University of East Piedmont

PhD Program in Medical Sciences and Biotechnology

Department of Translational Medicine

BIO/09-Fisiologia

PhD thesis

Direct/indirect protective effects elicited by anti-vascular endothelial growth factor drugs on retinal pigment epithelium cells (ARPE-19 cell line)

Mentor:

Prof. Grossini Elena

Candidate:

Farruggio Serena

ACADEMIC YEAR: 2018/2019

Index

Summary

BACKGROUND/AIMS: The Age-Related Macular Degeneration (AMD) is the leading cause of loss of vision in developed countries. Abnormalities of the choroidal blood flow have been hypothesized to contribute to the development of AMD. Regarding this issue, recent studies have suggested that changes in nitric oxide (NO) plasma levels in AMD patients could be involved in the modulation of choroidal perfusion. Furthermore, mitochondrial damage and reactive oxygen species (ROS) could play an important role in AMD pathogenesis, through the reduction of vascularization of choriocapillaris, apoptosis, and by increasing the formation of drusen (extracellular lipids formations, between RPE cells and Bruch's membrane), and the release of pro-angiogenic vascular endothelial growth factor (VEGF) from the retinal pigment epithelium (RPE) cells. Intravitreal anti-VEGF therapy with drugs like Aflibercept and Ranibizumab has hugely improved the vision prognosis of neo-vascular AMD. However, it is not clear up till now if those agents could act as modulator of NO release, oxidative stress and apoptosis.

In the present study, we planned to evaluate the effects of Aflibercept and Ranibizumab in human RPE cells (ARPE-19 cell line) cultured in physiologic/peroxidative conditions on cell viability/mitochondrial function, and proliferation/migration. Mechanisms related to NO release, and apoptosis were examined, as well. Furthermore, we conducted co-culture experiments between RPE and human umbilical vascular endothelial cells (HUVEC), in order to analyze the cross-talk between RPE cells and vascular endothelial cells, which is important for the maintenance of the outer-retina structure and function. Pathological alterations of retinal pigment epithelium and endothelial cells relationship, could be the primary event leading to vision-threatening pathologies such as macular degeneration.

METHODOLOGY: RPE and co-culture RPE/HUVEC, were exposed to Ranibizumab/Aflibercept in the absence or presence of NO synthase (NOS) inhibitor, phosphatidylinositol 3′-kinase (PI3K), extracellular-signal-regulated kinases 1/2 (ERK1/2) and p38 mitogen-activated protein kinase (p38 MAPK) blockers. Specific kits were used for cell viability, NO, ROS detection, apoptosis and mitochondrial membrane potential measurement. Western blot was performed for apoptosis markers, NOS isoforms, and other kinases detection. Cell migration ability was measured by wound healing assay and cell proliferation was analyzed by using xCELLigence.

RESULTS: In RPE alone or in co-culture with HUVEC, Aflibercept/Ranibizumab increased NO release in a dose and time-dependent way, in physiologic conditions. Opposite results were obtained in RPE pretreated with hydrogen peroxide. Moreover, both the anti-VEGF agents were able to prevent the fall of cell viability and of mitochondrial membrane potential. Those effects were

reduced by inhibitors of NOS, PI3K, ERK1/2 and p38MAPK. Both anti-VEGF drugs were able to increase cell viability and migration. Finally, Aflibercept and Ranibizumab counteracted the changes of apoptosis markers, NOS expression/activation, protein kinase B (PKB or Akt) and ERK1/2 activation caused by peroxidation.

CONCLUSION: This study has shown for the first time new mechanisms involving NO, and mitochondria, in the actions of Aflibercept and Ranibizumab in RPE. Although not fully examined, HUVEC stimulated with the two anti-VEGF drugs, could release some paracrine factors, which could modulate the RPE response to anti-VEGF drugs.

BACKGROUND/OBIETTIVI: La degenerazione maculare legata all'età (AMD) è la principale causa di cecità nei paesi sviluppati. Si ipotizza che, anomalie del flusso sanguigno coroidale, possano contribuire allo sviluppo della AMD. A tale proposito, studi recenti hanno suggerito che i cambiamenti nei livelli plasmatici di monossido d'azoto (NO) nei pazienti con AMD, potrebbero essere coinvolti nella modulazione della perfusione coroidale. Inoltre, il danno mitocondriale e le specie reattive dell'ossigeno (ROS) potrebbero svolgere un ruolo importante nella patogenesi dell'AMD, attraverso la riduzione della vascolarizzazione della coriocapillare, l'apoptosi e aumentando la formazione di drusen (accumuli lipidici extracellulari situati tra l'RPE e la membrana di Bruch) e il rilascio del fattore di crescita dell'endotelio vascolare pro-angiogenico (VEGF) da parte delle cellule dell'epitelio pigmentato retinico (RPE). La terapia intravitreale con farmaci anti-VEGF come Aflibercept e Ranibizumab, ha notevolmente migliorato la prognosi nei pazienti con la forma di AMD neovascolare. Tuttavia, fino a ora non è chiaro se tali agenti possano agire modulando il rilascio di NO, lo stress ossidativo e l'apoptosi. Nel presente studio, lo scopo è stato quello di valutare gli effetti di Aflibercept e Ranibizumab in cellule dell'epitelio pigmentato retinico (linea cellulare: ARPE-19) di origine umana, coltivate in condizioni fisiologiche/perossidative, e valutando i loro effetti sulla vitalità cellulare/funzione mitocondriale e proliferazione/migrazione. Sono stati esaminati anche i meccanismi relativi al rilascio di NO e all'apoptosi. Sono stati inoltre condotti esperimenti di co-coltura tra cellule RPE e cellule endoteliali vascolari ombelicali umane (HUVEC), al fine di analizzare il cross-talk tra cellule RPE e cellule endoteliali, che risulta fondamentale per il mantenimento della struttura e della funzione della retina esterna. Alterazioni patologiche dell'interazione tra RPE e cellule endoteliali potrebbero infatti essere l'evento principale che porta a patologie che alterano le capacità visive, come la degenerazione maculare.

METODOLOGIA: Le cellule RPE da sole o in co-coltura con le HUVEC, sono state esposte al trattamento con Ranibizumab/Aflibercept in assenza o presenza di inibitori della NO sintasi (NOS), della fosfatidilinositolo-3-chinasi (PI3K), della chinasi regolata dal segnale extracellulare 1/2 (ERK 1/2), e della proteina chinasi mitogena p38 attivata (p38 MAPK). Sono stati utilizzati kit specifici per l'analisi della vitalità cellulare, per il dosaggio dell' NO, per il dosaggio dei ROS, per esaminare l'apoptosi e per la misurazione del potenziale della membrana mitocondriale. La metodica del Western blot, in particolare, è stata eseguita per l'analisi dei marcatori dell'apoptosi, per analizzare le isoforme della NOS e per esaminare le variazioni dell'espressione o attivazione di altre chinasi coinvolte nella proliferazione e vitalità cellulare. La capacità di migrazione cellulare è stata misurata mediante il saggio di wound healing e la proliferazione cellulare è stata analizzata utilizzando lo strumento xCELLigence.

RISULTATI: Nelle cellule RPE coltivate da sole o in co-coltura con le HUVEC in condizioni fisiologiche, il trattamento con Aflibercept/ Ranibizumab ha aumentato il rilascio di NO in modo dose-dipendente e in funzione del tempo. Risultati opposti sono stati ottenuti nelle RPE pretrattate con perossido di idrogeno. Inoltre, entrambi gli agenti anti-VEGF hanno prevenuto la caduta della vitalità cellulare e del potenziale della membrana mitocondriale. Tali effetti sono stati ridotti dagli inibitori di NOS, PI3K, ERK1/2 e p38 MAPK. Entrambi i farmaci anti-VEGF hanno inoltre aumentato la vitalità cellulare e la migrazione. Infine, Aflibercept e Ranibizumab hanno ridotto le variazioni dell' espressione/attivazione dei marcatori di apoptosi, delle isoforme di NOS, della proteina chinasi B (PKB o Akt) e della chinasi ERK 1/2 causate dalla perossidazione.

CONCLUSIONE: Questo studio ha mostrato per la prima volta nuovi meccanismi che coinvolgono l'NO e i mitocondri, nel meccanismo di azione di Aflibercept e Ranibizumab nelle RPE. Sebbene non completamente esaminato, le HUVEC stimolate con i due farmaci anti-VEGF, potrebbero rilasciare alcuni fattori paracrini, che potrebbero modulare la risposta delle RPE ai farmaci anti-VEGF.

Introduction

2.1 ANATOMY AND PHYSIOLOGY OF THE EYE

The eye is the primary sensory organ for vision, responsible for collecting light, focusing it, and encoding the first neural signals of the visual pathway. To reach the retina, light must pass through the ocular media, consisting of the tear film, cornea, anterior chamber, lens, and the posterior chamber vitreous (Figure 1). The corneal epithelium and stroma are transparent to permit passage of light without distortion. The ciliary muscles dynamically adjust the shape of the lens in order to focus light optimally from different distances upon the retina (accommodation) (Prasad S. and Galletta S.L., 2011).

In the human eye, three layers can be distinguished:

The *outer region* consists of the cornea and the sclera. The cornea refracts and transmits the light to the lens and the retina, and protects the eye against infection and structural damage of the deeper parts. The sclera forms a connective tissue coat that protects the eye from internal and external forces and maintains its shape. The cornea and the sclera are connected at the limbus. The visible part of the sclera is covered by a transparent mucous membrane, the conjunctiva.

The *middle layer* of the eye is composed of the iris, the ciliary body and the choroid. The iris controls the size of the pupil, and thus the amount of light reaching the retina; the ciliary body controls the power and shape of the lens and is the site of aqueous production; and the choroid is a vascular layer that provides oxygen and nutrients to the outer retinal layers.

The *inner layer* of the eye is the *retina*, a complex layered structure of neurons, that capture and process light. The three transparent structures surrounded by the ocular layers are called the aqueous, the vitreous and the lens (Willoughby C.E. *et al.*, 2010).

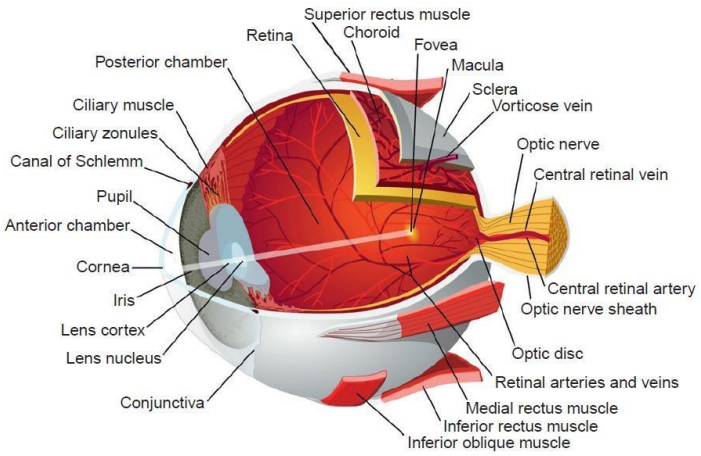

Figure 1: The anatomy of the eye. Light passes through the anterior chamber, the lens, and the posterior chamber, and is then focused upside-down and backwards upon the retina (Prasad S. and Galletta S.L., 2011).

Retina

The retina is the thin layer of cells at the back of the eye ball and is protected and held in the appropriate position by the surrounding sclera and cornea. In vertebrate embryonic development, the retina and the optic nerve originate as out growths of the developing brain, specifically the embryonic diencephalon; thus, the retina is considered part of the central nervous system and is actually a brain tissue. Retina is made up of nerve cells interconnected by synapses and sensitive to light. These cells are connected to the brain by the optic nerve, which sends information from the eye to the brain and allows us to see. The eyes of most vertebrates contain two types of photoreceptors: rods and cones (Figure 2). In humans, rods are approximately 20 times more abundant than cones (Willoughby C.E. *et al*., 2010). When light reaches the retina, its energy is converted by retinal photoreceptors into an electrochemical signal that is then relayed by neurons. For this purpose, the membranes of the outer segment discs of the photoreceptors contain pigments. Cones, which are responsible for color vision, have pigments with absorption peaks in the blue, green or yellow parts of the spectrum. Rods are active with low light levels, and are not involved in color vision. The density of rods and cones varies between different regions of the retina. In humans, about 50% of the cones are located in the central 30% of the visual field, roughly corresponding with the macula.

To arrive at the photoreceptors, light must first pass through transparent inner layers of the neurosensory retina, comprised of the nerve fiber layer, ganglion cells, amacrine cells, bipolar cells and horizontal cells. Immediately outside the photoreceptor layer there is the retinal pigment epithelium (RPE). The RPE provides structural and metabolic support for the photoreceptors, primarily through the vital function of vitamin A metabolism (Prasad S. and Galletta S.L., 2011).

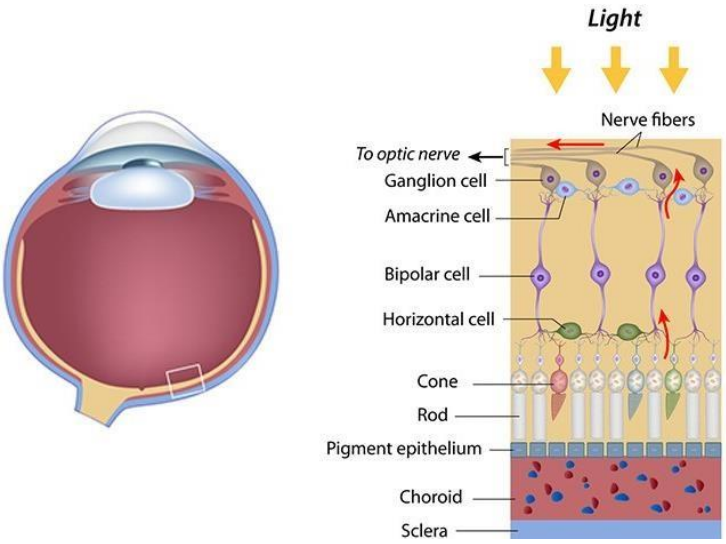

Figure 2: Cells and layers of the retina (https://discoveryeye.org/layers-of-the-retina).

The *macula lutea* is a highly specialized region of the central retina unique to humans and other primates that is normally responsible for achieving high acuity and color vision (Kaarniranta K. *et al*., 2013). The macula looks like an oval yellow 'spot' for the presence of carotenoids (zeaxanthin and lutein) and is more sensitive to light stimuli compared to the rest of the retina. In fact, the macula is rich in cones and rods. Histologically, the macula has several layers of ganglion cells, whereas in the surrounding peripheral retina the ganglion cell layer is only one-cell thick. The excavation near the centre of the macula is called the fovea (Figure 3). This area of the retina is responsible for sharp central vision and contains the largest concentration of cones in the eye. Visual acuity is highest in the foveola, the thin, avascular bottom of the fovea, which contains only densely packed cone cells. At the level of the internal nuclear layer, the foveola is surrounded by a circular system of capillaries, the vascular arcades. No photoreceptor cells are present at the optic disc or optic nerve head where the axons from the ganglion cells exit the eye to form the optic nerve (Handa J.T. *et al*., 2017)**.**

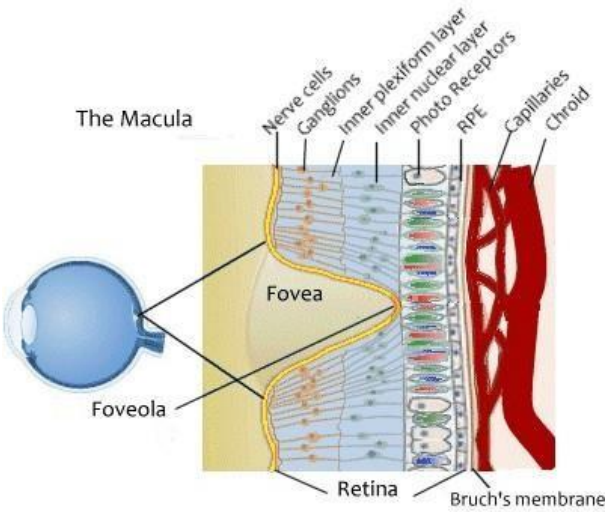

Figure 3: Macula structure. The macula is located at the back of the eye. It is a small area of about 1mm in diameter from which we get our sharpest vision. In the macula there is a high concentration of cone cells. These cells are responsible for color vision, sharp visual acuity and central vision. There is 6-7 million cone cells in the retina, the highest concentration of which is in the fovea, a tiny area in the center of the macula (https://www.naturaleyecare.com/glossary/macula-definition).

2.1.1 The retinal pigment epithelium

The RPE, is a monolayer of pigmented cells located between the neural retina and choroid and is essential for the maintenance and survival of overlying photoreceptor cells (Kauppinen A. *et al*., 2016; Zhao Z. *et al*., 2014; Mitter S.K. *et al.*, 2014). The RPE incorporates about 3.5 million epithelial cells arranged in a hexagonal pattern, with a density that is relatively uniform throughout

the retina. At the apical side, the cells of the RPE form long microvilli that reach up between the outer segments of rod photoreceptors. Numerous pigment (melanin and lipofuscin) granules are present in the apical cytoplasm of RPE cells (Figure 4). RPE cells are responsible for many tasks in the eye including maintaining the functionality of the overlying photoreceptor cells (including phagocytosis of photoreceptor wastes, regeneration and synthesis of pigments), protection of the retina from excessive light, immune defence of the central retina (macula), retinal adhesion, storage and metabolism of vitamin A, and production of growth factors necessary for nearby tissues and wound healing after injury or surgery. In addition, the RPE plays an important role in the blood retinal barrier function. The retina receives its blood supply from two circulatory systems: the retinal and the choroidal blood vessels. The retinal circulation supplies the inner retina, except for the avascular foveal zone. The outer avascular retinal layers receive their nutrients by diffusion from the choroid vessels. The choriocapillaris is fenestrated, which allows leakage of molecules to the RPE. Specialized transport systems in the RPE control the transportation of fluid and nutrients to the photoreceptors. Retinal function depends on several factors, including the region of the retina being illuminated, the wavelength and intensity of the and formation of blood-retinal barrier in conjunction with the vascular endothelium.

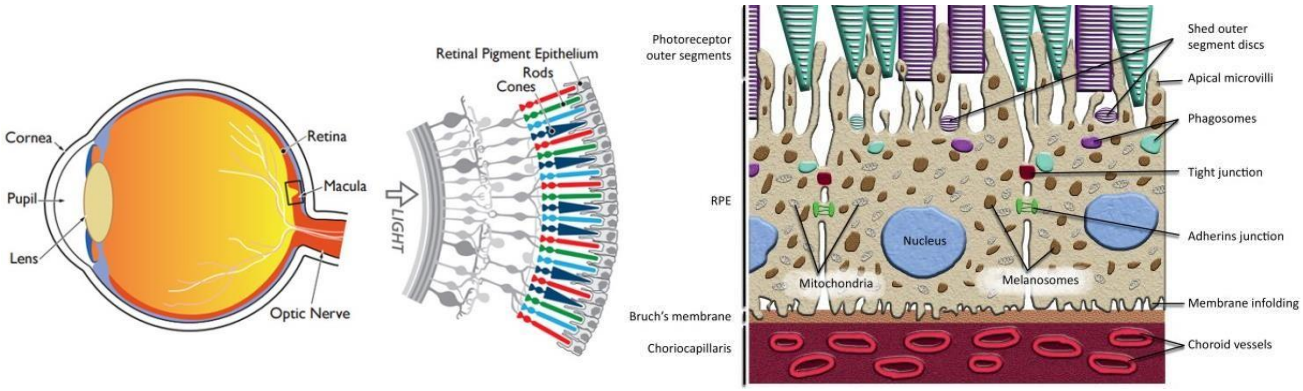

Figure 4: The retinal pigment epithelium. The RPE is a monolayer of highly polarized columnar epithelia that forms a barrier between the neural retina and the choroid. Barrier function is mediated by tight and adherin junctional complexes between adjacent cells. The apical surface of RPE cells forms microvilli protrusions, which extend between the outer segments of overlying photoreceptor cells and are involved in the removal of diurnally shed photoreceptor outer segment discs. The phagocytosed outer segments are ingested and form inclusion bodies, known as phagosomes, which are subsequently digested. Pigmentation of the RPE is due to the presence of melanosomes within cells. The basal membrane is highly infolded, which is common in cells involved in the transport of fluid and ions. The RPE cells reside on a layered extracellular matrix called Bruch's membrane, above the fenestrated choroidal capillaries of the eye, termed the 'choriocapillaris' (https://www.closerlookatstemcells.org/stem-cells-medicine/macular-degeneration; Carr A.J. et al., 2013).

2.2 RETINAL AGING

Our vision shows declining performance with increasing age including decrease visual acuity, decline in sensitivity of visual field, decreased contrast sensitivity, and increased dark adaptation threshold. Decreased visual function is a combination of mainly ageing changes in neuronal elements of visual system, changes in ocular media, and pupillary miosis (Salvi S.M. *et al*., 2006). RPE, which is vital for integrity of the rods and cones, shows with age increased pleomorphism, decrease in number of cells in the posterior pole, decreased melanin content, increased lipofuscin content, decreased volume of cytoplasm. All the above changes would prevent the normal switch of hydrophilic substances between choriocapillaris and retina, leading the cells to programmed cell death (apoptosis), retinal atrophy or pathological neovascularization such as in exudative form of age-related macular degeneration (AMD) (Salvi S.M. *et al*., 2006; Green W.R. and Key S.N. *et al*., 2005; Wetzig P.C., 1988; Spraul C.W. *et al*., 1999).

2.3 AGE-RELATED MACULAR DEGENERATION (AMD)

The AMD, is a complex chronic neurodegenerative disease and is the major cause of blindness among old people (more than 50 years old of age in developed countries) (Saenz-de-Viteri M. *et al*., 2015; Handa J.T., 2012). Although age is the most significant risk factor in AMD, the disease is also associated with hypertension, atherosclerosis, hypercholesterolemia, lifestyle (obesity, uncontrolled high blood pressure, smoking) and many environmental and genetic factors (Blasiak J. *et al*., 2014; Kaarniranta K. *et al*., 2011). Due to prolonged life expectancy in modern societies, AMD constitutes a severe medical and socio-economic problem (Zając-Pytrus H.M. *et al*., 2015). AMD is characterized by a progressive alteration of the central region of the retinal tissue, the macula, that is involved in the central vision, and allows us to distinguish forms and colors (Figure 5).

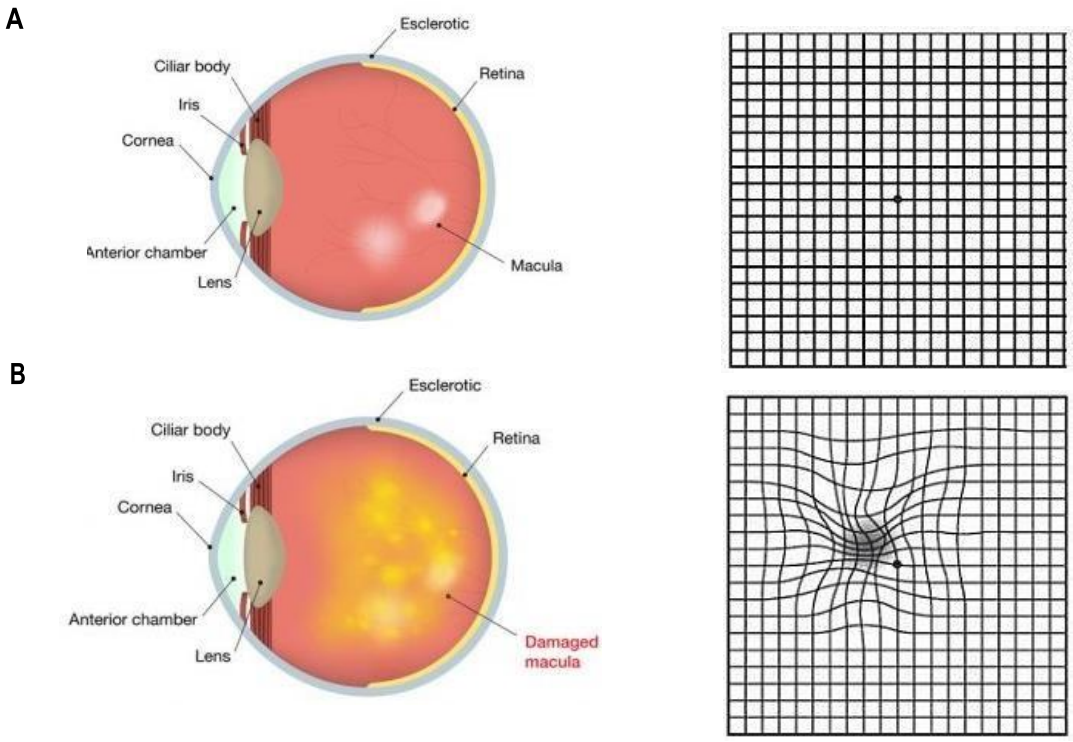

Figure 5: Loss of high acuity vision in patients with age-related macular degeneration. A simulated interpretation of vision in patients with late-stage AMD. In A, normal vision is depicted, whereas loss of central vision is illustrated in B. Photoreceptor cell death in the macular region of the eye leads to loss of central vision which is required for fine high acuity tasks, such as reading, face recognition, and driving (https://c60canada.com/2018/04/23/age-related-macular-degeneration-treatment-possibly; https://terraceeyecentre.com.au/conditions-treated/age-related-macular-degeneration).

The reason why the macula may be more susceptible to retinal degeneration is still a matter of debate, but there are some characteristics that probably can contribute to this susceptibility. Some of these characteristics are related to the structural organization of the macula with particular reference to its RPE. In macular degeneration and retinitis pigmentosa, it has been found to be dysfunctional and for this reason it has been suggested to be the initial site of pathogenesis. Also differences in the thickness of Bruch's membrane may contribute to this susceptibility.

Bruch's membrane or vitreous lamina is a thin layer between choriocapillaris and RPE and its function is to filter substances from fenestrated capillaries of choriocapillaris to RPE cells (Booij J.C. *et al*., 2010).

Macular degeneration is characterized by an initial step, which is not accompanied by important visual changes and is called "early AMD" (also called "dry" or "non exudative"), with

intermediate-size drusen (63–124 μm), which can evolve into "intermediate AMD" (with large drusen ≥125 μm). However, the intermediate stage can evolve into "late AMD", which includes two advanced forms: the geographic atrophy (GA), characterized by outer retinal and choroidal atrophy, specifically the photoreceptor layer, RPE, and choriocapillaris, and the choroidal neovascularization (CNV, also called "wet" or "exudative" or "neovascular") (Arya M. *et al*., 2018; Plyukhova A.A. *et al*., 2018) (Figure 6).

The **dry or non exudative AMD**, is the most common form of AMD and is characterized by slow progressive dysfunction of the RPE, photoreceptor loss, and retinal degeneration (Hernández-Zimbrón L.F. *et al*., 2018). It is usually asymptomatic and patients do not experience pain. In patients with dry AMD the straight lines look wavy or distorted (metamorphopsia), and dark spots appear in the central vision (Blasiak J. *et al*., 2014). The non exudative AMD is characterized by the presence of subretinal deposits (drusen), which are extracellular white-yellow lipids formations with round shape, between RPE cells and Bruch's membrane and can be clinically detected in the central posterior pole of the eye (Kauppinen A. *et al*., 2016). Drusen may be of various sizes (30– 50 μm or larger when confluent) and various compositions. Even if the exact proportion of protein and lipid in drusen is unknow, they can contain cholesterol in 2 chemical forms, unesterified and esterified to a long chain fatty acid, phosphatidylcholine (Wang L. *et al*., 2010), plasma derived (amyloid P component, prothrombin), vitronectin, complement proteins C3, C5, and C9, and apolipoproteins B and E (Bergen A.A. *et al*., 2018) Their occurrence signals the degree of advancement of the disease (Zając-Pytrus H.M. *et al*., 2015). The diagnosis usually is picked up on routin visit to the optometrist. The most common initial symptom is slightly blurred central vision when performing tasks that require seeing details. Glasses cannot correct this blurred spot, or sense there is dirt in the way of clear vision. Over time, the blurred area may increase in size and interfere with reading and recognizing faces.

The **wet or exudative or neovascular AMD**, is less frequent but is responsible for 90% of acute blindness due to AMD. It is characterized by choroidal neovascularization (CNV) with intraretinal or subretinal leakage, hemorrhage, and RPE detachments so, it is the most serious form of AMD and it can evolve from the dry form (Hernández-Zimbrón L.F. *et al*., 2018). The RPE produces excessive amounts of vascular endothelial growth factor (VEGF), and this contributes to the breakdown of the blood-retinal barrier and sprouting of fragile blood vessels from the choroid through Bruch's membrane into the retina in a process called neovascularization. Leakage of blood from these abnormal vessels causes oedema and an acute loss of vision. These subretinal neovessels

grow from choroid to Bruch's membrane so, in this way, they lift the sensorial retina causing an alteration of images and promoting a deterioration of the macula. The neovessels are very fragile so that they allow the exudation of blood and fluids below the macula and if this exudative form evolves into a hemorrhagic form, the patient can completely loss the central vision in few seconds (Kauppinen A. *et al*., 2016; Blasiak J. *et al*., 2014).

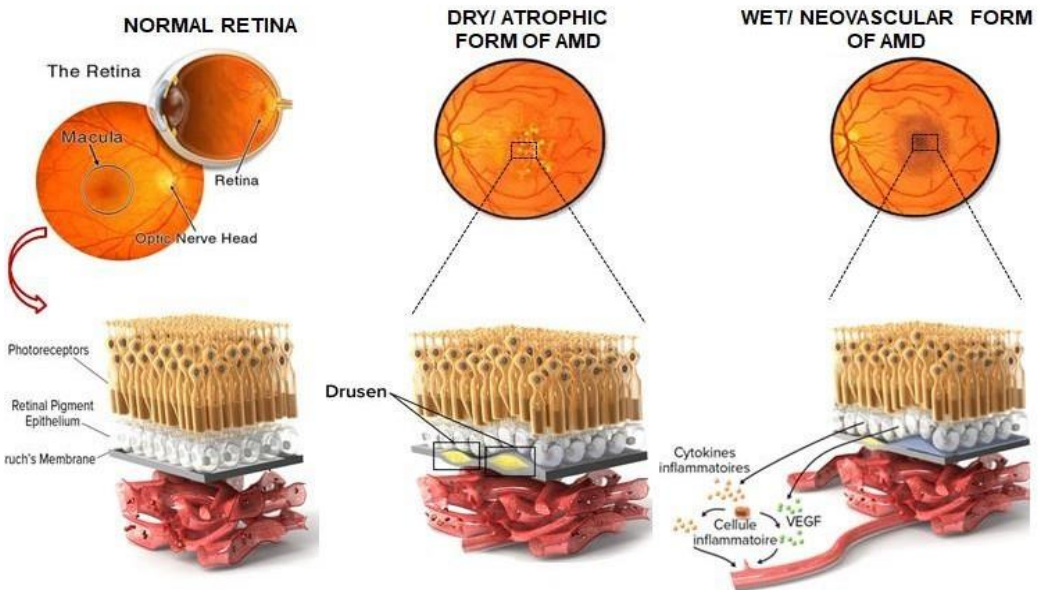

Figure 6: Examples of a normal macula, early AMD and dry AMD. Schematic rapresentation about the progression of AMD (https://www.scienceofamd.org).

2.4 AMD DIAGNOSIS

- *Amsler grid:* is used to check whether lines look wavy or distorted, or whether areas of the visual field are missing. In case of macular degeneration, some of the lines will appear faded, broken or distorted (Figure 7).

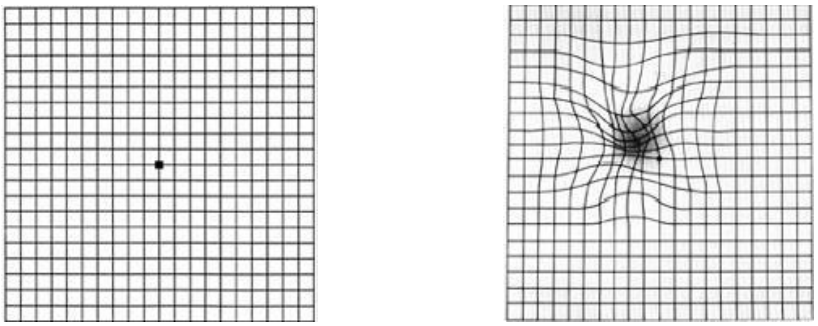

Figure 7: Comparison of the Amsler grid as seen by someone without AMD (left) and someone with AMD (right) (https://terraceeyecentre.com.au/conditions-treated/age-related-macular-degeneration).

Most of the advanced diagnostics tools for studying the presence or progression of macular degeneration involves making images of the fundus (the inside back of the eye ball) and the retina. The technology is constantly being updated, but currently includes:

- *Fundus Fluorescein Angiography (FFA):* a yellow dye called fluorescein is injected into a vein in the arm or hand. Sequential photographs of the eye are taken, using a camera that sits on a table (the person sits in front of it). The images show blood flow and possible leakage (wet AMD) in the retina and choroid. This method of imaging takes about 20 min altogether and requires dilation drops. Urine and saliva are sometimes dark orange afterwards, a result of the body metabolizing the dye.

- *Optical Coherence Tomography (OCT):* in this common, non-invasive (no injections) imaging method, infrared light waves are used to make cross-section photographs of the retina and choroid layer. OCT provides extremely useful information about drusen, retinal structure, new blood vessels, and hemorrhages. The person gets dilation drops then sits in front of the camera with his or her chin in a chin rest. The imaging equipment takes about 15 min.

- *Fundus Autofluorescence Imaging (AF):* this is an imaging non-invasive method which uses the body's natural fluorescence to study the retina. Certain structures (fluorophores) in the body will light up when exposed to certain wavelengths of light. These include RPE cells and lipofuscin (the residue of RPE cell waste). This imaging method is often used to study late dry AMD, or geographic atrophy because atrophied sections of the eye do not light up.

2.5 AMD PATHOGENESIS

The precise etiopathogenesis of AMD is still unknown; however, it is most probably a multifactorial disease of aging (Totan Y. *et al*., 2015).

Abnormalities of the choroidal blood circulation have been hypothesized to contribute to the development of AMD.

Hence, choroidal circulation plays an important role in providing nutrients and removing wastes from the RPE and retina layers. Many vasodilators are currently under investigation in clinical trials with the rationale that the use of these drugs may increase the blood flow of the choroid, and thus may delay the progression of d-AMD. It has been postulated that the reduced choroidal blood flow would result in changes in the RPE function with accumulation of lipoproteins that ultimately lead

to RPE cell degeneration and altered permeability of the Bruch's membrane as observed in early AMD.

As regarding the mechanisms, previous studies have suggested that a reduction of nitric oxide (NO) levels in AMD patients could be involved in changes of choroidal blood flow (Imran A. *et al*., 2010; Totan Y. *et al*., 2015). Furthermore, the levels of NO synthase (NOS) isoforms have been found to be significantly reduced in eyes with AMD. All together those findings could be associated with neuronal degeneration in retina and hemodynamic changes in AMD choroid (Bhutto I.A. *et al*., 2010). In spite of this the precise role of NO in the onset of AMD have not clearly examined, yet (Keles S. *et al*., 2014). Furthermore, mitochondrial damage (Mitter S.K. *et al*, 2014; Chen W.J. *et al*., 2017) and reactive oxygen species (ROS) could play an important role in AMD phatogenesis, through the reduction of vascularization of choriocapillaris and by increasing the formation of drusen (Blasiak J. *et al*., 2014) and the release of pro-angiogenic VEGF from the RPE cells (Ranjbar M. *et al*., 2016; Jarrett S.G. and Boulton M.E., 2012; Karunadharma P.P. *et al*., 2010).

2.5.1 The role of oxidative stress

Despite being a disease of unknown etiology, there is strong evidence suggesting that oxidative stress has a major role in the development and progression of AMD. The retina and RPE are extremely susceptible to oxidative stress damage: they both have high metabolic demands and require large amounts of adenosine triphosphate (ATP) to support their functions (Hernández-Zimbrón L.F. *et al*., 2018).

The retina is continually exposed to free radicals from its rich blood supply, numerous mitochondria (Peddada K.V. *et al*., 2018), and has the highest consumption of oxygen per gram of tissue in the human body. In addition, the constant exposure of both structures to UV radiation, especially UVA, which is able to excite ocular chromophores and induce DNA damage by secondary photoreactions and indirect photosensitizing reactions, is also a constant source of ROS like hydrogen peroxide (Hernández-Zimbrón L.F. *et al*., 2018). The outer segment of the rods has a high content of polyunsaturated fatty acids (PUFAs) that are particularly sensitive to peroxidation given their number of double bonds. The inner segments of the rods are particularly rich in mitochondria, which contain activated oxygen species that may cause damage if they leak out of cells. Furthermore, the light that hits the retina may trigger photooxidative processes. Visible light in the blue wavelength forms the toxic compound which targets cytochrome oxidase and induces irreversible DNA damage in RPE cells. Most pathological processes that take place in the retina, such as inflammation, cell apoptosis, or angiogenesis, can, hence, involve free radicals directly or indirectly (Peddada K.V. *et al*., 2018). With ageing, antioxidant levels decline accompanied by

ROS level increase in most tissues, thus resulting in oxidative damage to macromolecules such as membrane phospholipids (Totan Y. *et al*., 2001). Oxidative stress has gained increasing recognition and is now considered to be a major pathogenic factor in many age-related diseases such as Alzheimer's disease (Honda K. *et al*., 2004), atherosclerosis (Stocker R. and Keaney J.F., 2004), and cancer development (Halliwell B., 2007) among others. In the eye, oxidative stress contributes to the development of many common chronic ophthalmic disorders including AMD, cataract, open-angle glaucoma, diabetic retinopathy, uveitis and ocular surface disorders (Pinazo D. *et al*., 2014). Over the years numerous hypotheses have been put forward to explain the association between oxidative stress and age-related dysfunction at the cellular and whole organism level (Jarrett S.G. and Boulton M.E., 2014).

Oxidative stress results from disturbances in the prooxidative/antioxidative cellular balance due to elevated levels of oxidation reactions producing ROS such as hydrogen peroxide (H_2O_2), superoxide anion (O_2^-), hydroxyl radical (OH^-) (Blasiak J. *et al*., 2014).

Generation of reactive oxygen/nitrogen species

ROS and reactive nitrogen species (RNS) are highly reactive molecules which play an important role in the regulation of many physiological processes involved in intracellular signaling, but they can also induce serious damage to nucleic acids, carbohydrates and lipids, often resulting in dysfunction of the biomolecules (Figure 8). ROS and RNS are terms that commonly define either a free radical (species that contains one or more unpaired electrons in the outer molecular orbitals), powerful oxidizing agents (H_2O_2 or peroxynitrite ($ONOO^-$)) or a species that exists at a higher energy level (singlet oxygen; O_2). At a physiological level, ROS and RNS can function as signaling molecules in crucial regulatory pathways including cell proliferation, gene expression and apoptosis. However, ROS/RNS levels above physiological, or an imbalance in the oxidant/antioxidant ratio, can have significant pathophysiological consequences (Jarrett S.G. and Boulton M.E., 2014).

ROS and RNS can be formed in many ways: (Blasiak J. *et al*., 2014)

- as a product of the respiratory chain in mitochondria
- photochemical and enzymatic reactions
- as a result of the exposure to UV light
- ionizing radiation
- heavy metal ions

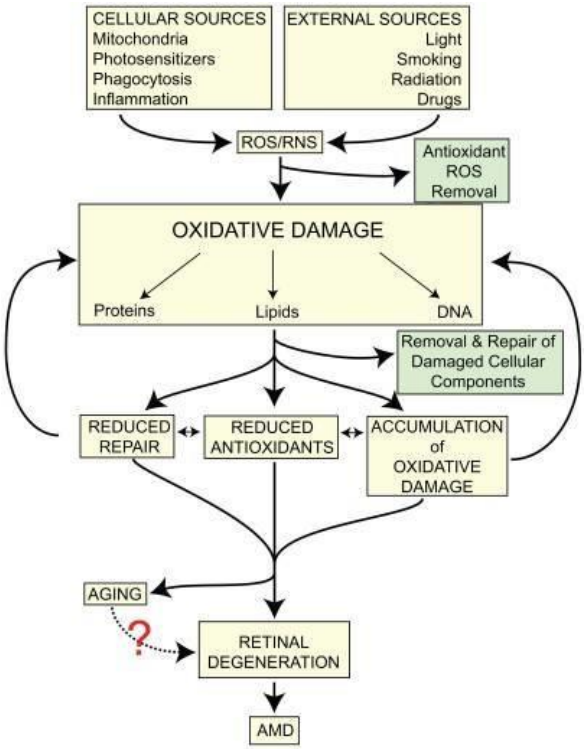

Figure 8: A diagram depicting the potential pathways leading from oxidative stress to AMD (Jarrett S.G. and Boulton M.E., 2014).

The cascade of oxygen radical production begins with a single electron reduction of molecular oxygen (O_2) to form superoxide anion ($O_2^{\cdot -}$), which dismutates in the presence of either superoxide dismutase 1 or 2 (SOD1/2) into H_2O_2 and O_2 ($2O_2^{\cdot -} + 2H^+ \rightarrow H_2O_2 + O_2$). H_2O_2 is a molecule with low reactivity, but it can readily penetrate cell membranes and generate the most reactive form of hydroxyl radical, via the Fentom reaction:

$Fe^{2+} + H_2O_2 \rightarrow Fe^{3+} + OH\cdot + OH^-$

Although $O_2^{\cdot -}$ is less reactive than OH^-, its reaction with NO forms the highly reactive oxidizing agent, peroxynitrite ($NO + O_2^{\cdot -} \rightarrow ONOO^-$).

The reaction of proteins with a variety of free radicals leads to oxidative protein modifications such as formation of protein hydroperoxides, hydroxylation of aromatic groups and aliphatic amino acid side chains, oxidation of sulfhydryl groups, oxidation of methionine residues, conversion of some amino acid residues into carbonyl groups, cleavage of the polypeptide chain, and formation of cross-linking bonds. Unless repaired or removed from cells, oxidized proteins are often toxic and can impair cellular viability since oxidatively modified proteins can form large aggregates (Santos A.L. *et al*., 2017).

Cells which are the most sensitive to oxidative damage are the non-proliferative post-mitotic cells, including photoreceptors and RPE cells, since they do not possess any DNA damage detection systems in the cell cycle checkpoints. Furthermore, the macular environment promotes the

production of ROS. In the macula, the predominant photoreceptors are cones, which have higher demand and production of energy than rods and, therefore, higher demand for oxygen. The macula is constantly exposed to a high metabolic rate and oxidative stress due to the high partial pressure of choriocapillaris and the amount of PUFAs from the retinal outer segments. Oxidized PUFAs are not efficiently digested in the lysosomes of aged RPE cells and become deposited in the form of lipofuscin (Jarrett S.G. and Boulton M.E., 2014) (Figure 9).

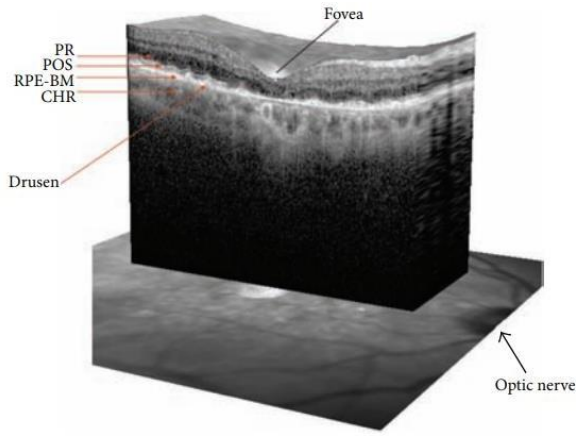

Figure 9: Optical coherence tomography (OCT) showing the major structures of the human retina in dry AMD patient. The structures marked are fovea, photoreceptors (PR), photoreceptor outer segments (POS), Retinal pigment epithelium-Bruch's complex (RPE-BM), and choroid (CHR). Drusen accumulate between RPE and Bruch's membrane. Optic nerve has been shown by thick arrow (Blasiak J. *et al.*, 2014).

This is thought to be important in inducing the formation of drusen between the RPE cells and Bruch's membrane. Lipofuscin is a chromophore, serving as the main RPE photosensitizer, which, after absorbing a high-energy photon, especially that of blue light, undergoes a variety of photochemical reactions involving ROS formation, which, in turn, evoke photochemical damage in the retina and RPE cells (Blasiak J. *et al*., 2014).

2.5.2 Mitochondrial role in ROS production and AMD pathogenesis

Due to its high metabolic activity, RPE cells are enriched with mitochondria, and as a result, these organelles are a major source of ROS in the RPE. Compared with young cells, aging mitochondria generate more ROS, and furthermore, aging cells are progressively susceptible to mitochondria derived ROS.

Under physiological conditions during ATP synthesis, the electron transport chain (ETC) complex generate ROS that leak out of the mitochondrial membrane. Under pathological conditions that

compromise the ETC components, the generation of ROS is significantly increased, principally at complexes I (NADH complex) and III (cytochrome complex). Not surprisingly, mutations in the genes that code for these complexes account for more than 50% of all mitochondrial ROS related pathological conditions. Additionally, the decrease in mitochondrial membrane potential facilitates the leakage of ROS into the cytoplasm (Datta S. *et al*., 2017; Jarrett S.G. and Boulton M.E., 2014). Direct evidence for mitochondrial damage in AMD has been documented in several studies. Feher and his colleagues, thanks to electron microscopic and morphometric studies, observed qualitative and quantitative alterations of mitochondria in human RPE from AMD and from age- and sex matched controls. They found that, increasing age, there was a significant decrease in number and area of mitochondria, as well as loss of cristae and matrix density, in both AMD and control specimens. These decreases were significantly greater in AMD than in normal aging (Fehér J. *et al*., 2007).

Blasiak *et al*. found that RPE of AMD patients have increased mitochondrial DNA (mtDNA) damage compared to RPE from age-matched controls (Blasiak J. *et al*., 2013). Human RPE cells exposed to oxidizing agents exhibit damage of mtDNA and this, in turn, leads to increased ROS generation. Unfortunately, unlike nuclear DNA (nDNA) repair, mtDNA repair in the RPE appears to be relatively slow and inefficient (Datta S. *et al*., 2017). The preferential susceptibility of mitochondria to oxidative damage and their poor repair capacity suggests that mitochondria are a weak link in the RPE cell's defenses against oxidative damage. Animal models of mitochondrial oxidative stress, involving knockdown of SOD2, have confirmed pathological lesions similar to those observed in "dry" AMD (Justilien V. *et al*., 2007) and over-expression of SOD2 protects against oxygen-induced apoptosis in mouse RPE and retinal cells (Kanwar M. *et al*., 2007; Kasahara E. *et al*., 2005). These findings strongly support that mitochondrial oxidative stress is a feature of aging and may be a pivotal factor in the development of AMD, by reducing cell function.

2.5.3 The role of NO

As mentioned above, evidence also suggests impaired choroidal blood flow in AMD pathogenesis. An abnormal choroidal blood supply may disrupt normal retinal function and lead to visual deterioration. Although NO could play an important role in the onset of AMD by its action on the vascular tone and ocular blood flow, there have been only a few studies to characterize the NOS isoforms in the choroid (Bhutto I.A. *et al*., 2009; Totan Y. *et al*., 2001).

NO is an important signaling molecule that acts in many tissues to regulate diverse range of physiological and cellular processes including neurotransmission, immune defense, regulation of cell death (apoptosis), and cell motility (Bhutto I.A. *et al*., 2009). Although the discovery of NO in

pharmacology has been known since 1979, it is only since the 90s that NO has already been related to numerous eye diseases, such as glaucoma, retinopathy, AMD, myopia and cataract (Chiou G.C., 2001).

Nitric oxide is a small, short-lived molecule synthesized from L-arginine by NOS and oxygen and nicotinamide adenine dinucleotide phosphate (NADPH) are necessary co-factors. There are three types of NOS in humans: two constitutive isoforms, which are called neuronal NOS (nNOS), the predominant isoform expressed in neurons, and endothelial NOS (eNOS), the predominant isoform in vascular endothelial cells. In normal conditions, both nNOS and eNOS produce low levels (picomolar) of NO and for short periods of time after activation by calcium/calmodulin-dependent protein kinase. Such small NO amount produces various biological responses, including vasodilation, increase of ocular blood flow, reduction of intraocular pressure, prevention of platelet aggregation, reduction of chemotaxis of polymorphonuclear cells, signal transduction of central nervous system and peripheral nervous system, inhibition of tumor cells (Chiou G.C., 2001; Bhutto I.A. *et al*., 2009; Keles S. *et al*., 2014). In abnormal conditions, however, large amounts of NO amounting to nanomolar levels are generated by the inducible NOS (iNOS) isoform. The iNOS isoform, is induced only in pathophysiological conditions, such as inflammation, lipopolysaccharide (LPS), endotoxin, and cytokines. NO will further oxidize into NO_2, nitrite, peroxynitrite, and free radicals to interact with thiols, iron-sulfur centers of various enzymes, cytochrome oxidase, glycolytic enzymes, endothelial cells, cardiomyocytes, neurons, hepatocytes, macrophages and calmodulin to alter biological function of cells, damage DNA, and result in apoptosis, neurotoxicity, optic nerve degeneration and numerous eye diseases (Chiou G.C., 2001).

Nitric oxide is influenced by a dynamic equilibrium between its synthesis and degradation in tissues. Free radicals rapidly inactivate NO. In normal physiological conditions, endogenous defense systems against oxidation maintain the equilibrium between NO synthesis and degradation by oxygen free radicals. However, this delicate balance may be altered, particularly in the course of aging and senile macular degeneration resulting in a reduced NO level and thus impaired vascular relaxation (Totan Y. *et al*., 2015).

Several studies have found lower levels of NO in AMD patients compared to the control. Indeed, in a recent study, it has been found that AMD patients had elevated levels of asymmetric dimethylarginine (ADMA), which is the primary inhibitor of eNOS (Keles S. *et al*., 2014).

In another study examining NO in AMD, the NO levels were found to be lower in AMD patients than in controls, but the underlying mechanism was not described. Friedman proposed that the decrease in NO levels may be a contributing factor in ocular system damage, as well as, playing a role in AMD pathogenesis (Friedman E. *et al*., 1997).

2.6 ROLE OF RPE CELLS IN AMD

A functional degeneration of the RPE results in impaired maintenance of sensory retina, which contributes to the vision loss in advanced AMD. Due to their high metabolic activity, the associated abundant oxygen consumption, the high contents of PUFAs and substantial exposure to light, the RPE is especially sensitive to excessive oxidative stress (Kauppinen A. *et al*., 2016). Increased mitochondrial damage and generation of ROS are associated with AMD, suggesting that damaged mitochondria and other oxidatively modified components are not efficiently removed by the aged-RPE cells (Mitter S.K. *et al*., 2014).

As shown by Young (Young R.W., 1988), the first sign of senescence in outer retinal layers is the appearance of residual bodies (lipofuscin) within the RPE. Progressive increase of the RPE cells with lipofuscin is accompanied by abnormal excretions, which accumulate in the basal part of the cells and within Bruch's membrane. This process of cellular impairment may finally culminate in the death of the RPE and visual cells. Lipofuscin is the generic name given to a heterogeneous group of complex, autofluorescent lipid/protein aggregates present in a wide variety of both neuronal and non-neuronal tissues. In the eye, lipofuscin accumulates within the RPE throughout life eventually occupying up to 19% of cytoplasmic volume by 80 years of age (Zhao Z. *et al*., 2014). Finally, as mentioned above, in neovascular AMD, RPE cells have been disclosed as the main source of VEGF-A. Especially the cells of the macular (central retinal) region in AMD patients show an increased expression of VEGF-A. This growth factor is an important regulator of angiogenesis, which acts as an autocrine growth and survival factor in VEGF-A-producing cells **(**Ranjbar M. *et al*., 2016; Ablonczy Z. *et al*., 2011).

2.6.1 Neovascularization in AMD: the role of VEGF

The AMD process starts as an atrophic formation, called dry AMD, which is characterized by decreased vision principally caused by retinal dysfunction, and subsequently can develop to a wet condition. The latter occurs when abnormal blood vessels behind the retina start to grow under the macula; these new blood vessels are very fragile and often have blood and fluid leaks. The blood and fluid raise the macula from its normal position in the back of the eye, and the macula is damaged quickly favoring the loss of central vision. The most studied factor related to ocular neovascularization is the VEGF. Vascular endothelial growth factor was first identified as a signal protein of vascular permeability (Hernández-Zimbrón L.F. *et al*., 2018; Enseleit F. *et al*., 2010), and is a trophic endothelial growth factor that promotes endothelial migration, proliferation, survival and differentiation. Overexpression of VEGF promotes vascular leak and ocular neovascularization (Shen W. *et al*., 2017).

The influence of VEGF in retinal diseases is profound. It has been implicated not only in AMD and diabetic retinopathy, but also in the retinopathy of prematurity, sickle cell retinopathy and retinal vascular occlusion. Moreover, it could play a non-causal secondary influence in neovascular glaucoma and inherited retinal dystrophies. Collectively, these conditions, all of which have critical angiogenic components, account for the vast majority of irreversible vision loss in developed countries (Yorston D., 2014). Five retinal cell types have the capacity to produce and secrete VEGF. These include RPE cells, astrocytes, Müller cells, vascular endothelium and ganglion cells. Evidence for the expression patterns and roles of VEGF receptor (VEGFR) in retinal tissues comes from a variety of species and experimental venues. In the human retina, VEGFR-1 and -2 can be expressed by neural, glial and vascular elements. Notably, in cultured RPE cells, both receptors are expressed and are induced by oxidative stress (Penn J.S. *et al*., 2008).

Molecular effects of VEGF

Vascular endothelial growth factors are a subfamily of growth factors that function as signaling proteins for both vasculogenesis (the de novo formation of the embryonic circulatory system) and angiogenesis (the growth of blood vessels from pre-existing vasculature) (Gupta N. *et al*., 2013). This growth factor, a dimeric glycoprotein of approximately 46 kDa, has a variety of functions including the control of developmental vasculogenesis and angiogenesis of new blood vessels, regulation of permeability, and promotion of cell survival (Saenz-de-Viteri M. *et al*., 2016). Furthermore, it is essential for angiogenesis during development and the deletion of a single allele arrests angiogenesis and causes embryonic lethality (Penn J.S. *et al*., 2008). There are several members of the VEGF family, including VEGF-A, VEGF-B, VEGF-C, VEGF-D and placental growth factor (PGF) (Fiebai B. and Odogu V., 2017). Within this group of proteins, it has been reported that the VEGF-A protein induces vascular proliferation and migration of endothelial cells and is essential for both physiological and pathological angiogenesis. In several diseases, such as rheumatoid arthritis, cardiac ischemia, psoriasis and diabetic retinopathy, as well as in AMD, the activity of the VEGF-A protein plays an important role (Hernández-Zimbrón L.F. *et al*., 2018). VEGF-A is expressed as five mRNA splice variants: isoforms 121, 145, 165, 189, and 206, depending upon the number of aminoacids present. In particular, VEGF-121, VEGF-165 (responsible for pathological ocular neovascularization), VEGF-189 and VEGF-206 are believed to play a key role in the human eye (Fiebai B. and Odogu V., 2017).

All members of the VEGF family stimulate cellular responses by binding to tyrosine kinase receptors on the endothelial cell surface, causing them to dimerize and become activated through transphosphorylation (Gupta N. *et al*., 2013). VEGF-A has two types of receptors: VEGF receptor 1

(VEGFR-1) and 2 (VEGFR-2), which belong to the receptor tyrosine kinase family and are primarily involved in angiogenesis.

The VEGFRs contain an approximately 750-amino-acid-residue extracellular domain, which is organized into seven immunoglobulin-like folds, a single transmembrane hydrophobic spanning region, and an intracellular portion containing a split tyrosine kinase domain. Signal transduction is propagated when activated VEGFRs phosphorylate SH2 domain-containing protein substrates (Penn J.S. *et al*., 2008; Gupta N. *et al*., 2013). Once VEGF-A binds to its receptor, several signaling pathways are activated (Figure 10):

(1) the Mitogen-activated protein kinase- (MAPK-)p38 signaling pathway, where the effector protein (the heat shock protein HSP27) acts by reorganizing actin;

(2) the phosphatidylinositol 3-kinase- (PI3K-) Akt pathway, promoting the formation of NO by direct phosphorylation and activation of eNOS and inducing endothelial cell survival;

(3) the phospholipase C-gamma (PLCγ), triggering the intracellular calcium release, promoting prostaglandin (PGE_2) production, and increasing vascular permeability.

All three pathways promote angiogenesis (Penn J.S. *et al*., 2008; Gupta N. *et al*., 2013).

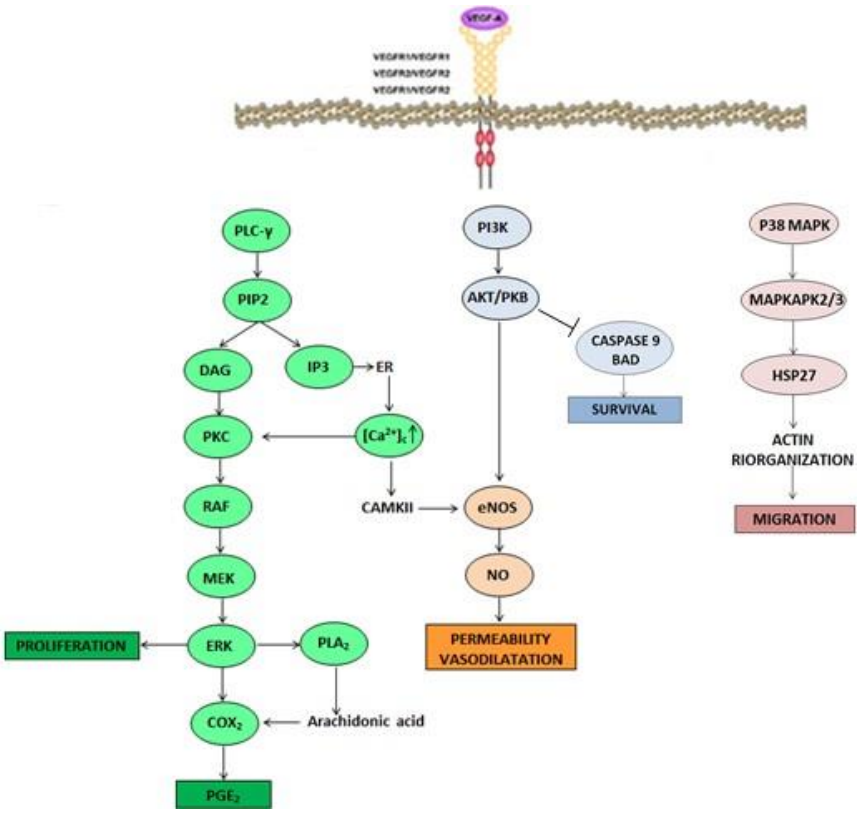

Figure 10: VEGF-A signalling pathways. The pathways are simplified, and only selected components are shown.

Currently, other proteins associated with VEGF-A signaling have been discovered to be involved in corneal neovascularization. The best-described proteins related to these processes are metalloproteinases 2 and 9 (MMP-2 and MMP-9). These proteins have acidic properties, are rich in cysteine, and promote angiogenesis as they act to degrade the extracellular matrix; by increasing the filtering of molecules that modify the microenvironment finally promote the formation of new blood vessels (Hernández-Zimbrón L.F. *et al*., 2018).

2.7 AMD TREATMENTS

Up to date there are no approved treatments for dry AMD, the US National Eye Institute has found that a specific formulation at high dosage of antioxidants and zinc taken orally, reduces significantly the risk of advanced AMD and the loss of vision associated with it. The risk of developing dry AMD can be reduced by avoiding smoking, exercising regularly and following a diet rich in vegetables and fruit. There are also some evidences that suggest that reducing exposure to strong UV light, by using sunglasses, can lead to a reduction of the risk. These preventative measures are strongly correlated with the reduction of the risk of cardiovascular disease, of some neoplasms and other chronic diseases.

With the discovery of VEGF as a driving factor in CNV development and associated edema, since 2006, anti-VEGF therapy has become the gold standard treatment modality in the treatment of neovascular AMD (Schottler J. *et al*., 2018; Ehlken C. *et al*., 2014).

2.7.1 Anti-VEGF drugs

Currently, intravitreal injections of anti-VEGF molecules are the best practice for the treatment of exudative AMD and are widely used in other ocular pathologies (such as diabetic retinopathy and retinal vascular occlusions, and retinopathy of prematurity) with new vessel growth and excessive vascular permeability (Saenz-de-Viteri M. *et al*., 2016; Kimoto K. and Kubota T., 2012). In clinics, different VEGF blockers are currently in use: the first approved Pegaptanib, the approved Ranibizumab, the off-label Bevacizumab, and the recently approved Aflibercept (Figure 11) (Klettner A. *et al*., 2014). Up to date, however, it is not clear if those agents could act as modulator of NO release, oxidative stress and apoptosis.

Pegaptanib (Macugen), is a pegylated aptamer, a modified oligonucleotide, which adopts a three-dimensional conformation that enables it to bind to extracellular VEGF with high affinity and selectivity. Pegaptanib binds to extracellular VEGF 165 isoform, with high affinity and specificity, thereby inhibiting VEGF165 binding to its VEGF receptors.

Bevacizumab (Avastin), a full-length murine-derived humanized, monoclonal, nonselective antibody against VEGF-A (Agrawal S. *et al*., 2013), has been initially approved by the Food and Drug Administration (FDA) for the treatment of metastatic colorectal carcinomas, renal carcinomas and glioblastoma multiforme of the brain and is one of the least expensive options; it is being used as an off-label therapy in the field of ophthalmology (Malik D. *et al*., 2014; Klettner A. *et al*., 2014; Kimoto K. and Kubota T., 2012). In comparison to ranibizumab, which is an antibody fragment, bevacizumab has an Fc fragment which may make it more immunogenic or proinflammatory (Agrawal S. *et al*., 2013).

Ranibizumab (Lucentis), is a humanized monoclonal antibody with a molecular weight of 48 kDa, and with a high affinity Fab-fragment against VEGF-A (Kimoto K. and Kubota T., 2012; Klettner A. *et al*., 2014). Ranibizumab, compared to its parent bevacizumab, has a higher affinity for VEGF with a greater potency (Agrawal S. *et al*., 2013).

Aflibercept (Eylea), is a fusion protein with a molecular weight of 115 kDa, composed by the 2nd Ig domain of the VEGFR-1 and the 3rd Ig domain of the VEGFR-2 connected to a Fc-fragment. These molecular differences may result in different effects on retinal cells. (Malik D. *et al*., 2014; Klettner A. *et al*., 2014). It binds with higher affinity to multiple isoforms of VEGF-A as well as VEGFR1 ligands, VEGF-B, and placental growth factor (PIGF) (Agrawal S. *et al*., 2013).

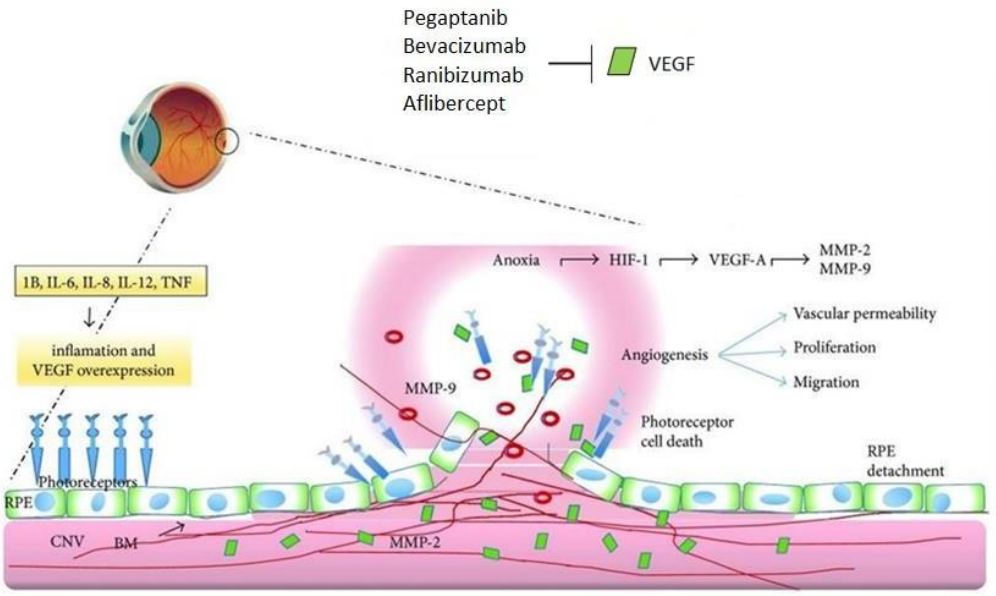

Figure 11: Wet AMD in which neovascularization from invading choroid vessels and the Bruch's membrane (BM) rupture causes photoreceptor damage. Besides, neovascularization of the retina ruptures the Bruch's membrane, which damages the macula and results in blurry or spotty vision. Anoxia and hypoxia-inducible factor 1 (HIF-1) induce the expression of VEGF-A and metalloproteinases 2 and 9 (MMP-2 and MMP-9). Additionally, Pagaptanib, Bevacizumab, Ranibizumab and Aflibercept could be used to block the angiogenic effects of VEGF (Hernández-Zimbrón L.F. *et al*., 2018).

Despite encouraging results in halting the disease and improving the vision, intravitreal injection of anti-VEGF agents may be associated with systemic adverse events and ocular complications (Falavarjani K.G. and Nguyen Q.D., 2013) such as endophthalmitis, intraocular inflammation, retinal detachment, elevated intraocular pressure and subretinal and vitreous hemorrhage. Many of these adverse events are more related to the mechanical action of intravitreal injection rather than to the drug-class (Modi Y.S. *et al*., 2015).

In eyes with neovascular AMD undergoing multiple anti-VEGF injections (Lois N. *et al*., 2013) reported progression of RPE atrophy in approximately 60% of eyes. However, it is impossible to distinguish if these events are a normal consequence of the natural course of the disease or they are caused by the anti-VEGF therapy.

Finally, VEGF is important for the growth of new blood vessels. Although the dose of anti-VEGF needed to treat eye diseases is very small, it has been shown to reduce the level of VEGF in the bloodstream. This means that there is a theoretical risk that, in adults, anti-VEGF drugs may increase the risk of cardiovascular disease, including heart attacks and strokes. However, clinical trials have not shown conclusive evidence of an increased risk of cardiovascular disease in patients

treated with anti-VEGF drugs compared to those given sham injections. In babies and young children, VEGF is essential for the growth of blood vessels and normal growth and development of many other organs including the lungs, kidney and brain. This is one of the reasons why anti-VEGF drugs are absolutely contraindicated in pregnancy.

2.8 AIMS

Intravitreal anti-VEGF therapy with drugs like Aflibercept and Ranibizumab has hugely improved the vision prognosis of neovascular AMD (Sreekumar P.G. *et al*., 2006; Kannan R. *et al*., 2006; Scott A.W. and Bressler S.B., 2013; Huo X. *et al*., 2015). However, it is not clear, up to date, if those agents could act as modulator of NO release, oxidative stress and apoptosis.

Thus, in the first part of the present study, we have planned to compare the effects of Aflibercept and Ranibizumab against oxidative stress in human RPE cell line (ARPE-19). In particular, we examined the involvement of NO, cell viability, mitochondrial function, proliferation and migration, apoptosis and activation/expression of various kinases involved in NO release and cell survival. Furthermore, various studies have demonstrated that in the early stages of the disease, the choroidal layer shows dramatic alterations in its composition (Bandello F. *et al*., 2017), and abnormal choroidal blood flow can be observed compared with healthy control eyes. This would suggest that choroidal vascular changes, such as decreasing density and diameter of the choriocapillaris, and intermediate-sized vessels, may be associated with aging and early stages of AMD (Bergen A.A. *et al*., 2018). The presence of abnormal choroidal circulation induces ischemia and hypoxia, which may trigger the development of angiogenesis, changes in the RPE and the formation of drusen (Boltz A. *et al*., 2010). Therefore, the normal interaction between RPE and choroidal endothelial cells appears critical for the maintenance of the outer-retina structure and function. For this reason, a better characterization of the homeostatic RPE-choroidal endothelial cell relationships could be of particular relevance. Thus, in the second part of the study, we have also conducted co-culture experiments between RPE cells and human umbilical vascular endothelial cells (HUVEC). It is suggested that co-culture systems are useful in evaluating the intercellular communication and composition of two different cell types. The choice of this cellular type is due to the key role of the choroid vasculature in the pathogenesis of AMD; furthermore, human choroidal endothelial cells are not of common use and are difficult to find. About this issue, it's to note that the choroidal endothelial cells used in previous studies are mainly isolated from bovine eyes. Moreover, the main cellular model used for the angiogenesis studies is represented by the HUVEC (Wang Y. *et al*., 2004; Schicht M. *et al*., 2017; Brandt M.M. *et al*., 2018)

Materials and methods

3.1 CULTURE OF RPE CELLS AND HUVEC

RPE cell line, was obtained from the American Type Culture Collection (ATCC; Rockville, Maryland, USA; catalog. no. CRL-2302^{TM}; ARPE-19; Figure 1A), and was maintained in Dulbecco's modified Eagle's medium (DMEM; Sigma, Milan, Italy) supplemented with 10% fetal bovine serum (FBS; Euroclone, Pero, Milan, Italy), 2 mM L-glutamine (Euroclone), 1% penicillin-streptomycin (P/S; Euroclone), at 37°C with 5% CO_2 in incubator.

Human umbilical vein endothelial cell line (HUVEC), was purchased from ATCC (catalog. no. CRL-1730^{TM}; Figure 1B), and was maintained in Kaighn's Modification of Ham's F-12 Medium (F-12K Medium; ATCC; catalog.no. 30-2004^{TM}), containing 2 mM L-glutamine, 1500 mg/L sodium bicarbonate, and supplemented with 0.1 mg/ml heparin (Sigma), 100 µg/ml endothelial cell growth supplement (ECGS; Sigma), 1% P/S, and 10% FBS.

When cells have reached confluence, the cell growth tends to stop and it is necessary to decrease their density. The culture medium was aspirated with vacuum pump, the plate was washed twice with sterile phosphate buffer saline (PBS; Sigma) 1X, which was then aspirated leaving the cells dry; 1 ml of Trypsin/ ethylenediaminetetraacetic acid (EDTA; Euroclone) solution was added and left to act for 3 min in an incubator to detach cells. Trypsin degrades the proteins of the cellular matrix that keep the cells connected each other, while the EDTA chelates magnesium (Mg^{2+}) and calcium (Ca^{2+}) which are essential for the adhesion to the plate: the combination of these two substances allows not only to detach the cells from the bottom of the plate, but also to separate them from each other. However, it must be remembered that trypsin is a specific hydrolase for Arginine (L-Arg) and Lysine (L-Lys) and does not discriminate between matrix proteins and membrane proteins, so if cells are left in trypsin for too long time, the enzyme will also digest membrane proteins, thus damaging cells. After 3 min, in order to verify if cells were detached, they have been observed by using optical microscope and then, complete growth medium was added to inhibit the action of the trypsin/EDTA. The cell suspension was centrifuged at 800 rpm for 5 min. After centrifugation, supernatant was removed and pellet resuspended by adding fresh complete medium and an appropriate aliquots of the cell suspension was added to a new 75 cm^2 culture flask (Sigma).

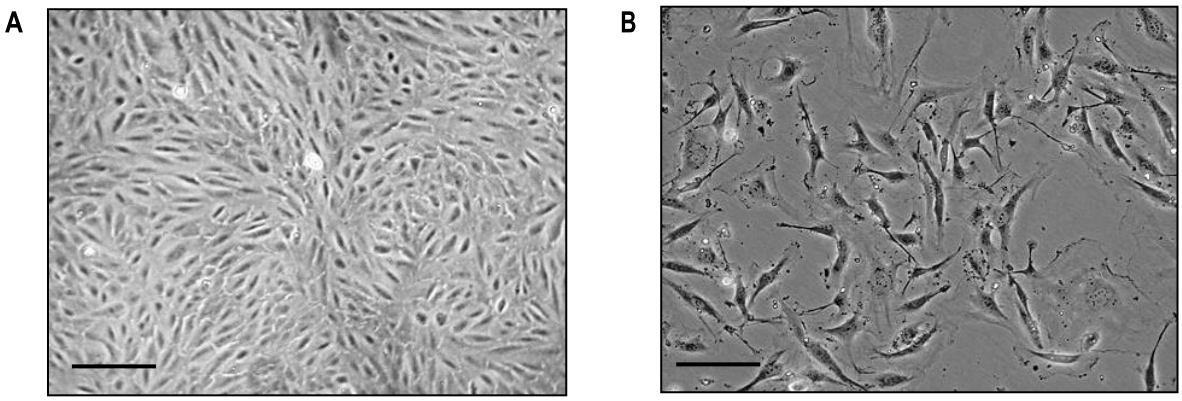

Figure 1: In A, retinal pigment epithelium (RPE) cells scale bar 50 µm. In B, human umbilical vein endothelial cells (HUVEC), scale bar 50 µm.

3.2 FIRST PART OF THE STUDY: EXPERIMENTS ON RPE AND HUVEC

3.2.1 Treatment with anti-VEGF drugs

RPE and HUVEC were treated with Aflibercept (0.025 mg/ml, 0.05 mg/ml, 0.2 mg/ml, 0.5 mg/ml; Novartis, Varese, Italy) or Ranibizumab (0.025 mg/ml, 0.05 mg/ml, 0.2 mg/ml; Bayer, Milan, Italy), at doses similar to the ones achievable in humans after intravitreal injection (Table 1). The clinical dose was calculated by assuming that the amount of intravitreally injected anti-VEGF agent was diluted equally throughout the 4 ml average volume of human vitreous, as previously performed in same cellular models (Malik D. *et al*., 2014; Kang S. *et al*., 2016; Weiyong S. *et al*., 2017). The corresponding molar concentrations of the anti-VEGF drugs doses used, are shown in Table 2.

Anti-VEGF drug	Clinical dose	Final concentration after intravitreal injection, in 4 ml of vitreous
Aflibercept	2 mg/ 0.05 ml	0.5 mg/ml
Ranibizumab	0.5 mg/ 0.05 ml	0.125 mg/ml

Table 1: Clinical doses of Aflibercept and Ranibizumab

Aflibercept	Molar concentration	Ranibizumab	Molar concentration
0.025 mg/ml	0.21 µM	0.025 mg/ml	0.52 µM
0.05 mg/ml	0.43 µM	0.05 mg/ml	1 µM
0.2 mg/ml	1.7 µM	0.2 mg/ml	4 µM
0.5 mg/ml	4 µM	-	-

Table 2: Molar concentrations of the two anti-VEGF drugs

3.2.2 Evaluation of nitric oxide release by using Griess Assay

Nitric oxide (NO) is an important physiological messenger and effector molecule in many biological systems, including immunological, neuronal and cardiovascular tissues. One tool to investigate nitric oxide formation is to measure nitrite (NO_2^-), which is one of the two primary, stable and non-volatile breakdown products of NO. The Griess Reagent System (Promega, Milan, Italy) is based on the chemical reaction shown in Figure 2, which uses sulfanilamide and N-1-napthylethylenediamine dihydrochloride (NED) under acidic (phosphoric acid) conditions.

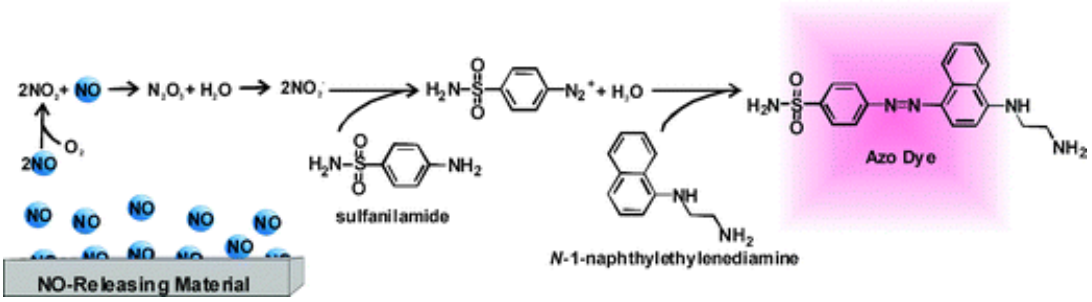

Figure 2: Chemical reactions involved in the measurement of NO^2, by using the Griess Reagent System (https://www.semanticscholar.org/paper/Nitric-oxide-release%3A-part-III.-Measurement-and-Coneski-Schoenfisch/4a96a285be5db3a74681e598a34b83e3754c70ff/figure/1)

The NO production was measured on RPE and HUVEC culture supernatants, by using the Griess method, as previously performed in same or similar cellular models (De Cillà S. *et al.*, 2017; Grossini E. *et al.*, 2014; 2015; 2016; Surico D. *et al.*, 2015). In RPE (7500 cells/well) plated in 96-well plate, and using culture medium without phenol red, a time-course and dose-response study was performed by treating cells with Aflibercept (0.025 mg/ml, 0.05 mg/ml, 0.2 mg/ml, 0.5 mg/ml) or Ranibizumab (0.025 mg/ml, 0.05 mg/ml, 0.2 mg/ml) for 5 min, 30 min, and 6 h.

In addition, in other experiments, both RPE (7500 cells/well) and HUVEC (7500 cells/well), were treated with Aflibercept (0.025 mg/ml, 0.05 mg/ml, 0.2 mg/ml, 0.5 mg/ml) or Ranibizumab (0.025 mg/ml, 0.05 mg/ml, 0.2 mg/ml) only for 30 min. Furthermore, the highest dose of the two anti-VEGF drugs (0.5 mg/ml for Aflibercept, and 0.2 mg/ml for Ranibizumab) was also administrated after 15 min pretreatment with the NOS blocker, Nω-nitro-L-arginine methylester (L-NAME; Sigma) 4 µM. Time and dose were chosen on the base of time-course and dose-response studies. In order to induce oxidative stress, in some samples, the effects on NO release of 200 µM hydrogen peroxide (H_2O_2), administrated 30 min after the anti-VEGF drugs, were also examined. Some samples were not stimulated and were used to obtain the baseline value (positive control). At the end of each treatment, 50 µl/well of supernatant was collected and transferred in a new plate in which, an equal volume of the reagents included in the kit, was added.

To ensure accurate NO_2^- quantification, a reference curve with the Nitrite Standard was prepared by using the known nitrite standard concentration (the range was 0-100 µM).

After preparing the straight line, 50 µl/well SULFAMIDE (1% sulfamide in 5% phosphoric acid) was added for 10 min, in all experimental samples. Likewise, 50 µl/well NED solution (0.1% N-1-naphthylethylenediamine) was added for 10 min, in all experimental samples in the absence of light because photosensitive. Finally, the absorbance (Abs) was read by a spectrophotometer (VICTOR™ X Multilabel Plate Reader; PerkinElmer; Waltham, Massachusetts, USA) with a filter between 520 nm and 550 nm.

This reading must be done within and no later than 30 min from the addition of the NED solution, because the compound formed is subject to decay, and the measurement would therefore be inaccurate. The value of each sample was quantified in respect to nitrite standard curve and expressed as nitrite production (µM). For dose-response and time-course study, data were normalized versus control cells. Experiments were conducted in triplicate and repeated at least five times.

3.2.3 Evaluation of cell viability by using MTT Assay

Cell viability was examined by using the 1% 3-[4,5-dimethylthiazol-2-yl]-2,5-diphenyl tetrazolium bromide (MTT; Life Technologies Italia, Monza, Italy) dye, as previously performed in same or similar cellular models (De Cillà S. *et al*., 2017; Grossini E. *et al.*, 2014; 2015; 2016; Surico D. *et al.*, 2015). This assay uses the reaction shown in Figure 3.

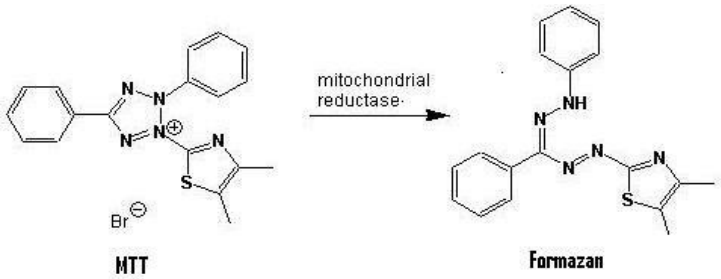

Figure 3: Chemical reaction happening when the MTT solution is added to the cells. The MTT is reduced by the mitochondria to form formazan crystals (https://www.researchgate.net/figure/Conversion-of-MTT-to-formazan-by-NADH-dependent-reductases_fig36_265025671)

MTT is reduced by metabolically active cells to insoluble purple formazan dye crystals. Formazan is a chromogen that absorbs at a wavelength of 570 nm; its production is catalyzed by the mitochondrial enzyme dehydrogenase. The rate of tetrazolium reduction is proportional to the rate of cell viability.

The experimental protocol was the same used for Griess assay, but using 10 000 cells/well in 96-well plate. After each treatment, the medium was removed, and 50 µl/well fresh culture medium without red phenol and FBS but with MTT dye, was added in 96-well plate containing the cells, and incubated for 2 h at 37°C. Thereafter, the medium was removed, and an MTT solubilization solution (dimethyl sulfoxide; DMSO, Sigma) in equal volume to the original culture medium was added and mixed until the complete dissolution of formazan crystals. Cell viability was determined by measuring the absorbance through a spectrophotometer (VICTOR™ X Multilabel Plate Reader; PerkinElmer) with a wavelength of 570 nm and cell viability was calculated by setting control cells as 100%. Experiments were conducted in triplicate and repeated at least five times.

3.2.4 Evaluation of mitochondrial membrane potential by using JC-1 Assay

Variation in mitochondrial membrane potential (ΔψM) is an important parameter of mitochondrial function and is an indicator of cell health. Mitochondrial membrane potential was measured in RPE by using 5,51,6,61-tetrachloro-1,11,3,31tetraethylbenzimidazolyl carbocyanine iodide (JC-1; Cayman, Ann Arbor, Michigan, USA), as previously performed in same or similar cellular models (De Cillà S. *et al*., 2017; Grossini E. *et al.*, 2014; 2015; Surico D. *et al.*, 2015). JC-1 is able to enter the mitochondria and change its fluorescent properties based on the aggregation probe. In healthy cells with high ΔψM, JC-1 forms complexes known as J-aggregates with intense red fluorescence. However, in cells with low ΔψM, JC-1 remains in the monomeric form, which exhibits green fluorescence. The higher the ratio of red to green fluorescence, the higher the polarization of the mitochondrial membrane is.

RPE (10 000 cells/well in 96-well plate), were treated with Aflibercept (0.025 mg/ml, 0.05 mg/ml, 0.2 mg/ml, 0.5 mg/ml) or Ranibizumab (0.025 mg/ml, 0.05 mg/ml, 0.2 mg/ml) for 30 min, in the presence/absence of 4 µM L-NAME administrated 15 min before Aflibercept (0.5 mg/ml) or Ranibizumab (0.2 mg/ml). Experiments were also conducted in peroxidative conditions, stimulating cells with 200 µM H_2O_2, administrated 30 min after the anti-VEGF drugs. After stimulations, the medium of cells was removed and cells were incubated with JC-1 diluted in Assay Buffer 1X for 15 min at 37°C, following the manufacturer's instruction. After incubation, cells were washed twice with Assay Buffer 1X and then the mitochondrial membrane potential was determined by measuring the red (excitation 535 nm/emission 595 nm) and green (excitation 485 nm/emission 535 nm) fluorescence through a spectrophotometer (VICTOR™ X Multilabel Plate Reader, PerkinElmer). The ratio of fluorescence intensity of J-aggregates to fluorescence intensity of monomers can be used as an indicator of cell health. The data were normalized versus control cells. Experiments were conducted in triplicate and repeated at least five times.

3.2.5 Proliferation rate by using xCELLigence

To evaluate the effects of anti-VEGF drugs on cell proliferation, xCELLigence™ MP Instrument (Roche, Basel, Switzerland) was used as previously performed (De Cillà S. *et al*., 2017). The system measures the electrical impedance across interdigitated microelectrodes integrated at the bottom of E-plates. The measurement of impedance provides quantitative information about the biological status of the cells, including cell proliferation in real time. The relative change in the electrical impedance is displayed by the system as arbitrary units called the Cell Index, which is proportional to the number and pattern of attached cells. RPE (3000 cells/well) plated in 16-well plate (E-Plate; Acea Bioscences, Inc.; San Diego, California, USA), were stimulated with Aflibercept (0.5 mg/ml) or Ranibizumab (0.2 mg/ml) alone, or in the presence of 200 µM H_2O_2 in order to induce oxidative stress. First, the background impedance was measured according to manufacturer´s instructions with 100 µl standard medium. Subsequently, 100 µl cell suspension was added in triplicate to the appropriate wells. After equilibration to 37°C, plates were inserted into the xCELLigence station and the base-line impedance was measured to ensure that all wells and connections were working within acceptable limits. The software automatically informs the researcher if any connection problems arise. The proliferation rate, determined by the Cell Index, was analyzed after 12 h, 24 h and 48 h from the anti-VEGF agents administration. The Cell Index at each time point is defined as (Rn-Rb)/15, where Rn is the cell-electrode impedance of the well when it contains cells and Rb is the background impedance of the well with the media alone. Having measured the impedance curves of these cell lines, we calculated the slope of the curves starting from the minimum Cell Index value after an initial cell adhesion phase, to the maximum of the Cell Index curve. The data were analyzed with real-time cell analysis (RTCA) software, which includes real-time data display and analysis functions. Experiments were conducted in triplicate and repeated at least five times.

3.2.6 Wound-healing migration assay

Cell migration was evaluated by the *in vitro* scratch assay. In 24-well plate, 25 000 cells/well were seeded and cultured in starvation medium (DMEM without FBS, in order to prevent false positives) to reach a confluent monolayer. Cell monolayers were then mechanically scratched with a sterile yellow tip (diameter = 2 mm) along the center of the plate and cell debris were removed by gentle wash with PBS. Some samples were treated with Aflibercept (0.025 mg/ml and 0.5 mg/ml) or Ranibizumab (0.025 mg/ml and 0.2 mg/ml) and incubated at 37°C in a humidified atmosphere containing 5% CO_2 for maximum 48 h. Images of cell monolayers were taken using an optical microscope (Leica ICC50HD) with a digital camera to evaluate wound closure. Migration was

quantified by calculating the area of wound at time points T0 (time of wound), T24 (24 h after wound) and T48 (48 h after wound) by using ImageJ software (National Institutes of Health, Bethesda, MA, USA). For each condition, the percentage of wound closure at several time points throughout the course of the assay, was obtained through the formula:

% wound closure: [WA_0-WA/ WA_0]*100, where WA= wound area and WA_0=original size of the wound area. Experiments were conducted in triplicate and repeated at least five times.

3.2.7 ROS quantification by using DCFDA-Cellular ROS Detection Assay kit

The DCFDA-Cellular Reactive Oxygen Species (ROS) Detection Assay Kit (Abcam, Cambridge, United Kindom), quantitatively measures ROS in cells by using a microplate assay. The assay uses the cell permeant reagent 2',7'-dichlorofluorescin diacetate (DCFDA), a fluorogenic dye that measures hydroxyl, peroxyl and other ROS activity within the cell. After diffusion into the cell, DCFDA is deacetylated by cellular esterases to a non-fluorescent compound, which is later oxidized by ROS into 2',7'dichlorofluorescein (DCF), a highly fluorescent compound which can be detected by spectrophotometer (Figure 4).

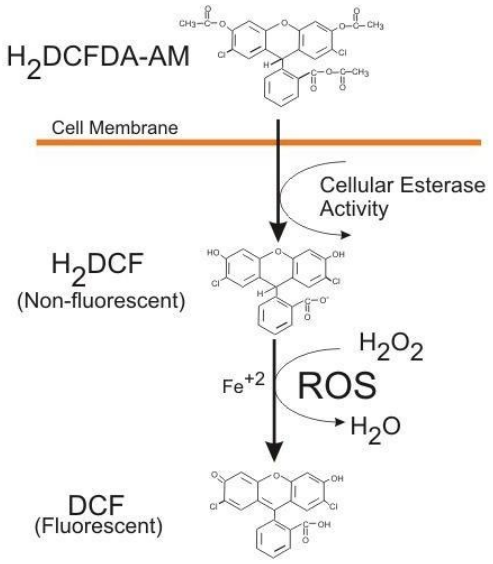

Figure 4: Formation of fluorescent compound DCF by ROS (https://www.abcam.com/dcfda--h2dcfda-cellular-ros-assay-kit-ab113851.html)

For the experiments, 25 000 cells/well in 96-well plate were plated and stimulated with 30 min 200 µM H_2O_2 alone or in the presence of Aflibercept (0.025 mg/ml, 0.05 mg/ml, 0.2 mg/ml, 0.5 mg/ml, for 30 min) or Ranibizumab (0.025 mg/ml, 0.05 mg/ml, 0.2 mg/ml, for 30 min). After treatments, the reactions were stopped by removing medium and washing with PBS followed by staining with 10 µM DCFDA for 20 min at 37°C, following the manufacturer's instructions and as

previously performed (De Cillà S. *et al*., 2017; Grossini E. *et al*., 2015; 2018; Surico D. *et al*., 2017). The fluorescence intensity of DCF was measured by using a spectrophotometer (VICTOR™ X Multilabel Plate Reader; PerkinElmer), with maximum excitation and emission spectra of 495 nm and 570 nm, respectively. The amount of intracellular ROS was proportional to the intensity of DCF fluorescence, and the fluorescence intensity was recorded directly to indicate the relative amount of ROS. Results were expressed as DCF fluorescence intensity, which is proportional to the amount of intracellular ROS Experiments were conducted in triplicate and repeated at least five times.

3.2.8 Apoptosis assay by using Annexin V, FITC Apoptosis Detection Kit

Apoptotic cells were determined by using flow cytometry with Annexin V, FITC Apoptosis Detection Kit (NBS Biologicals; Huntingdon, UK). During early induction of apoptosis, cells translocate the membrane phosphatidylserine (PS) from the inner face of the plasma membrane to the cell surface. Once on the cell surface, PS can be easily detected by staining with a fluorescent conjugate of Annexin V, a protein-dependent Ca^{2+} ion, that has a high affinity for PS (Figure 5).

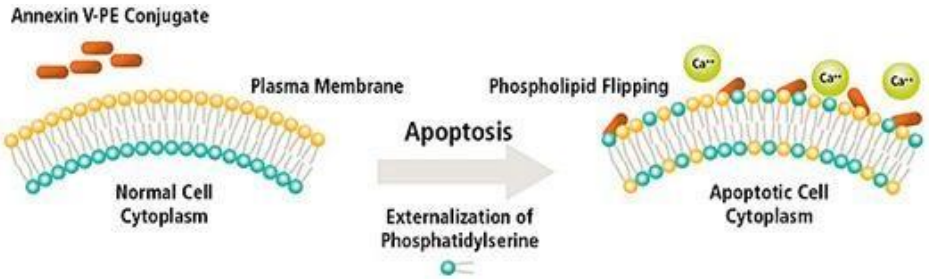

Figure 5: How Annexin V staining detects apoptosis (http://bdbiosciences. com/kr/instruments/accuri/ a rticles/archive/2015_02/index.jsp)

The kit can differentiate apoptosis vs necrosis performing both Annexin V-FITC and propidium iodide (PI) staining (an impermeable dye excluded from cells with an intact membrane). For the experiments, 300 000 cells/well in 6-well plate were plated and stimulated with 6 h 200 µM H_2O_2 alone or in the presence of Aflibercept (0.025 mg/ml and 0.5 mg/ml, for 6 h) and Ranibizumab (0.025 mg/ml and 0.2 mg/ml, for 6 h). After treatments, the reactions were stopped by removing medium and washing with PBS. Cells were detached with trypsin-EDTA thereafter, an appropriate volume of culture medium was added and cell suspension was transferred to a tube and centrifuged at 1000 rpm for 3 min. After centrifuged, supernatant was removed and 1 ml Annexin V Binding Solution was added to make a final concentration of $1*10^6$ cells/ml. Thereafter, 100 µl of this cell suspension was transferred to a new tube and 5 µl Annexin V, FITC Conjugate and 5 µl PI Solution

were added and incubated for 15 min at room temperature with protection from light. Annexin V Binding Solution (400 µl) was added, and the analysis was performed by using Attune NxT (Life Technologies). The results were interpreted as follow: cells that were Annexin V(-)/PI(-) (lower left quadrant) were considered as living cells; Annexin V(+)/PI(-) (lower right quadrant) as apoptotic cells; Annexin V(+)/PI(+) (upper right quadrant) as a necrotic cells; and Annexin V (-)/PI(+) (upper left quadrant) may be bare nuclei, cells in late necrosis or cellular debris, as shown in Figure 6. Experiments were conducted in triplicate and repeated at least five times.

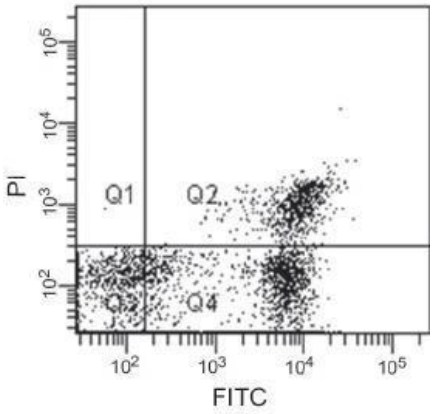

Figure 6: Flow cytometric analysis of apoptosis. Q1 is Annexin V(-)/PI(+); Q2 is Annexin V(+)/PI(+); Q3 is Annexin V(-)/PI(-); Q4 is Annexin V(+)/PI(-)(https://www.nbsbio.co.uk).

3.2.9 Cell lysates

In order to extract proteins, 400 000 cells/well in 6-well plate, were plated overnight at 37°C with 5% CO_2. Western blot analysis was performed on RPE treated with Aflibercept (0.5 mg/ml, for 6 h) or Ranibizumab (0.2 mg/ml, for 6 h) in the presence or absence of 200 µM H_2O_2 administrated 6 h after the anti-VEGF drugs. At the end of stimulations, the plate was kept on ice for all steps in order to block the reaction. Therefore, RPE were lysed by adding 200 µl iced-Ripa-buffer (Table 3) supplemented with 1 mM phenylmethanesulfonyl fluoride (PMSF; Sigma), 2 mM sodium orthovanadate (Na_3VO_4; Sigma) and protease inhibitor cocktail (1 mM; Thermo Fisher Scientific, Waltham, MA, USA). Using a cell scraper, cells were scraped and the lysate was transferred to a 1.5 ml vial. The lysates were centrifuged at 14 000 rpm for 20 min at 4°C. The supernatants were collected into new microtubes. In each sample, the protein concentration was determined by the bicinchoninic acid (BCA) method (De Cillà S. *et al*., 2017; Surico D. *et al.*, 2015; Grossini E. *et al*., 2014; 2015; 2018).

50 mM	Tris-Hcl, pH 7.4
0.1%	sodium dodecyl sulfate (SDS)
0.1%	Tergitol (NP-40)
150 mM	Sodium Chloride (NaCl)
1 mM	Ethylenediaminetetraacetic acid (EDTA)
50 mM	Sodium Fluoride (NaF)

Table 3: Recipe Ripa lysis buffer

3.2.10 Bicinchoninic acid (BCA) assay

The "Pierce® BCA Protein Assay Kit" (Pierce, Rockford, IL, USA) can be set up to measure the concentration of the unknown protein sample (mg/ml), starting from protein standard (Bovine Serum Albumin; BSA) solution. The principle of the BCA assay is based on the formation of a Cu^{2+} protein complex under alkaline conditions, followed by reduction of the Cu^{2+} to Cu^{1+}. The amount of reduction is proportional to the protein present. It has been shown that cysteine, tryptophan, tyrosine, and the peptide bond are able to reduce Cu^{2+} to Cu^{1+}. BCA forms a purple-blue complex with Cu^{1+} in alkaline environments, thus providing a basis to monitor the reduction of alkaline Cu^{2+} by proteins (Biuret reaction). The protein concentration was calculated by interpolation of the absorbance values with the standard BSA curve.

3.2.11 Western blotting

Protein extracts, quantified with BCA method, were dissolved in Laemmli buffer 5X and boiled 5 min at 95°C, and thereafter 30 µg of each sample were loaded onto sodium dodecyl sulfate polyacrylamide gel electrophoresis (SDS-PAGE) 8-12% gel. After electrophoresis (180 V for about 1.30 h), proteins were transferred to polyvinylidene fluoride (PVDF; Sigma) membranes, activated in 100% methanol (Sigma) and washed with Transfer Buffer (25 mM Tris-Cl, 192 mM glycine, with 20% methanol). After proteins transfer, the PVDF membranes were blocked in Tris Buffer Saline 1X (TBS; 50 mM Tris-Cl pH 7.5, 50 mM NaCl) + 0.1% Tween 20 + 5% BSA at room temperature for 30 min. After this, membranes were incubated overnight at 4°C with specific primary antibodies (listed in Table 4):

Primary antibodies	Diluition	Source
Ab anti phospho-Akt	1:1000 in TBS 1X, 0.1% Tween and 5% BSA	Santa Cruz Biotechnology
Ab anti Akt	1:1000 in TBS 1X, 0.1% Tween and 5% BSA	Santa Cruz Biotechnology
Ab anti phospho-ERK1/2	1:1000 in TBS 1X, 0.1% Tween and 5% BSA	Cell-Signalling Technologies
Ab anti phospho-eNOS	1:1000 in TBS 1X, 0.1% Tween and 5% BSA	Cell-Signalling Technologies
Ab anti eNOS	1:1000 in TBS 1X, 0.1% Tween and 5% BSA	Cell-Signalling Technologies
Ab anti iNOS	1:1000 in TBS 1X, 0.1% Tween and 5% BSA	Santa Cruz Biotechnology
Ab anti Cleaved Caspase 9	1:1000 in TBS 1X, 0.1% Tween and 5% BSA	Santa Cruz Biotechnology
Ab anti Cytochrome C	1:1000 in TBS 1X, 0.1% Tween and 5% BSA	Santa Cruz Biotechnology
Ab anti β-actin	1:5000 in TBS 1X, 0.1% Tween and 5% BSA	Santa Cruz Biotechnology

Table 4: Primary antibodies used for Western blot analysis on RPE cells

Membranes were washed in 1X TBS 0.1% Tween 20 and then incubated with horseradish peroxidase-coupled goat anti-rabbit IgG (Sigma), or horseradish peroxidase-coupled goat anti-mouse IgG (Sigma) for 45 min. Next, signal was developed through a non-radioactive method using Western Lightning Chemiluminescence (PerkinElmer Life and Analytical Sciences, Waltham, MA, USA). Quantity of chemiluminescence was detected using ChemiDoc™ Imaging System (Bio-Rad, Hercules, California, USA) and data were analyzed with Image Lab™ Softwer (Bio-Rad). Phosphorylated protein expression was calculated as a ratio towards specific total protein expression or β-actin detection.

3.3 SECOND PART OF THE STUDY: EXPERIMENTS ON CELL CO-CULTURE MODEL

The culture of one cell type (monoculture) presents some limitations, since the interaction with other cell types cannot be considered. Consequently, the monoculture model does not mimic the real multicellular interaction during the progression of the disease. Simultaneous co-culture is a system where two cell types are seeded together and allows the study of cell-to-cell interactions. This approach reproduces more accurately cell connections observed in the *in vivo* microenvironment. The development of more complex and sophisticated co-culture models, can reproduce more accurately the intercellular interactions and the biochemical response. To investigate whether HUVEC, stimulated with anti-VEGF drugs, have protective effects against oxidative stress on RPE, and can have effects on NO release, proliferation, migration, viability, apoptosis and mitochondrial membrane potential, we co-cultured RPE with HUVEC by using Transwell inserts (Life Science; Gerenzano, Milan, Italy, and ACEA Bioscience) (Figure 7). Experiments were performed both in physiological and peroxidative conditions. Cell and tissue culture techniques are becoming increasingly important for basic and applied life science research. The development of new culture vessels and cell attachment substrates is currently being driven by the need to produce an environment that resembles the *in vivo* state as closely as possible to enable the growth of specialized cell types. Consequently, using permeable supports with microporous membranes has become a standard method for culturing these cells. These permeable supports have allowed significant improvements in culturing polarized cells since these permeable supports permit cells to uptake and secrete molecules on both their basal and apical surfaces and thereby carry out metabolic activities in a more natural fashion. In Table 5, the characteristics of the Transwell inserts which were used, are shown.

Multiple well plate	96-well insert	24-well insert	6-well insert	E-plate insert 16
Company	Life Science	Life Science	Life Science	ACEA Biosciences
Membrane material	polyester	polyester	polyester	polyester
Membrane thickness	10 µm	10 µm	10 µm	10 µm
Collagene treated	no	no	no	no
Cell visibility	good	good	good	good
Optical properties	clear	clear	clear	clear
Transwell insert diameter	4.26 mm	6.5 mm	24 mm	4.26 mm
Insert membrane growth area	0.143 cm^2	0.33 cm^2	4.67 cm^2	0.143 cm^2
Pore size	0.4 µm	0.4 µm	0.4 µm	0.4 µm
Pore density	$4*10^6$ pores/cm^2	$4*10^6$ pores/cm^2	$4*10^6$ pores/cm^2	$4*10^6$ pores/cm^2
Volume added per plate well	0.235 ml	0.6 ml	2.6 ml	0.235 ml
Volume added to inside of Transwell insert	0.075 ml	0.1 ml	1.5 ml	0.075 ml

Table 5: Characteristics of Transwell inserts

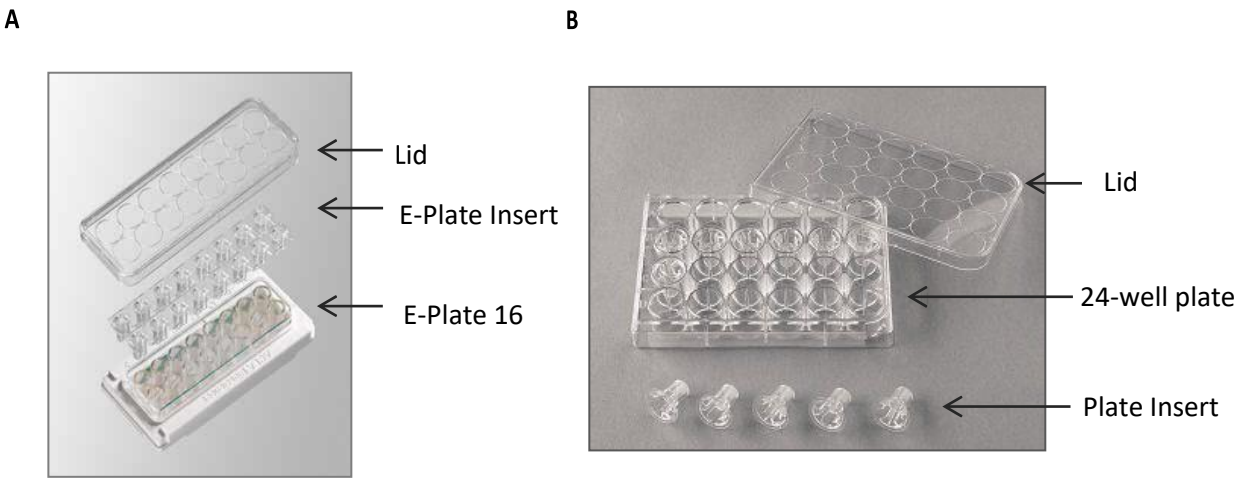

Figure 7: In A, an example of E-Plate Insert in combination with the E-Plate 16. In B, an example of Insert in combination with the 24-well plate

For co-culture experiments, HUVEC were plated in the apical compartment of the insert while, RPE cells, were plated in the basal compartment. Transwell inserts were used by first adding medium to the multi-well plate, followed by adding the Transwell inserts, and lastly adding the medium and cells to the inside compartment. An initial equilibrium period may be used to improve cell attachment. The plate should then be incubated for at least one hour at the same temperature that will be used to grow the cells. The cells are then added in fresh medium to the Transwell insert and returned to the incubator over-night. Next day, HUVEC were stimulated with Aflibercept

(0.025 mg/ml and 0.5 mg/ml, for 30 min) or Ranibizumab (0.025 mg/ml and 0.2 mg/ml, for 30 min). In addition, in some experiments, Aflibercept (0.5 mg/ml) or Ranibizumab (0.2 mg/ml) were also given after pre-treatment with the NOS inhibitor, L-NAME (4 μM, for 15 min; Sigma), the p38 MAPK inhibitor, SB203580 (4 μM, for 30 min; Sigma), the phosphatidylinositol 3′-kinase (PI3K) inhibitor, wortmannin (4 μM, for 15 min; Sigma), or the MAPK/ERK inhibitor, UO126 (4 μM, for 15 min; Sigma). After the treatment, medium was changed and new completed fresh medium was added for 24 h, in order to give the HUVEC time to induce any responses from the RPE cells. Next day, using a sterile forceps, all Transwell inserts were removed, and some samples of RPE cells were treated with 200 μM H_2O_2, in order to induce oxidative stress. At the end of stimulations, various assays were performed as described above (Figure 8).

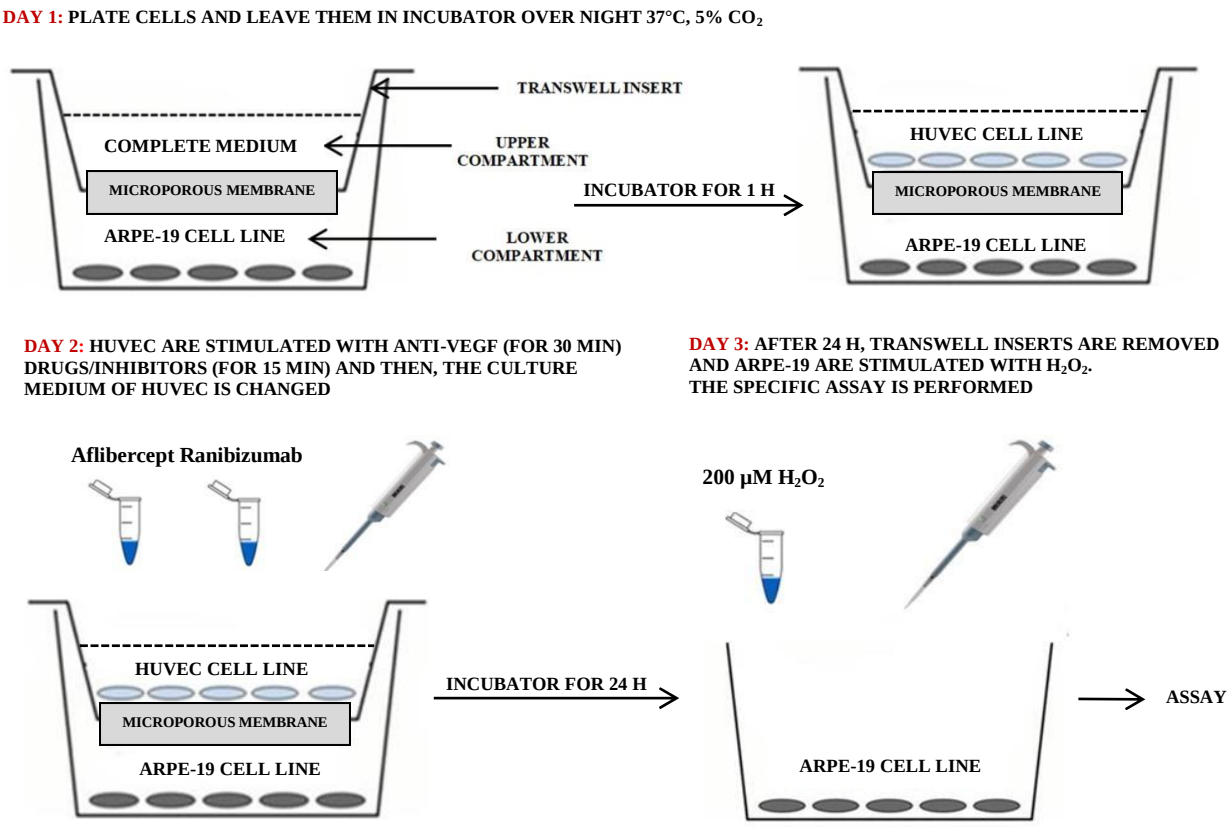

Figure 8: Schematic representation of experimental models, is shown

3.3.1 Evaluation of NO release, cell viability, mitochondrial membrane potential and ROS production in RPE cells

NO release (Griess assay), cell viability (MTT assay), mitochondrial membrane potential (JC-1 assay), and ROS production (DCFDA-Cellular ROS Detection Assay Kit), were measured in RPE, co-cultured with HUVEC, by following the manufacturer´s instructions as described in paragraphs

3.2.2, 3.2.3, 3.2.4, and 3.2.7. For co-culture, HUVEC (7500 cells/insert in 96-Transwells plate for Griess assay, and 10 000 cells/insert in 96-Transwell plate for MTT and JC-1 methods), were stimulated with Aflibercept (0.025 mg/ml and 0.5 mg/ml, for 30 min) or Ranibizumab (0.025 mg/ml and 0.2 mg/ml, for 30 min). Another pool of cells was treated with Aflibercept (0.5 mg/ml, for 30 min) and Ranibizumab (0.2 mg/ml, for 30 min), after pre-treatment with various inhibitors, as described above. After stimulations, medium was changed and new F-12K medium was added for 24 h. Next day, each Transwell insert was removed and some RPE samples (7500 cells/well in 96-Transwell plate for Griess assay and 10 000 cells/well in 96-Transwell plate for MTT and JC-1 assays) were treated with for 30 min, in order to induce oxidative stress (Figure 9). Finally, the absorbance (as specified in previous paragraphs) was read by using a spectrophotometer (VICTOR™ X Multilabel Plate Reader; PerkinElmer).

For ROS production (25 000 HUVEC cells/insert in 96-Transwell plate and 25 000 RPE cells/well in 96-Transwell plate), the same experimental protocol was used but in the absence of inhibitors (Figure 10). Experiments were conducted in triplicate and repeated at least five times.

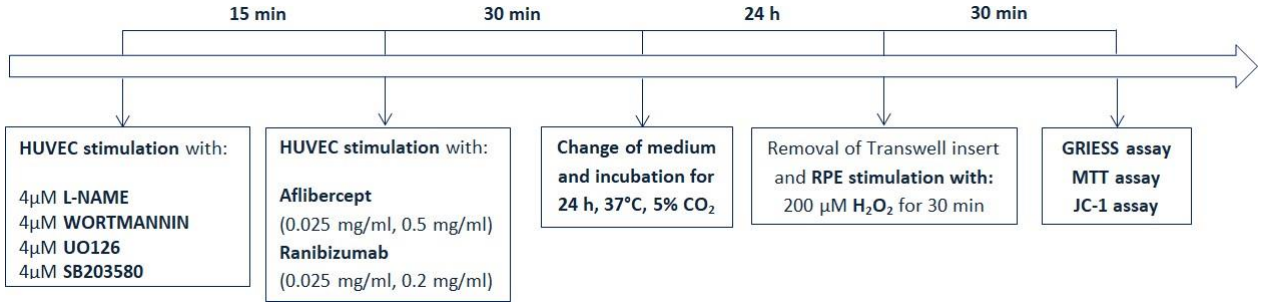

Figure 9: The Flowchart shows a schematic representation about the co-culture experiments performed by using Griess, MTT and JC-1 methods

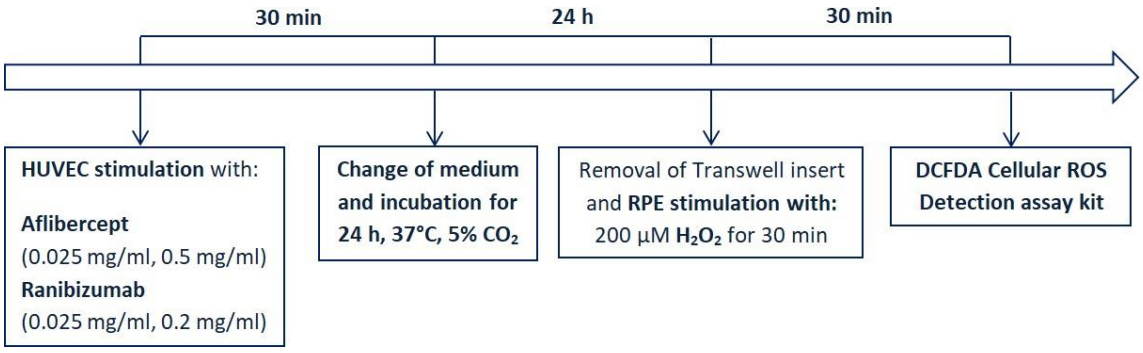

Figure 10: The Flowchart shows a schematic representation about the co-culture experiments performed by using DCFDA-Cellular ROS Detection Assay Kit

3.3.2 Evaluation of cell proliferation in RPE cells

Cell proliferation (xCELLigence), was measured in RPE, co-cultured with HUVEC, by following the manufacturer´s instructions as described in paragraph 3.2.5. For co-culture, HUVEC (3000 cells/insert in 16-well E-plate) were stimulated with Aflibercept (0.5 mg/ml, for 30 min) or Ranibizumab (0.2 mg/ml, for 30 min). After stimulations, the medium of HUVEC was changed and new F-12K medium was added. In the same time, in order to induce peroxidation, some RPE samples were treated with 200 µM H_2O_2, and left to act all the time of the analysis. The proliferation rate, determined by the Cell Index, was analyzed at 12 h, 24 h and 48 h (Figure 11). Experiments were conducted in triplicate and repeated at least five times.

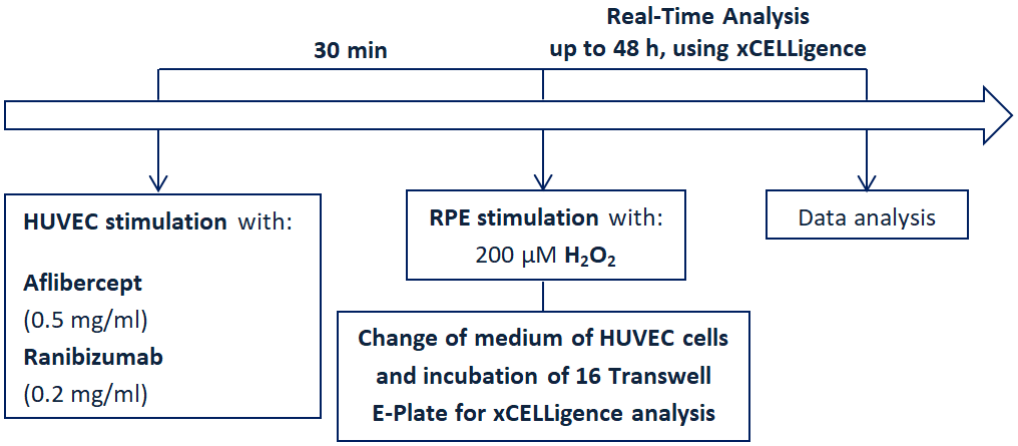

Figure 11: The Flowchart shows a schematic representation about the co-culture experiments performed by using xCELLigence

3.3.3 Evaluation of cell migration in RPE cells

Cell migration (wound-healing assay), was measured in RPE cells, co-cultured with HUVEC, by following the manufacturer´s instructions as described in paragraph 3.2.6. For co-culture, HUVEC (25 000 cells/insert in 24-Transwell plate) were stimulated with Aflibercept (0.025 mg/ml and 0.5 mg/ml, for 30 min) or Ranibizumab (0.025 mg/ml and 0.2 mg/ml, for 30 min), in the presence or absence of the NOS inhibitor, L-NAME (4 µM for 15 min before anti-VEGF drugs). After stimulations, RPE cell monolayers were mechanically scratched, and in the same time, the medium of HUVEC was changed and new F-12K medium was added. Cells were then incubated for a maximum of 48 h. The migration rate, at time points T0 (time of wound), T24 (24 h after wound), and T48 (48 h after wound) was analyzed (Figure 12). Experiments were conducted in triplicate and repeated at least five times.

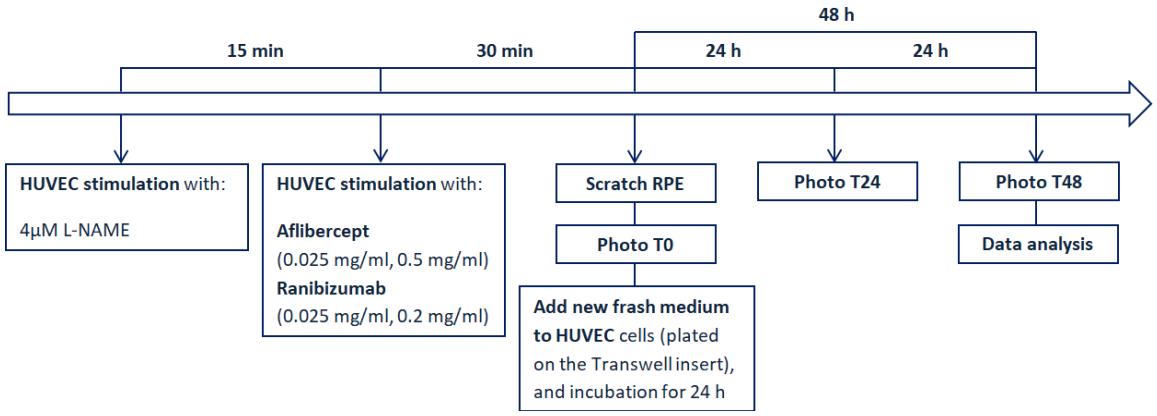

Figure 12: The Flowchart shows a schematic representation about the co-culture experiments performed for migration analysis

3.3.4 Evaluation of protein expression/activation in RPE cells

Protein expression/activation, was evaluated by Western blot in RPE cells, co-cultured with HUVEC, by following the manufacturer´s instructions as described in paragraphs 3.2.9, 3.2.10, 3.2.11. For co-culture, HUVEC (400 000 cells/insert in 6-Transwell plate) were stimulated with Aflibercept (0.5 mg/ml, for 30 min) or Ranibizumab (0.2 mg/ml, for 30 min). After stimulations, medium was changed and new F-12K medium was added for 24 h. Next day, each Transwell insert was removed, and some RPE samples (400 000 cells/well in 6-Transwell plate) were treated with 200 µM H_2O_2 for 6 h, in order to induce peroxidation.

In order to confirm the data obtained on NO release, the activation/expression of NOS isoforms, were investigated, in physiological and peroxidative conditions. To study the role of anti-VEGF drugs on cell cycle, the expression of the cyclin-dependent kinase inhibitor p21, which activates cell cycle check-points by inhibiting cyclin/cdk, was analyzed, in physiological and peroxidative conditions. Furthermore, in order to study the involvement of Aflibercept and Ranibizumab, in the process of apoptosis under peroxidative condition, the expression of Cleaved Caspase 9 and Cytochrome C, was evaluated. Finally, the effect of anti-VEGF on the activation of Akt and ERK1/2, kinases implicated in the cell survival mechanism, was further investigated, in physiological and peroxidative conditions. The studies were conducted on RPE cells treated with anti-VEGF drugs, in the presence or absence of 200 µM H_2O_2. Experiments were conducted in triplicate and repeated at least five times (Figure 13).

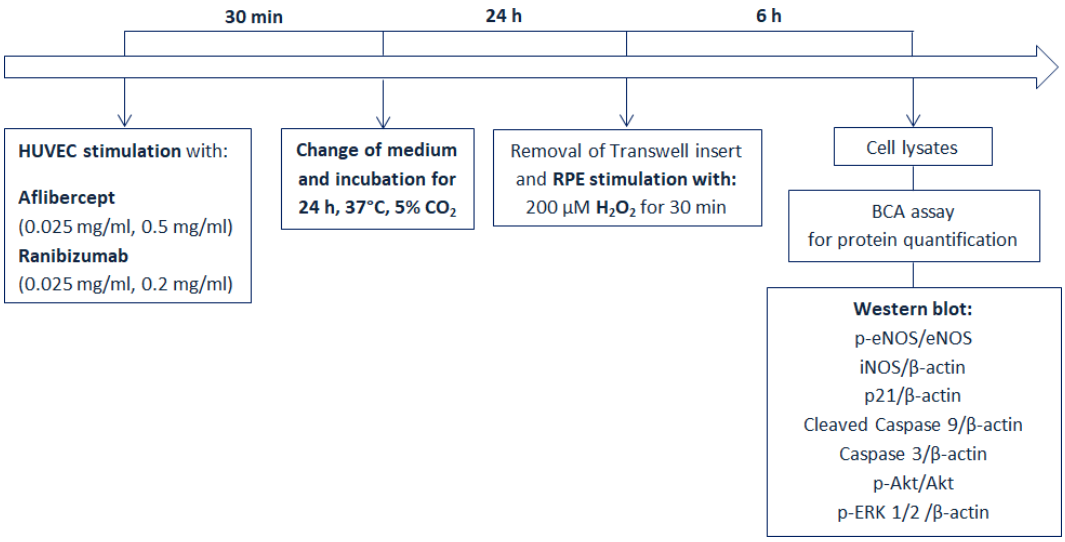

Figure 13: The Flowchart shows a schematic representation about the co-culture experiments performed for Western blot analysis

3.4 STATISTICAL ANALYSIS

All data were recorded using the Institution's database. Statistical analysis was performed by using STATVIEW version 5.0.1 for Microsoft Windows (SAS Institute Inc., Cary NC, USA). Data were checked for normality before statistical analysis. All the results obtained were examined through one-way ANOVA followed by Bonferroni post hoc tests. The non-parametric Mann Whitney U test for unpaired data was used to compare percentage responses. All data are presented as means ± standard deviation (SD) of five independent experiments for each experimental protocol. A value of $P < 0.05$ was considered statistically significant.

Results

4. FIRST PART OF THE STUDY: RESULTS ON RPE CELLS AND HUVEC

4.1 Effects of Aflibercept and Ranibizumab on NO release

4.1.1 Dose-and time-response effects of anti-VEGF agents on NO release in RPE cells by using the Griess assay

The effects of anti-VEGF agents on NO release, were analyzed by a dose-response study (also called "grading"), as shown in Figure 1, and a time-course study, as shown in Figure 2. In particular the results obtained with different concentrations of Aflibercept (0.025 mg/ml, 0.05 mg/ml, 0.2 mg/ml, 0.5 mg/ml) or Ranibizumab (0.025 mg/ml, 0.05 mg/ml, 0.2 mg/ml), are shown in Figure 1. While, the release of NO caused by 5 min, 30 min, and 6 h Aflibercept and Ranibizumab, is shown in Figure 2.

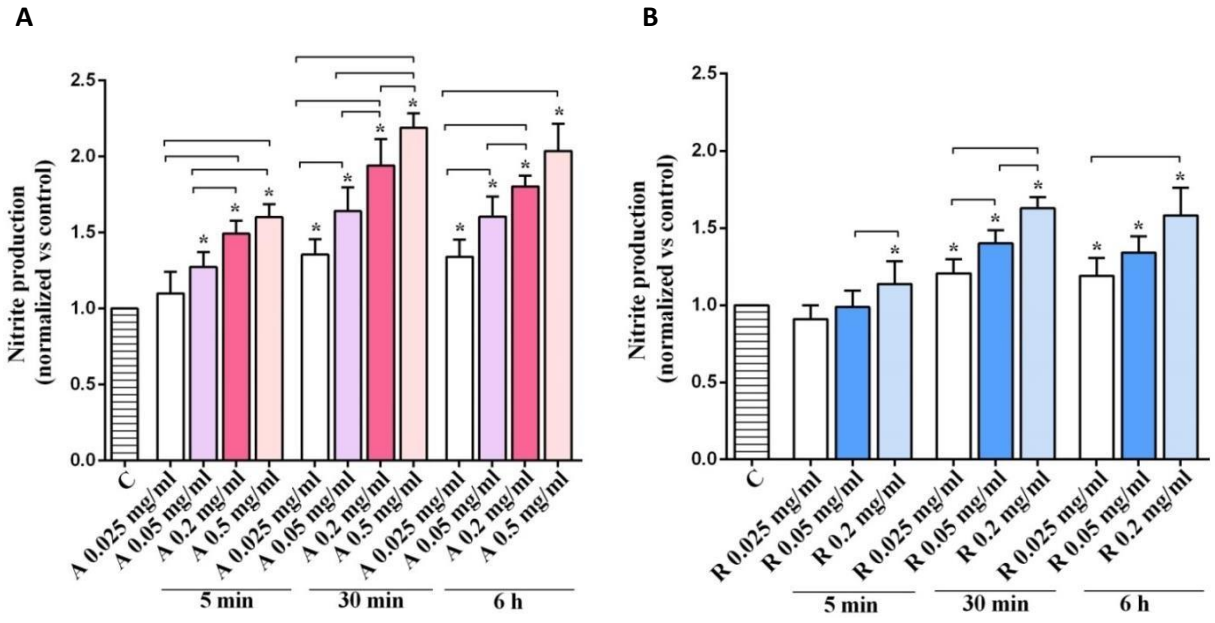

Figure 1: Dose-response effects of anti-VEGF agents on NO release in RPE cells. In A, Aflibercept (A), in B, Ranibizumab (R). C=Control (untreated cells). The data were normalized versus control cells. Reported data are means ± SD of five independent experiments. Significance between groups: *P<0.05 vs C. Short square brackets indicate significance between groups (P<0.05).

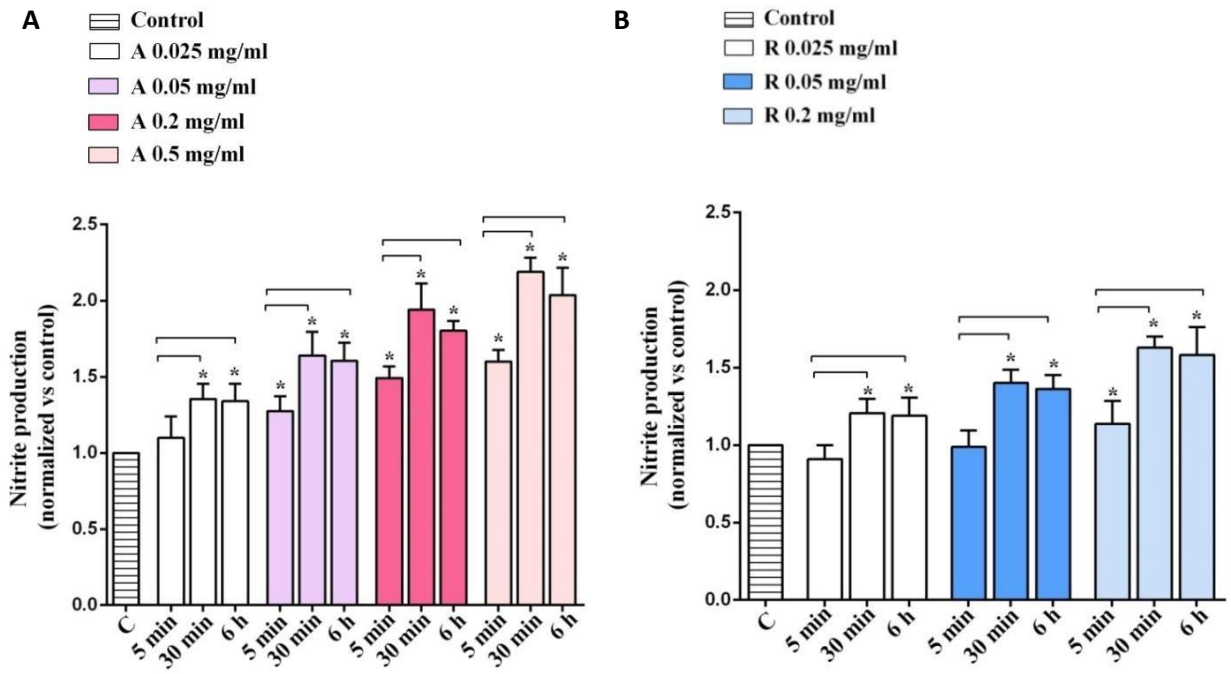

Figure 2: Time-course effects of anti-VEGF agents on NO release in RPE cells. In A, Aflibercept, in B, Ranibizumab. Abbreviations are as in Figure 1. Data were normalized versus control cells. Reported data are means ± SD of five independent experiments. Significance between groups: *P<0.05 vs C. Short square brackets indicate significance between groups (P<0.05).

As illustrated in Figure 1A, for each stimulation time, a general dose-dependent increase of NO release, induced by Aflibercept, was observed. Similar findings were observed with Ranibizumab, but with a dose-dependent increase of NO release, less marked than Aflibercept. The maximum effect was observed with Aflibercept 0.5 mg/ml, and Ranibizumab 0.2 mg/ml.

In addition, as shown in the time-course study in Figure 2, a time-dependent response was observed in RPE cells treated with Aflibercept (from 0.025 mg/ml to 0.5 mg/ml) and Ranibizumab (from 0.025 mg/ml to 0.2 mg/ml), only up to 30 min stimulation. Hence, the maximum effect was reached with Aflibercept 0.5 mg/ml and Ranibizumab 0.2 mg/ml administrated for 30 min.

4.1.2 Effects of Aflibercept and Ranibizumab on NO release by RPE cells and HUVEC cultured in physiological and peroxidative conditions in the presence/absence of the NOS blocker by using the Griess assay

The effects of anti-VEGF agents on RPE cells (Figures 3A and B) and HUVEC (Figures 3C and D), were tested also in the presence/absence of the NOS antagonist (L-NAME, 4 µM for 15 min), administrated alone, or before the treatment with Aflibercept (0.5 mg/ml) or Ranibizumab (0.2 mg/ml), administrated both for 30 min. Concentrations and time were chosen based on the

results obtained with dose-response and time-course study. The experiments were conducted in physiological and peroxidative conditions inducted by 200 µM H_2O_2 for 30 min.

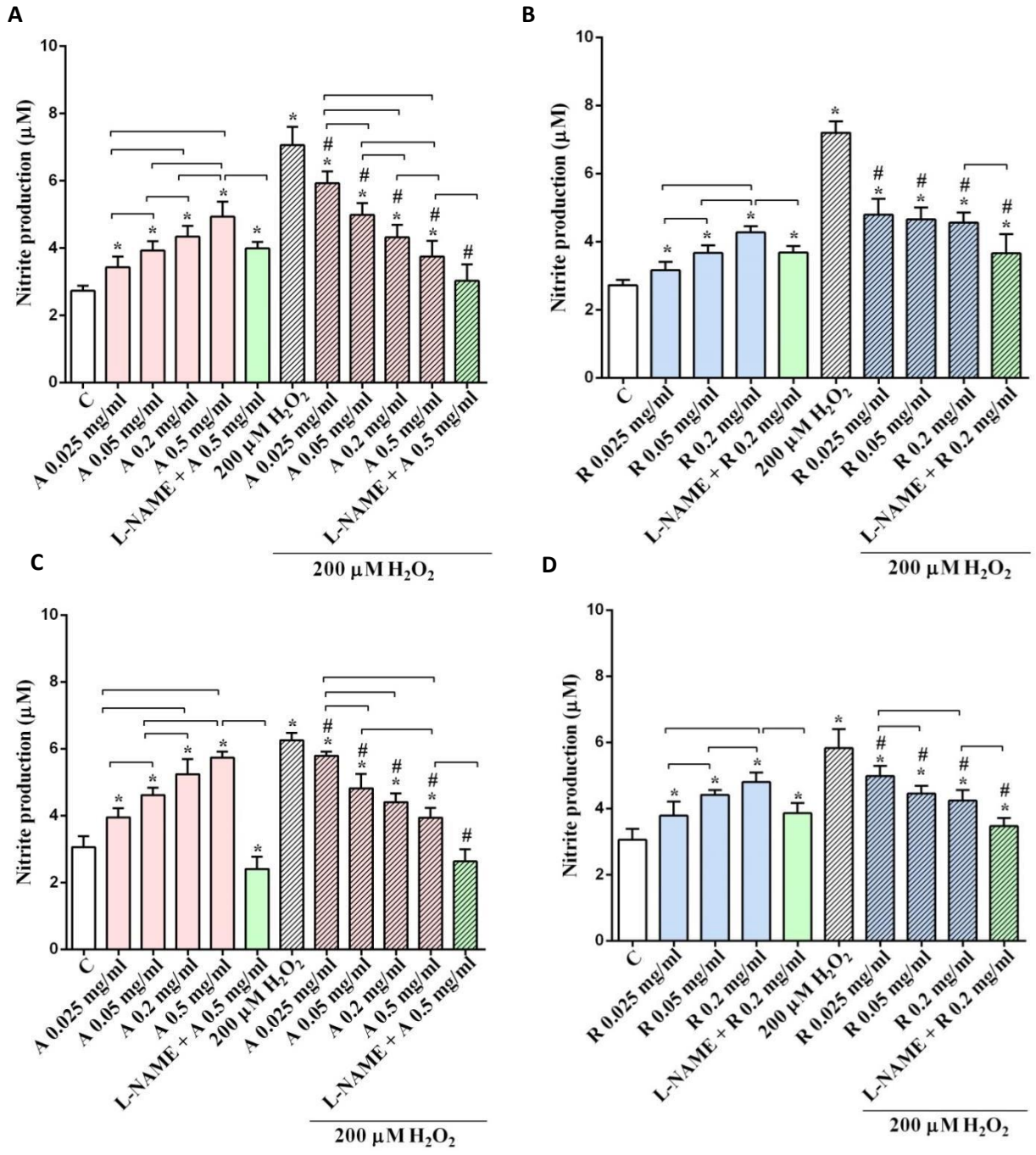

Figure 3: Effects of anti-VEGF agents on NO release in RPE cells (A and B) and HUVEC (C and D), cultured in physiological or peroxidative conditions. Abbreviations are as in previous Figures. The values obtained correspond to the nitrite (µM) produced, after each stimulation. Reported data are means ± SD of five independent experiments for each experimental protocol. Significance between groups: *P<0.05 vs C; #P<0.05 vs 200 µM H_2O_2. Short square brackets indicate significance between groups (P<0.05).

As shown in Figure 3, Aflibercept (Figure 3A) and Ranibizumab (Figure 3B), caused a dose-dependent increase of NO release by RPE cells cultured in physiological conditions. It is to note that, the pre-treatment with L-NAME, reduced the effects of two agents on NO release in physiological conditions. In addition, both agents were able to reduce NO release caused by peroxidation, and the pretreatment with the NOS inhibitor, potentiated these protective effects. Furthermore, similar findings were observed in HUVEC (Figures 3C and D), which would highlight the involvement of NO in the mechanisms of action of the anti-VEGF agents on vasculature, too.

4.1.3 Effects of anti-VEGF agents on activation/expression of eNOS and iNOS in RPE cells cultured in physiological and peroxidative conditions by using Western blot analysis

In order to confirm the involvement of eNOS/iNOS proteins in the intracellular signaling involved in the production of NO caused by Aflibercept (0.5 mg/ml for 6 h) or Ranibizumab (0.2 mg/ml for 6 h), the degree of eNOS/iNOS expression and eNOS phosphorylation was investigated. Experiments were conducted in the presence/absence of 200 µM H_2O_2 for 6 h. Since, changes in expression of proteins need time to be observed, we decided to choose 6 h stimulation. It is to note that results obtained about NO release showed no difference between 30 min and 6 h stimulation

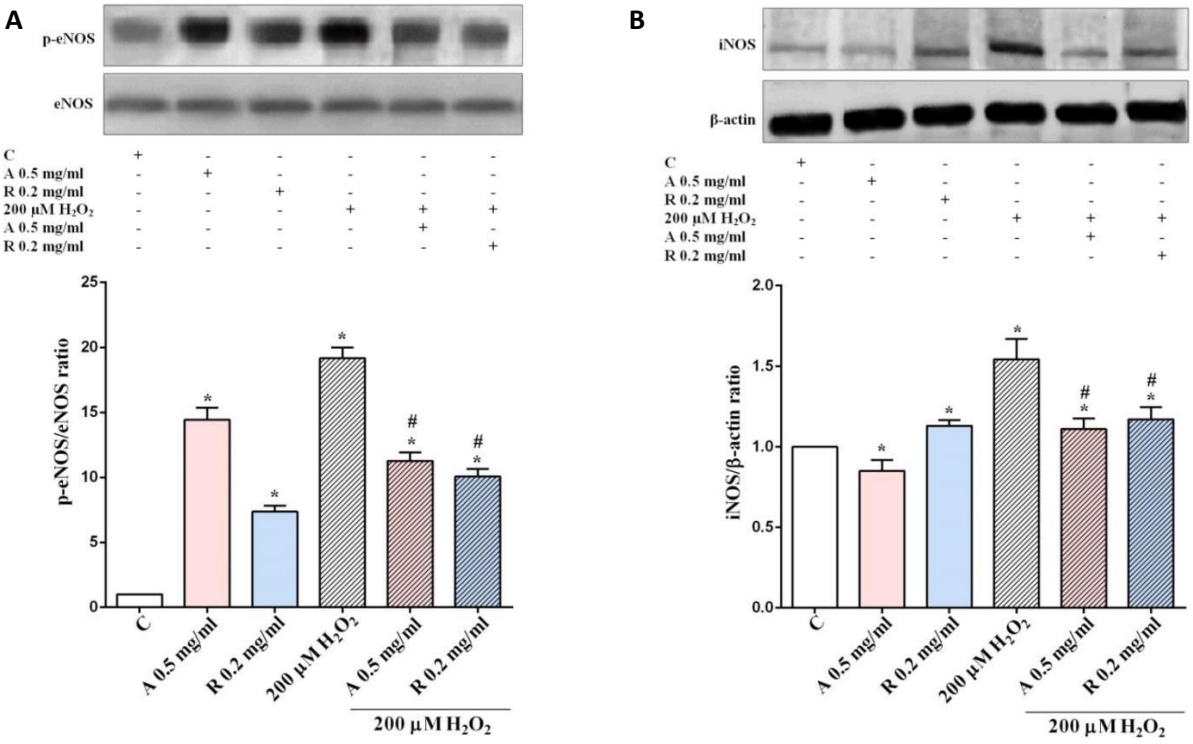

Figure 4: Variation in eNOS phosphorylation and iNOS expression measured in RPE cells by Western blot and densitometric analysis. In A and B densitometric analysis and an example of Western blot p-eNOS and iNOS, respectively, are shown. Abbreviations are as in previous Figures. The data were normalized versus control cells. Reported data are means ± SD of five independent experiments for each experimental protocol. Significance between groups: *P<0.05 vs C; #P<0.05 vs 200 µM H_2O_2.

As shown in Figure 4, the effects of the anti-VEGF agents on NO release were accompanied by changes in eNOS/iNOS activation/expression. While in physiological conditions these synthases were activated or their expression was increased (except for iNOS after stimulation with Aflibercept 0.5 mg/ml), in RPE subjected to peroxidation, eNOS/iNOS were inhibited.

All together these findings showed the involvement of eNOS and iNOS in the mechanisms of action of anti-VEGF agents.

4.2 Effects of Aflibercept and Ranibizumab on cell viability and mitochondrial membrane potential in RPE cells by using the MTT and the JC-1 assays

4.2.1 Dose-and time-response effects of anti-VEGF agents on cell viability in RPE cells

The effects on cell viability caused by anti-VEGF drugs, were analyzed by a dose-response study, as shown in Figure 5, and a time-course study, as shown in Figure 6. In particular the results obtained with different concentrations of Aflibercept (0.025 mg/ml, 0.05 mg/ml, 0.2 mg/ml, 0.5 mg/ml) or Ranibizumab (0.025 mg/ml, 0.05 mg/ml, 0.2 mg/ml), administrated for 5 min, 30 min and 6 h, are shown in Figure 5 and 6. In Figure 6, in particular, the comparison between the effects of anti VEGF obtained with the time-course study is highlighted.

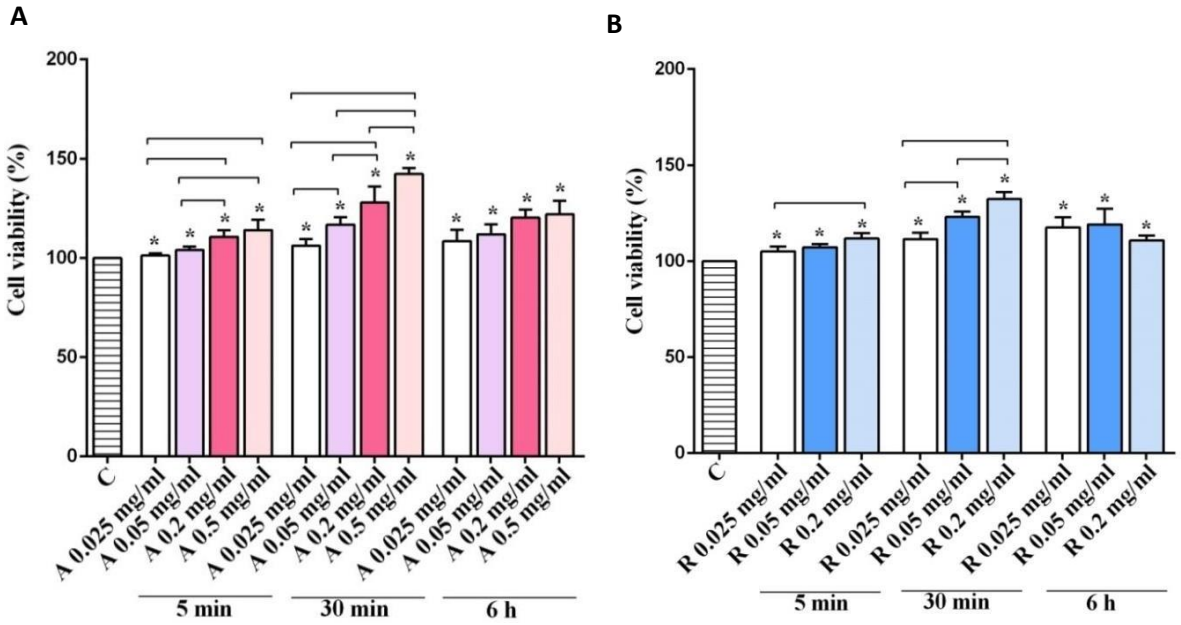

Figure 5: Dose-response effects of anti-VEGF agents on cell viability in RPE cells. In A, Aflibercept, in B, Ranibizumab. Abbreviations are as in previous Figures. The data were normalized versus control values. Reported data are means ± SD of five independent experiments. Significance between groups: *P<0.05 vs C. Short square brackets indicate significance between groups (P<0.05).

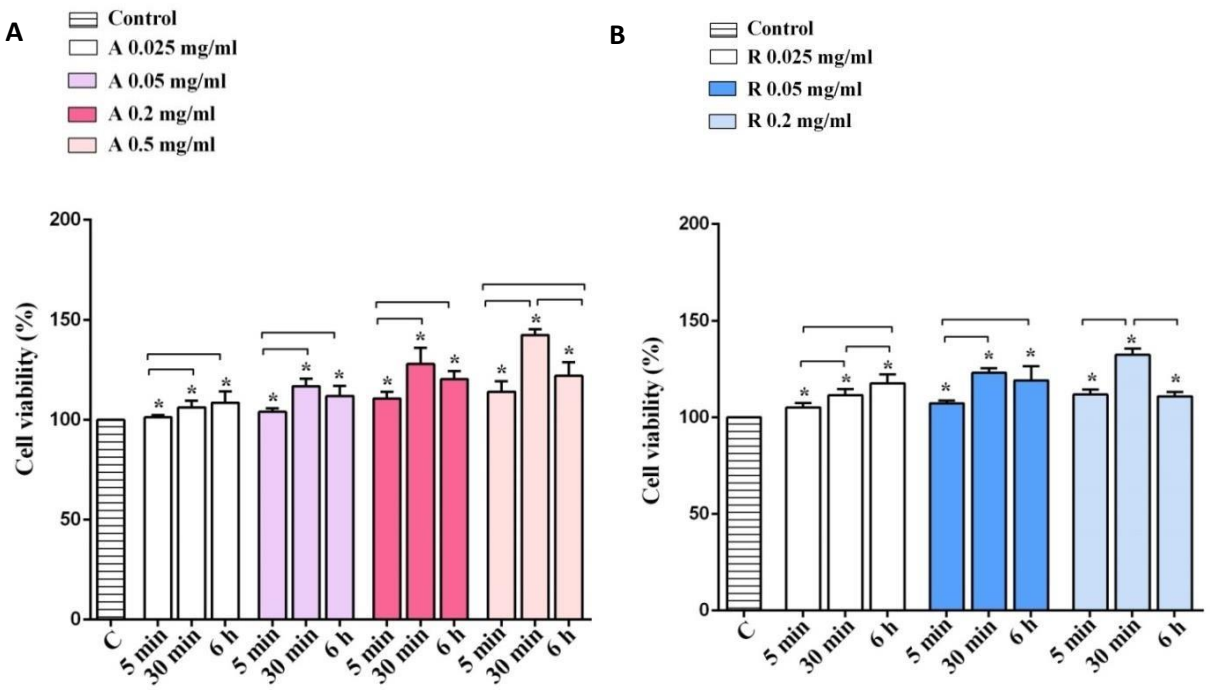

Figure 6: Time-course effects of anti-VEGF agents on cell viability in RPE cells. In A, Aflibercept, in B, Ranibizumab. Abbreviations are as in previous Figures. The data were normalized versus control value. Reported data are means ± SD of five independent experiments. Significance between groups: *P<0.05 vs C. Short square brackets indicate significance between groups (P<0.05).

As illustrated in Figure 5, all doses of Aflibercept (Figure 5A) and Ranibizumab (Figure 5B), were able to increase cell viability, in a dose-dependent way, until 30 min stimulation. As observed for the Griess assay, also in this case, the major effect was observed with Aflibercept 0.5 mg/ml and Ranibizumab 0.2 mg/ml. In addition, the time course study shown that, the smallest dose of Aflibercept (Figure 6A) and Ranibizumab (Figure 6B), had the greatest effect after 6 h, while the other doses had maximum effects at 30 min stimulation.

4.2.2 Effects of Aflibercept and Ranibizumab on cell viability and mitochondrial membrane potential of RPE cells, cultured in physiological and peroxidative conditions, in the presence/absence of the NOS blocker

For these experiments, the same experimental protocol used for the Griess assay was followed.

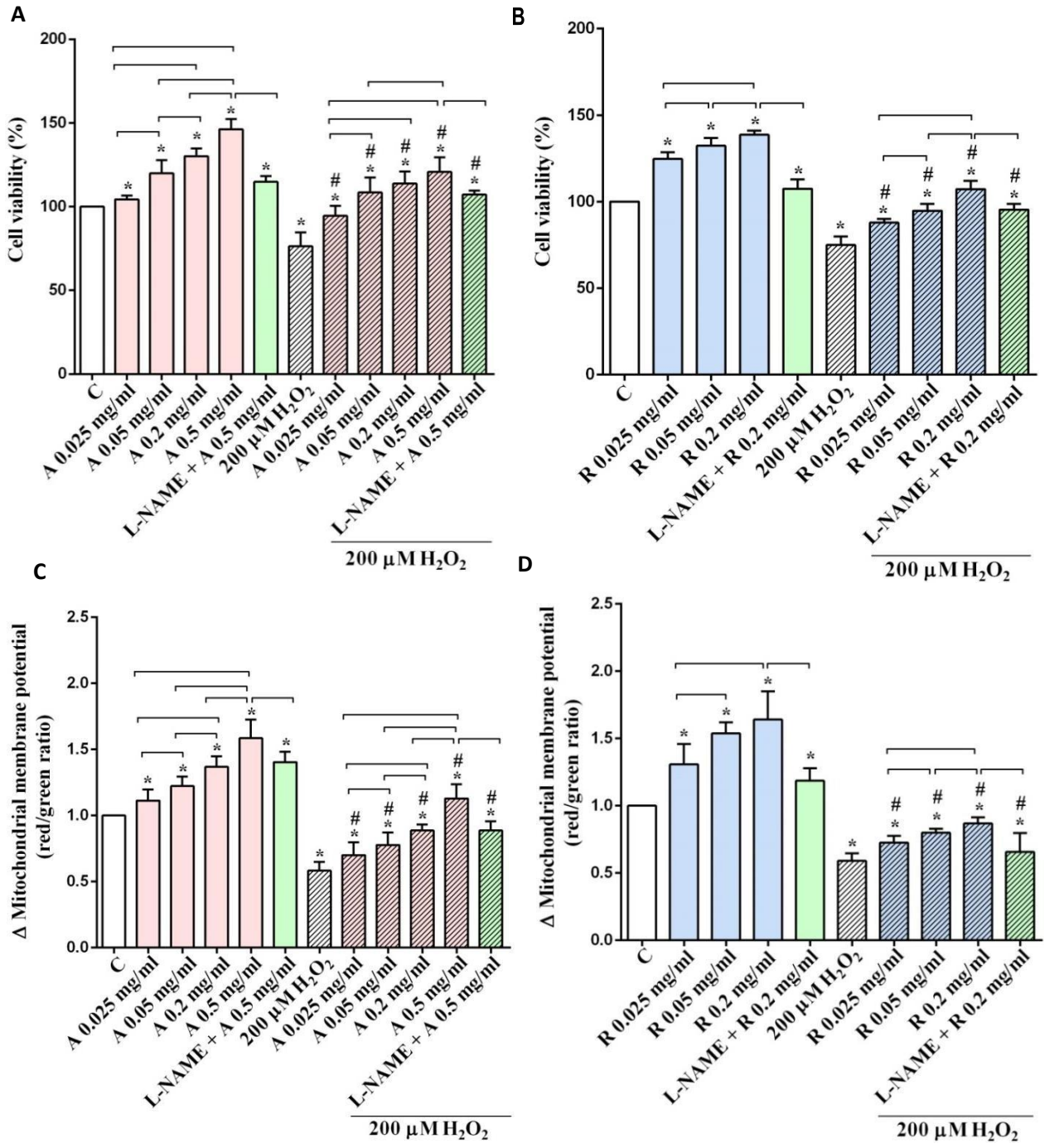

Figure 7: Effects of anti-VEGF agents on cell viability (A and B), and mitochondrial membrane potential (C and D) in RPE cells cultured in physiological or peroxidative conditions. Abbreviations are as in previous Figures. Reported data are means ± SD of five independent experiments for each experimental protocol. The data were normalized versus control value. Significance between groups: *P<0.05 vs C; #P<0.05 vs 200 µM H_2O_2. Short square brackets indicate significance between groups (P<0.05).

Aflibercept and Ranibizumab dose-dependently increased cell viability (Figures 7A and B), and mitochondrial membrane potential (Figures 7C and D) in RPE cells cultured in physiological medium and prevented the effects of H_2O_2. It is to note that both in physiological and peroxidative

conditions, L-NAME reduced the responses of RPE on cell viability and mitochondrial membrane potential to Aflibercept and Ranibizumab. Thus, the protective effects elicited by Aflibercept and Ranibizumab in RPE were found to be related to the modulation of NO release.

4.3 Effects of Aflibercept and Ranibizumab on RPE cell proliferation and migration

4.3.1 Effects of Aflibercept and Ranibizumab on RPE cell proliferation in physiological and peroxidative conditions by using xCELLigence

For these experiments, cells were stimulated with Aflibercept 0.5 mg/ml or Ranibizumab 0.2 mg/ml, alone or in the presence of 200 μM H_2O_2, and cell proliferation was analyzed at 12 h, 24 h and 48 h of stimulation. Results are shown in Figures 8 and 9.

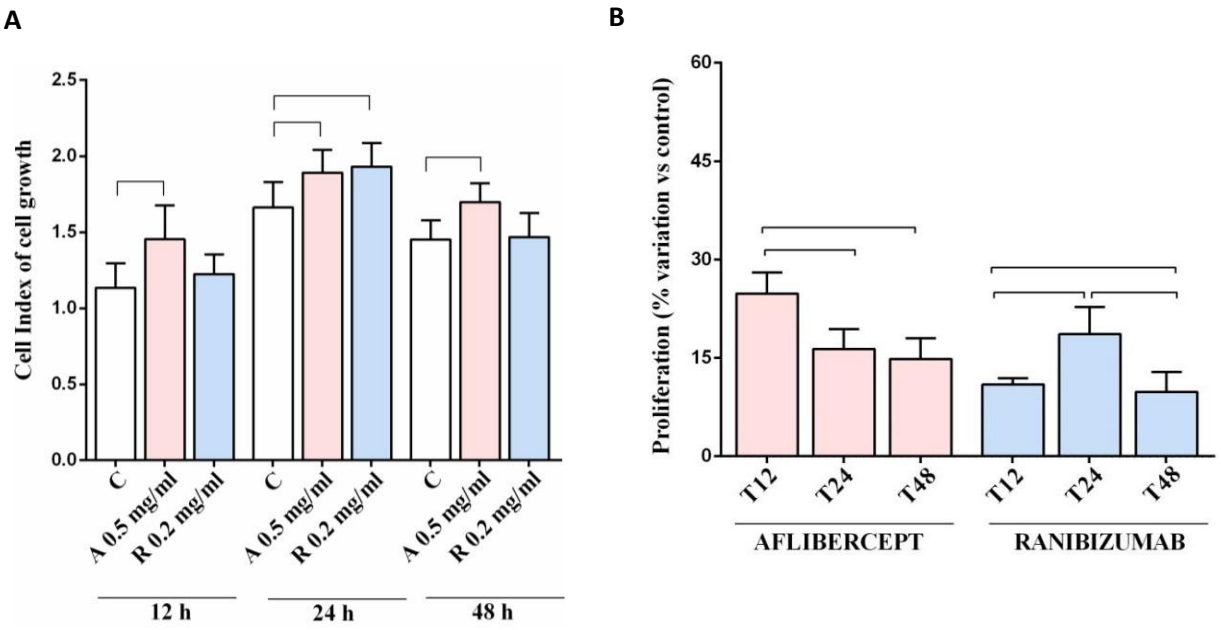

Figure 8: Effects of anti-VEGF agents on RPE cell proliferation in physiological conditions. In A, Cell index obtained from the xCELLigence system. In B, the percentage variation calculated with respect to each control value for each time. Abbreviations are as in previous Figures. Reported data are means ± SD of five independent experiments for each experimental protocol. Short square brackets indicate significance between groups ($P<0.05$).

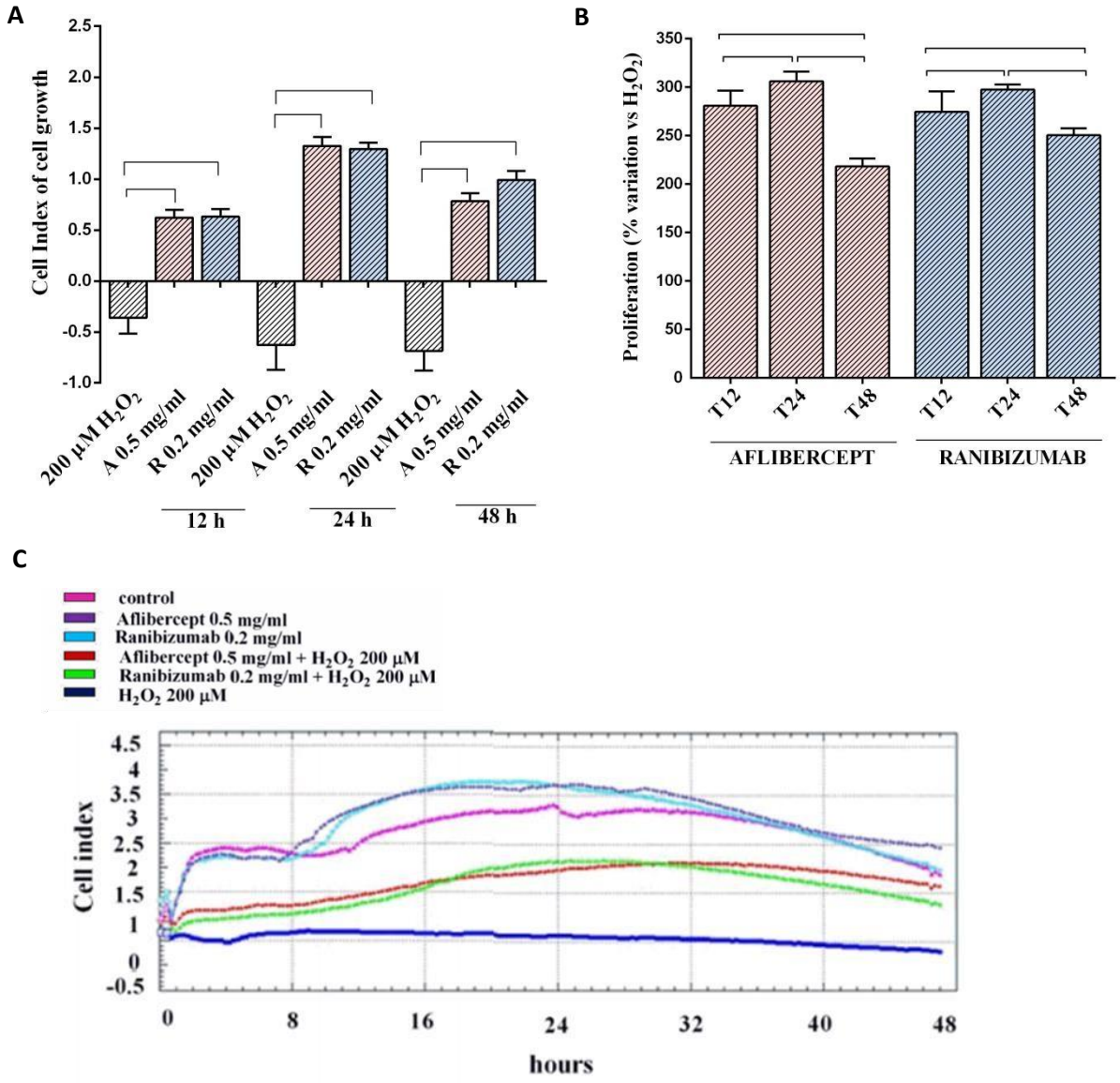

Figure 9: Effects of anti-VEGF agents on RPE cell proliferation in peroxidative conditions. In A, Cell index obtained from the xCELLigence system. In B, the percentage variation calculated with respect to each H_2O_2 value for each time. In C, an example of tracing taken from xCELLigence is shown. Abbreviations are as in previous Figures. Reported data are means ± SD of five independent experiments for each experimental protocol. Short square brackets indicate significance between groups ($P<0.05$).

As shown in Figures 8A and 9C, both Aflibercept was able to increase RPE cell proliferation in physiological conditions up to 48 h of stimulation, while Ranibizumab only up to 24 h. Both anti-VEGF were able to counteract the effects of hydrogen peroxide (Figures 9A and 9C). However, as shown in Figure 8B comparing each effect with its specific control time, the major effect of Aflibercept and Ranibizumab were observed at 12 h and 24 h respectively. In peroxidative conditions, in respect to H_2O_2, the major effect of both Aflibercept and Ranibizumab was reached at 24 h, in a time-dependent way (Figure 9B).

4.3.2 Effects of Aflibercept and Ranibizumab on RPE cell migration by using the wound-healing assay

For these experiments, "scratched" cells were stimulated with Aflibercept (0.025 mg/ml and 0.5 mg/ml) or Ranibizumab (0.025 mg/ml and 0.2 mg/ml), and then the time of closure was analyzed at T0, and after 24 h (T24) and 48 h (T48) from the wound.

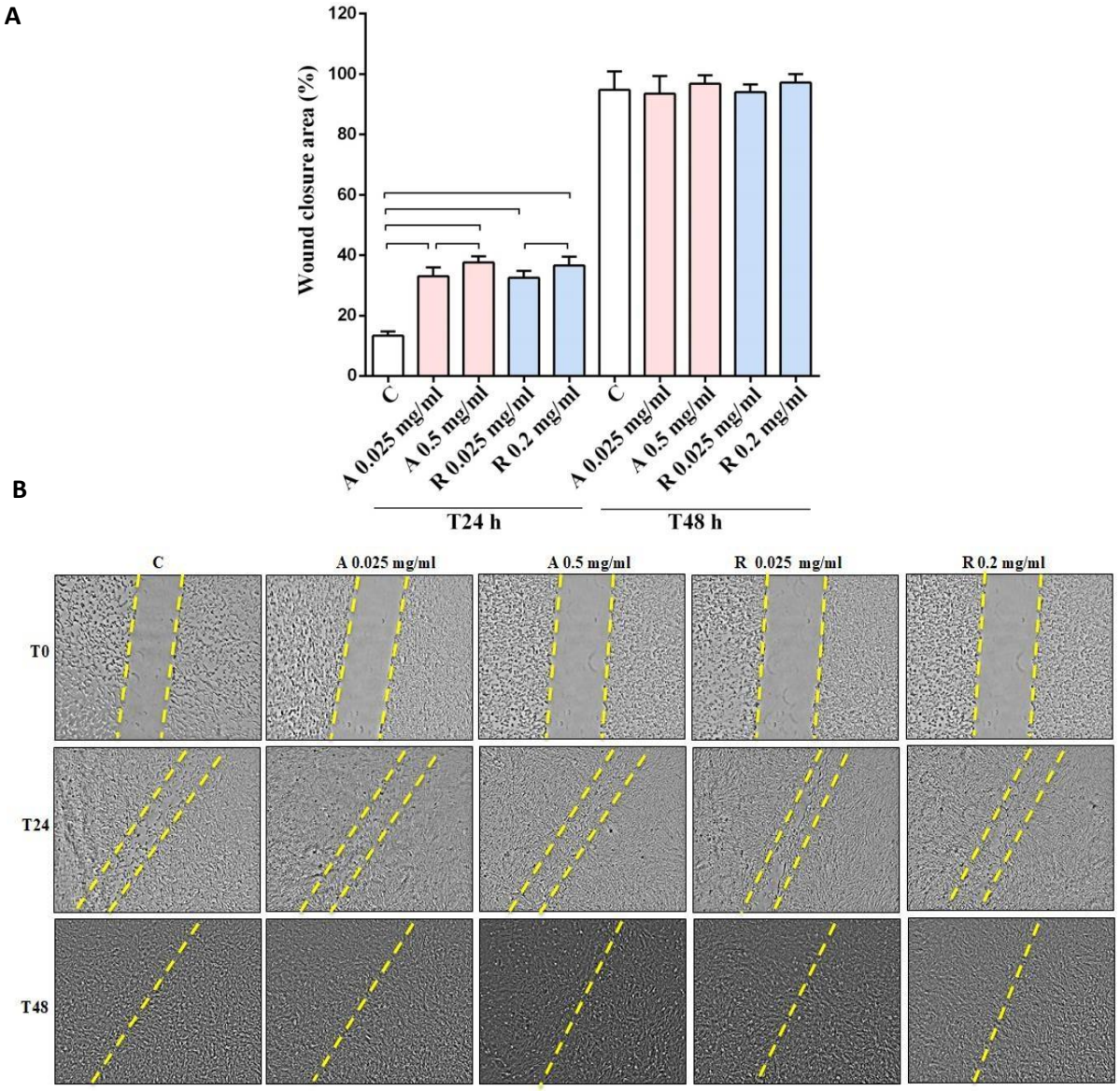

Figure 10: Effects of anti-VEGF agents on RPE cell migration. Abbreviations are as in previous Figures. In A, summary bar graph illustrating percentage wound closure at indicated time points during the scratch wound assay. In B, representative images from in vitro scratch wound healing assays, demonstrating that cell migration into the cell-free region (outlined) is significantly accelerated in the presence of anti-VEGF drugs when compared to control. The images were taken at 4X magnification. The wound area and the percentage of healing were calculated for each time point. Reported data are means ± SD of five independent experiments for each experimental protocol. Short square brackets indicate significance between groups ($P<0.05$).

As shown in Figure 10, the stimulation with anti-VEGF drugs increases, in a dose-dependent way, cell migration up to 24 h after wound. After 48 h, no difference was observed compared to control cells.

4.4 Effects of Aflibercept and Ranibizumab on reactive oxygen species (ROS) production by using the DCFDA-Cellular ROS Detection Assay Kit

Effects of Aflibercept and Ranibizumab on ROS release were examined by a dose-response study using the DCFDA-Cellular ROS Detection Assay Kit. The study was performed by testing Aflibercept (0.025 mg/ml, 0.05 mg/ml, 0.2 mg/ml, 0.5 mg/ml, for 30 min) or Ranibizumab (0.025 mg/ml, 0.05 mg/ml, 0.2 mg/ml, for 30 min) alone, or in the presence of 200 µM H_2O_2 for 30 min. The acute effects of anti-VEGF on ROS release were therefore examined: the doses used and the effect produced by their stimulation are visible in Figure 11.

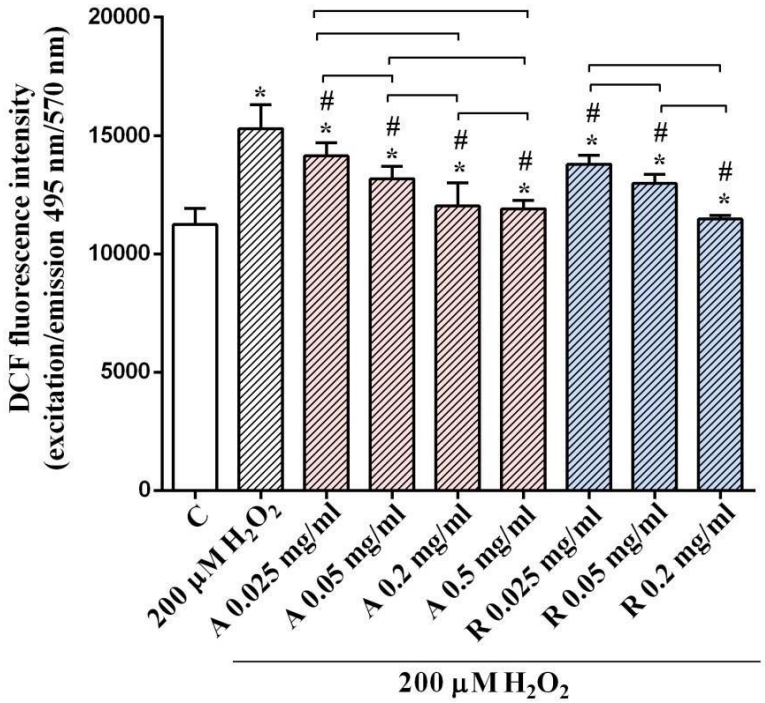

Figure 11: ROS release in RPE cells caused by hydrogen peroxide in the presence or absence of Aflibercept and Ranibizumab. Abbreviations are as in previous Figures. Results are expressed as DCF fluorescence intensity, which is proportional to the amount of intracellular ROS. Reported data are means ± SD of five independent experiments for each experimental protocol. Significance between groups: *P<0.05 vs C; #P<0.05 vs 200 µM H_2O_2. Short square brackets indicate significance between groups (P<0.05).

As shown from the graph in Figure 11, anti-VEGF drugs were able to reduce ROS production induced by the treatment with H_2O_2, in a dose-dependent manner with a maximum effect at 0.5 mg/ml for Aflibercept and 0.2 mg/ml for Ranibizumab.

4.5 Effects of Aflibercept and Ranibizumab on RPE cell apoptosis by using flow cytometry and Western blot analysis

To study the role of anti-VEGF drugs in the process of apoptosis under physiological and peroxidative conditions, Annexin V/PI detection was performed. In parallel experiments, the expression of Cleaved Caspase 9 and Cytochrome C, was evaluated by Western blot and densitometric analysis. Furthermore, the effect of anti-VEGF on the activation of Akt and ERK1/2, kinases implicated in the cell survival mechanism, was further investigated. The studies were conducted on RPE cells treated with anti-VEGF drugs, in the presence or absence of 200 µM H_2O_2. As performed for eNOS/iNOS also in this case, we decided to choose 6 h stimulation in order to see any protein expression changes. Although the results obtained about cell viability with 6 h simulation were lower than those observed with 30 min, they were higher than control.

4.5.1 Effects of anti-VEGF agents on RPE cell apoptosis by using Annexin V/PI staining

For these experiments, RPE cells were stimulated with Aflibercept (0.025 mg/ml and 0.5 mg/ml, for 6 h) or Ranibizumab (0.025 mg/ml and 0.2 mg/ml, for 6 h), in the presence or absence of 200 µM H_2O_2 for 6 h.

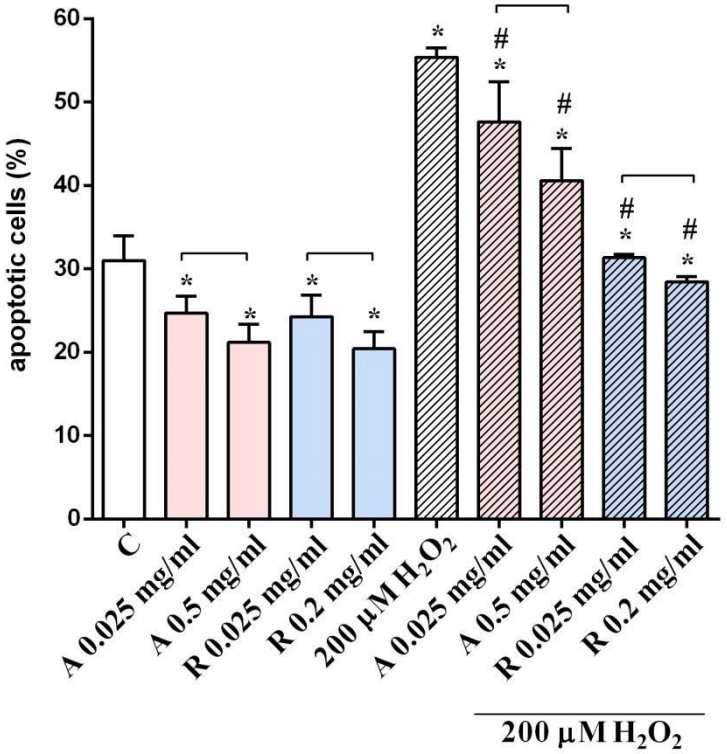

Figure 12: Effects of Aflibercept and Ranibizumab on RPE cell apoptosis. Abbreviations are as in previous Figures. Reported data are means ± SD of five independent experiments for each experimental protocol. Significance between groups: *P<0.05 vs C; #P<0.05 vs 200 µM H_2O_2. Short square brackets indicate significance between groups (P<0.05).

As shown in Figure 12, apoptosis was reduced by treating cells with both doses of Aflibercept, and Ranibizumab. Furthermore, the anti-VEGF agents were able to counteract the effects of H_2O_2. In both cases the two drugs acted in a dose-dependent way.

4.5.2 Effects of anti-VEGF agents on RPE cell apoptosis analyzed by Cleaved Caspase 9 and Cytochrome C expression by using Western blot analysis

For these experiments, RPE cells were stimulated with Aflibercept (0.5 mg/ml for 6 h) or Ranibizumab (0.2 mg/ml for 6 h), in the presence or absence of 200 µM H_2O_2 for 6 h.

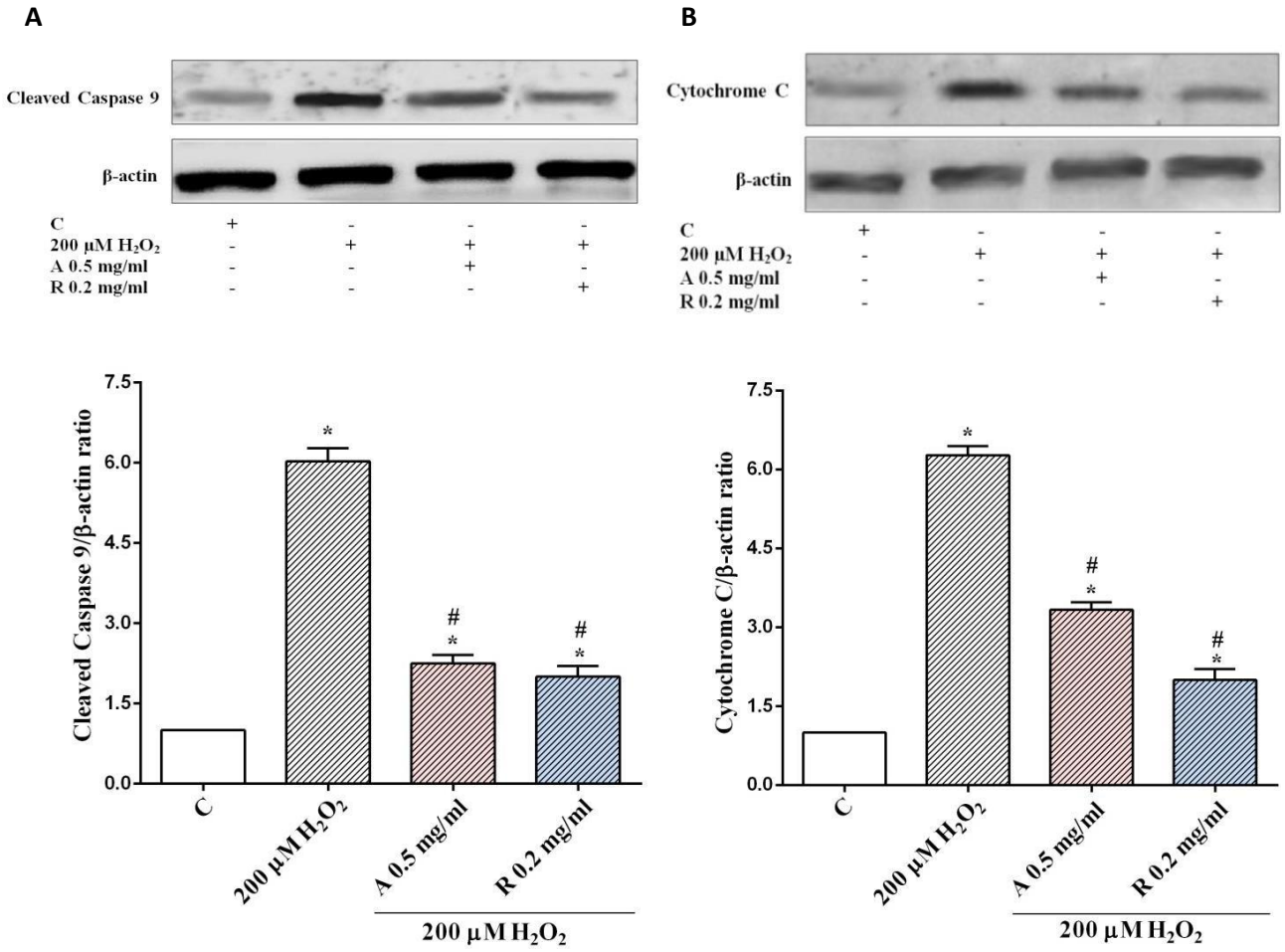

Figure 13: Variation in Cleaved Caspase 9 and Cytochrome C expression in RPE measured by Western blot and densitometric analysis in RPE cells. In A and B densitometric analysis and an example of Western blot Cleaved Caspase 9 and Cytochrome C, respectively, are shown. Abbreviations are as in previous Figures. The data were normalized versus control cells. Reported data are means ± SD of five independent experiments for each experimental protocol. Significance between groups: *P<0.05 vs C; #P<0.05 vs 200 µM H_2O_2.

As shown in Figure 13, anti-VEGF agents were able to counteract the effects of H_2O_2 on apoptosis in RPE cells, as evidenced by the inhibition of the expression of the Cleaved Caspase 9 and Cytochrome C.

4.5.3 Effects of anti-VEGF agents on Akt and ERK1/2 activation, in RPE cells cultured in physiological and peroxidative conditions by using Western blot analysis

For these experiments, cells were stimulated with Aflibercept (0.5 mg/ml for 6 h) or Ranibizumab (0.2 mg/ml for 6 h), in the presence or absence of 200 µM H_2O_2 for 6 h.

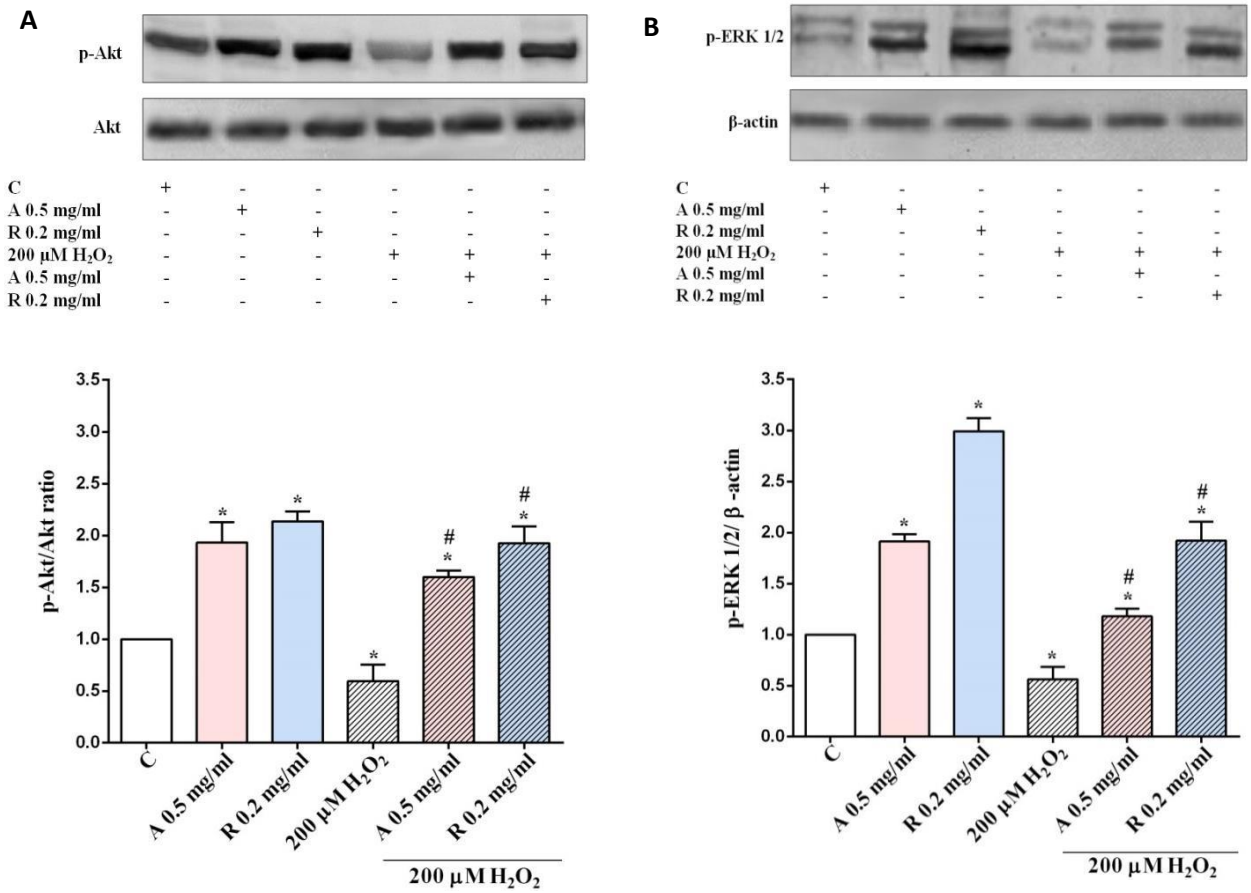

Figure 14: Akt and ERK 1/2 phosphorylation in RPE cells measured by Western blot and densitometric analysis. In A and B densitometric analysis and an example of p-Akt and p-ERK1/2 respectively, are shown. Abbreviations are as in previous Figures. The data were normalized versus control cells. Reported data are means ± SD of five independent experiments for each experimental protocol. Significance between groups: *P<0.05 vs C; #P<0.05 vs 200 µM H_2O_2.

As shown in Figure 14, Aflibercept and Ranibizumab were able to increase Akt and ERK1/2 activation in RPE cells cultured in physiological conditions, and prevented the inhibition of these survival kinases, caused by H_2O_2.

5. SECOND PART OF THE STUDY: RESULTS ON HUVEC AND RPE CELL CO-CULTURE

5.1 Effects of HUVEC/RPE cell co-culture on NO release in RPE cells

5.1.1 Griess assay

For these experiments, HUVEC were stimulated with Aflibercept (0.025 mg/ml and 0.5 mg/ml) or Ranibizumab (0.025 mg/ml and 0.2 mg/ml) for 30 min, in the presence or absence of various inhibitors administrated 15 min before the two drugs. RPE were treated in physiological or peroxidative conditions, caused by 200 µM H_2O_2 for 30 min.

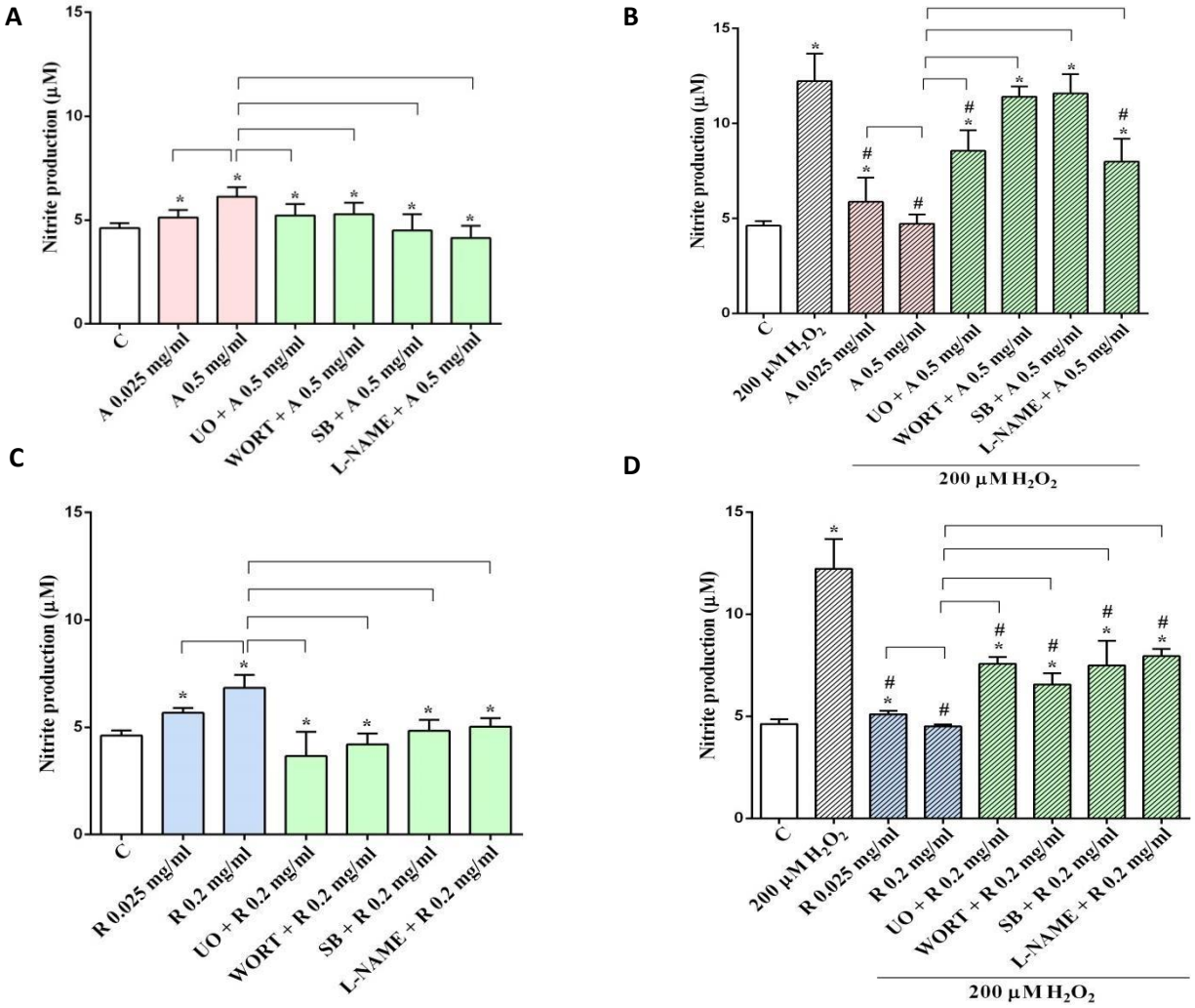

Figure 15: Effects of HUVEC/RPE cell co-culture on NO release in RPE cells, in physiological (A and C) or peroxidative (B and D) conditions. In A and B, the effects of Aflibercept, and in C and D, the effects of Ranibizumab, are shown. The values obtained correspond to the nitrite (µM) produced, after each stimulation. Abbreviations are as in previous Figures. UO (UO126 4 µM for 15 min); WORT (wortmannin 4 µM for 15 min); SB (SB203580 4 µM for 15 min); L-NAME (4 µM for 15 min). Reported data are means ± SD of five independent experiments for each experimental protocol. Significance between groups: *P<0.05 vs C; #P<0.05 vs 200 µM H_2O_2. Short square brackets indicate significance between groups (P<0.05).

As illustrated in Figures 15A and C, the HUVEC treatment induced a dose-dependent increase of NO release in RPE cultured in physiological conditions, and reduced the NO release caused by peroxidation (Figures 15B and D). It is to note that the pre-treatment with inhibitors reduced the effects on NO release in physiological conditions (Figures 15A and C), and the protective effects of the two anti-VEG drugs against NO release in peroxidation (Figures 15B and D).

5.1.2 Activation/expression of eNOS and iNOS in RPE cells cultured in physiological and peroxidative conditions by using Western blot

In order to confirm the involvement of eNOS/iNOS proteins in the intracellular signaling involved in the production of NO caused on RPE, after HUVEC stimulation with Aflibercept (0.5 mg/ml for 30 min) or Ranibizumab (0.2 mg/ml for 30 min), the degree of eNOS/iNOS expression and eNOS phosphorylation was investigated. Experiments were conducted in the presence/absence of 200 µM H_2O_2 for 6 h.

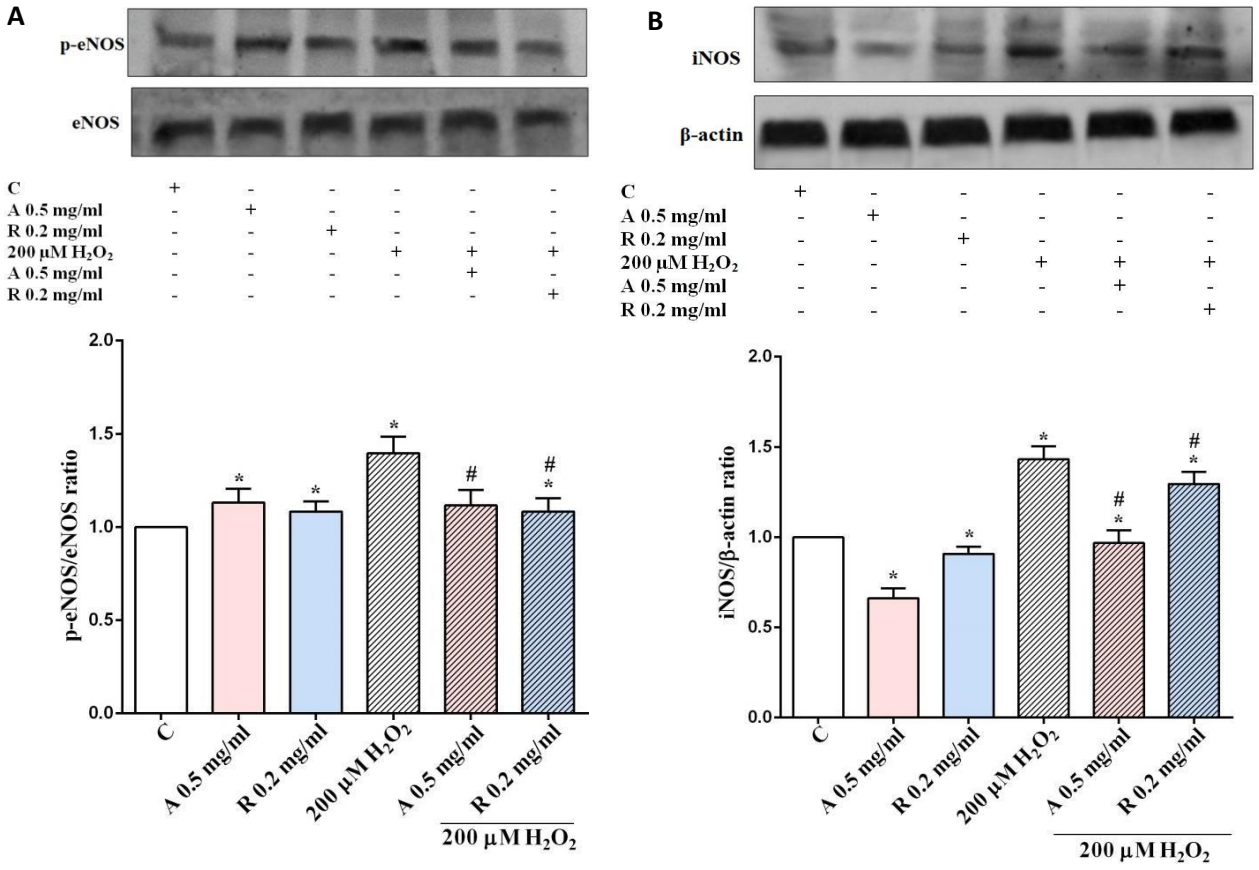

Figure 16: Variation in eNOS phosphorylation and iNOS expression measured in RPE cells by Western blot and densitometric analysis. In A and B densitometric analysis and an example of Western blot of p-eNOS and iNOS, respectively, are shown. Abbreviations are as in previous Figures. The data were normalized versus control cells. Reported data are means ± SD of five independent experiments for each experimental protocol. Significance between groups: *P<0.05 vs C; #P<0.05 vs 200 µM H_2O_2.

As shown in Figure 16, the effects of HUVEC/RPE cell co-culture on NO release by RPE cells, were accompanied by changes in eNOS/iNOS activation/expression. In physiological conditions, eNOS phosphorylation was increased (Figure 16A), but iNOS expression was reduced (Figure 16B). In RPE cells subjected to peroxidation both activation/expression of these synthases was inhibited.

5.2 Effects of HUVEC/RPE cell co-culture on RPE cell viability and mitochondrial membrane potential, by using the MTT and the JC-1 assays

For the experiments, the same experimental protocol used for the Griess assay was followed. Data about MTT and JC-1 assays are shown in Figures 17 and 18 respectively.

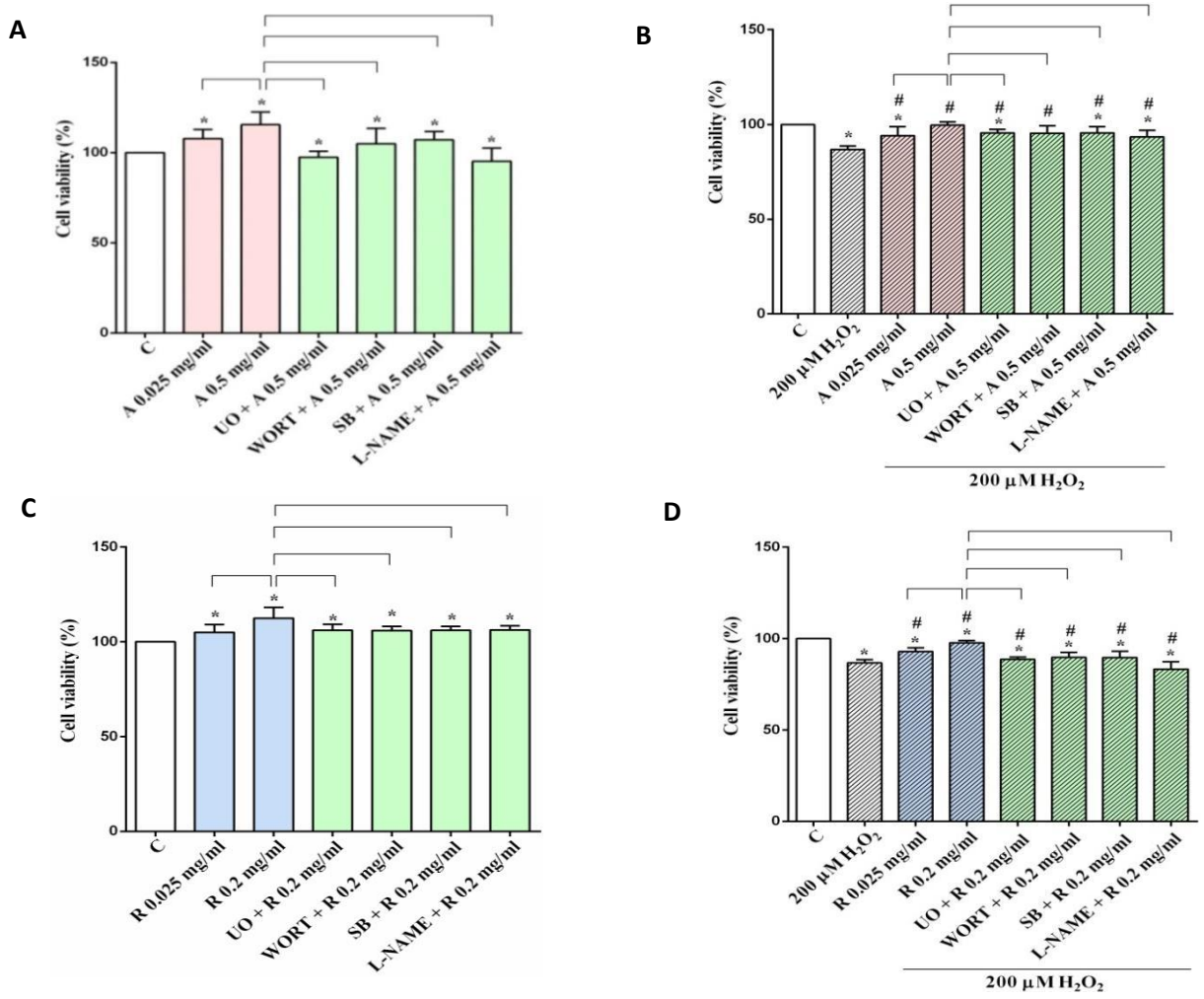

Figure 17: Effects of HUVEC/RPE cell co-culture on RPE cell viability in physiological (A and C) and peroxidative (B and D) conditions. In A and B the effects of Aflibercept, and in C and D the effects of Ranibizumab, are shown. Abbreviations are as in previous Figures. The data were normalized versus control value. Reported data are means ± SD of five independent experiments for each experimental protocol. Significance between groups: *P<0.05 vs C; #P<0.05 vs 200 µM H_2O_2. Short square brackets indicate significance between groups (P<0.05).

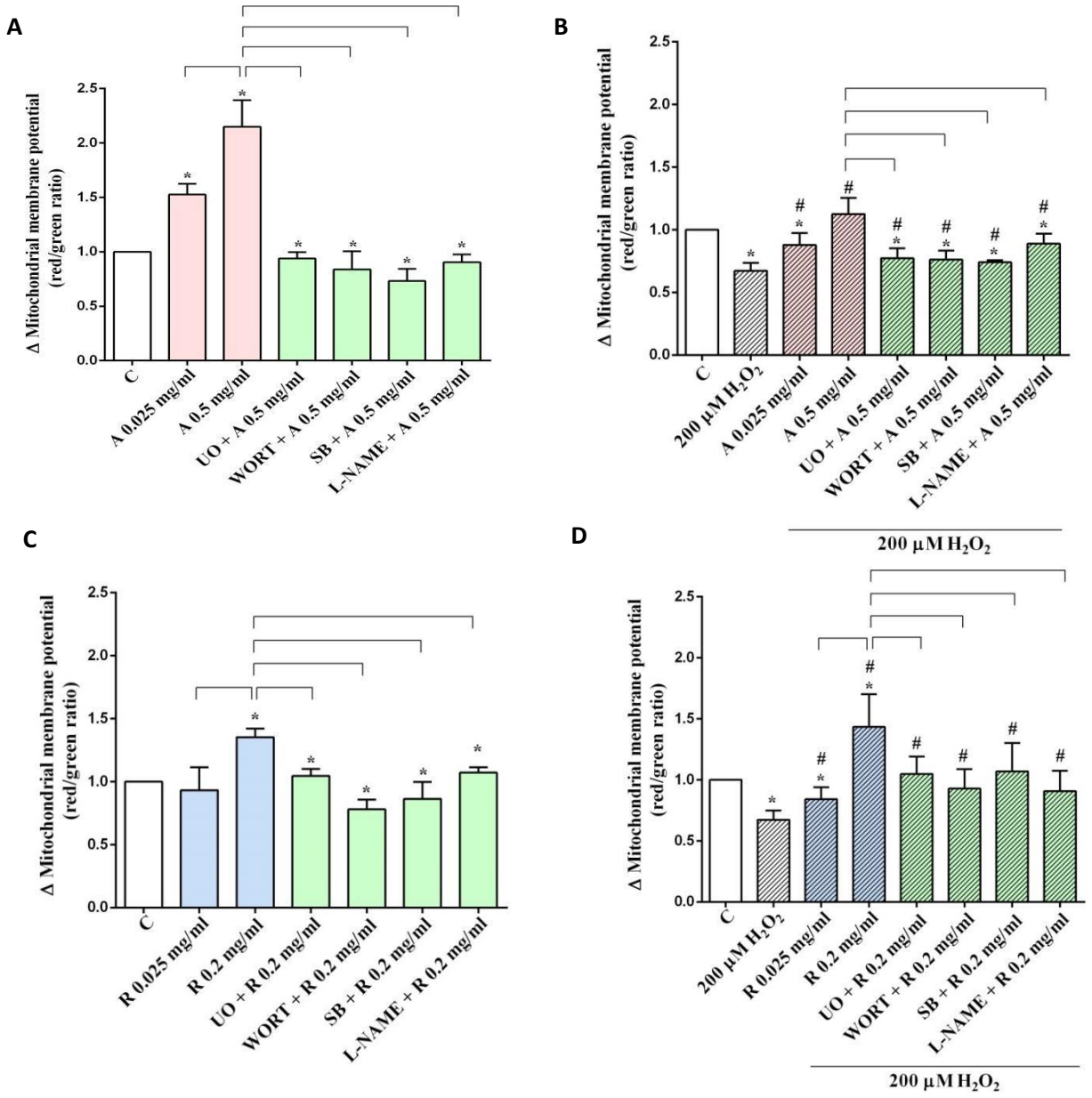

Figure 18: Effects of co-culture on mitochondrial membrane potential in RPE cells, in physiological (A and C) and peroxidative (B and D) conditions. In A and B the effects of Aflibercept, and in C and D the effects of Ranibizumab, are shown. Abbreviations are as in previous Figures. The data were normalized versus control value. Reported data are means ± SD of five independent experiments for each experimental protocol. Significance between groups: *P<0.05 vs C; #P<0.05 vs 200 µM H_2O_2. Short square brackets indicate significance between groups (P<0.05).

As shown in Figure 17, the HUVEC/RPE cell co-culture caused a dose-response increase in cell viability (Figures 17A and C). As regarding the mitochondrial membrane potential (Figures 18A and C) both doses Aflibercept were able to induce an increase in a dose-dependent way, an effect that was observed with only 0.2 mg/ml Ranibizumab in RPE cells cultured in physiological medium. In peroxidative conditions, the co-culture with HUVEC was able to prevent the reduction

of cell viability (Figures 17B and D) and the collapse of mitochondrial membrane potential (Figures 18B and D) caused by H_2O_2. It is to note that, in both physiological and peroxidative conditions, the protective effects elicited by HUVEC on RPE cells, were reduced or abolished by UO126, wortmannin, SB203580 and L-NAME (Figures 17 and 18).

5.3 Effects of HUVEC/RPE cell co-culture on RPE cell proliferation and migration

5.3.1 Effects of HUVEC/RPE cell co-culture on RPE cell proliferation, in physiological and peroxidative conditions, by using XCELLigence

For these experiments, HUVEC were stimulated with Aflibercept (0.5 mg/ml) or Ranibizumab (0.2 mg/ml), and the effects on RPE cells, were analyzed in physiological and peroxidative conditions, caused by 200 µM H_2O_2. Cell proliferation was analyzed at 12 h, 24 h and 48 h of treatment. Results are shown in Figures 19 and 20.

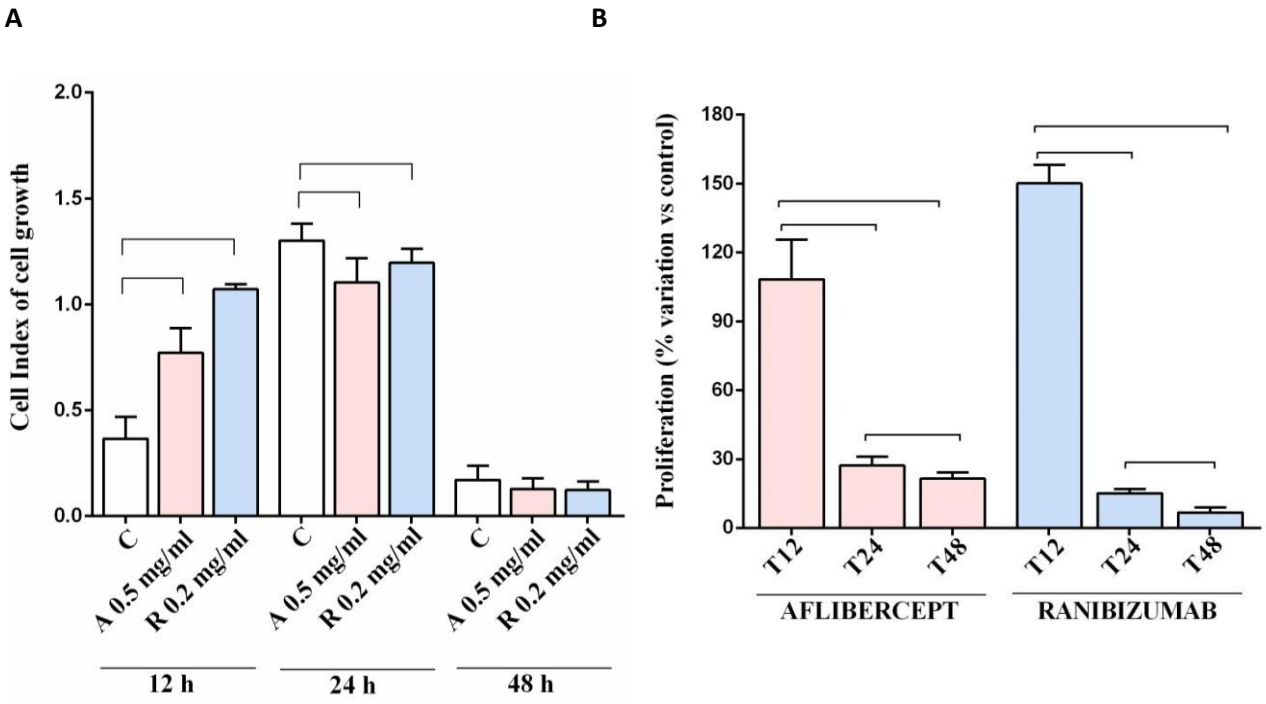

Figure 19: Effects of HUVEC/RPE cell co-culture on RPE cell proliferation in physiological condition. In A, Cell index obtained from the xCELLigence system. In B, the percentage variation calculated with respect to each control value for each time. Abbreviations are as in previous Figures. Reported data are means ± SD of five independent experiments for each experimental protocol. Short square brackets indicate significance between groups ($P<0.05$).

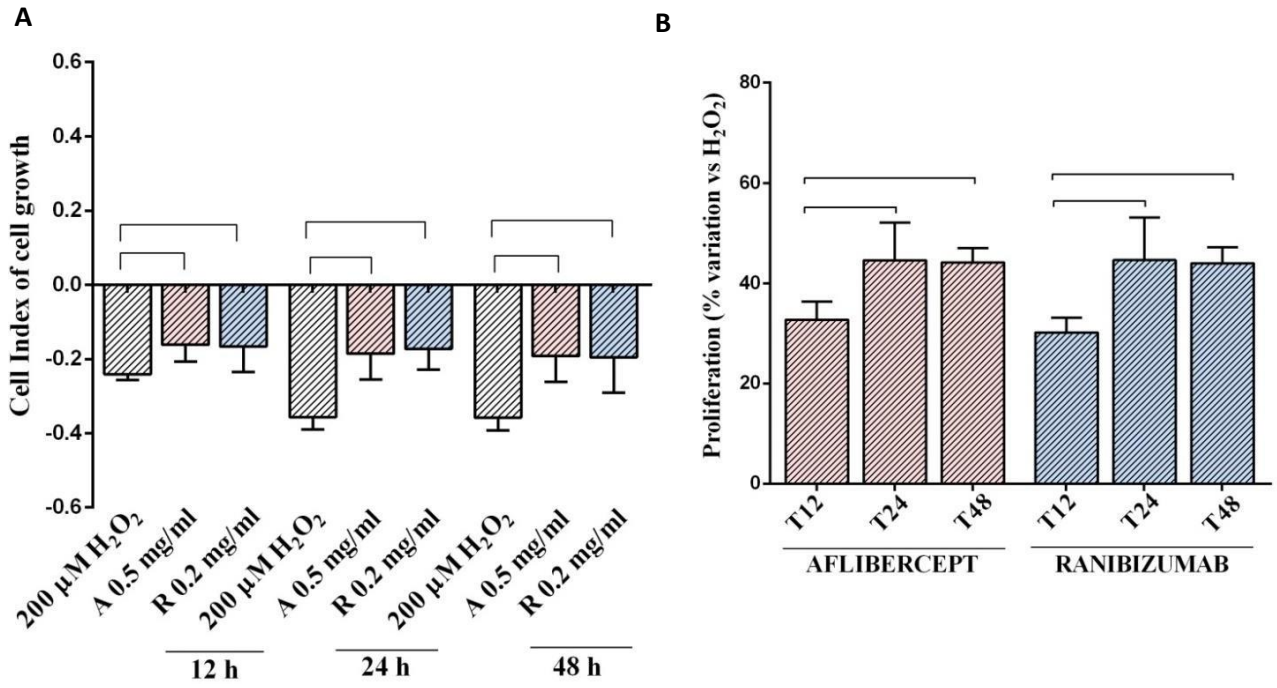

Figure 20: Effects of HUVEC/RPE cell co-culture on RPE cell proliferation in peroxidative condition. In A, Cell index obtained from the xCELLigence system. In B, the percentage variation calculated with respect to each H_2O_2 value for each time. Abbreviations are as in previous Figures. Reported data are means ± SD of five independent experiments for each experimental protocol. Short square brackets indicate significance between groups ($P<0.05$).

As shown in Figures 19A and B, in physiological conditions, HUVEC stimulated with Aflibercept or Ranibizumab, were able to increase RPE cell proliferation, only up to 12 h of stimulation, while after 24 h and 48 h, cell proliferation was reduced in a time-dependent way. Both agents were able to counteract the effects of H_2O_2 (Figure 20A) after 12 h to 48 h of stimulation. However, as shown in Figure 20B, comparing each effect to H_2O_2, the maximum effect of Aflibercept and Ranibizumab was reached at 24 h, in a time-dependent way.

5.3.2 Western blot

In order to confirm the results obtained with xCELLigence, the expression of p21 protein, was investigated by using Western blot. HUVEC were stimulated with Aflibercept (0.5 mg/ml) or Ranibizumab (0.2 mg/ml) for 6 h and the effects on RPE cells, were analyzed in physiological and peroxidative conditions caused by 200 µM H_2O_2 for 6 h.

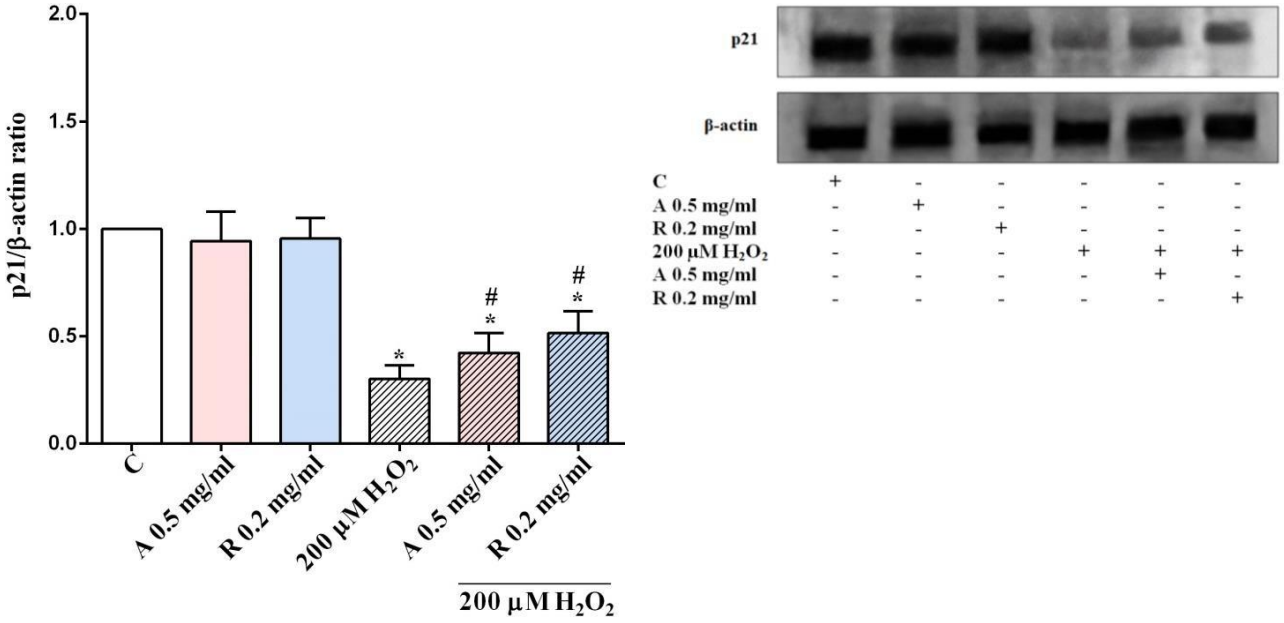

Figure 21: Variation in p21 expression measured in RPE cells by Western blot and densitometric analysis. Densitometric analysis and an example of Western blot taken from 5 different experiments of p21, are shown. Abbreviations are as in previous Figures. The data were normalized versus control value. Reported data are means ± SD of five independent experiments for each experimental protocol. Significance between groups: *P<0.05 vs C; #P<0.05 vs 200 µM H_2O_2.

As shown in Figure 21, the HUVEC/RPE cell co-culture was able to counteract the effects of oxidative stress on p21 expression in RPE cells.

5.3.3 Effects of HUVEC/RPE cell co-culture on RPE cell migration by using the wound-healing assay

For these experiments, HUVEC were stimulated with Aflibercept (0.025 mg/ml and 0.5 mg/ml) or Ranibizumab (0.025 mg/ml and 0.2 mg/ml) for 30 min, in the presence/absence of 15 min pretreatment with 4 µM L-NAME. After stimulations, RPE cells were "scratched" and new medium was added to HUVEC. The closure was analyzed at T0, and after 24 h (T24) and 48 h (T48) from the wound. Results are shown in Figures 22 (Aflibercept) and 23 (Ranibizumab).

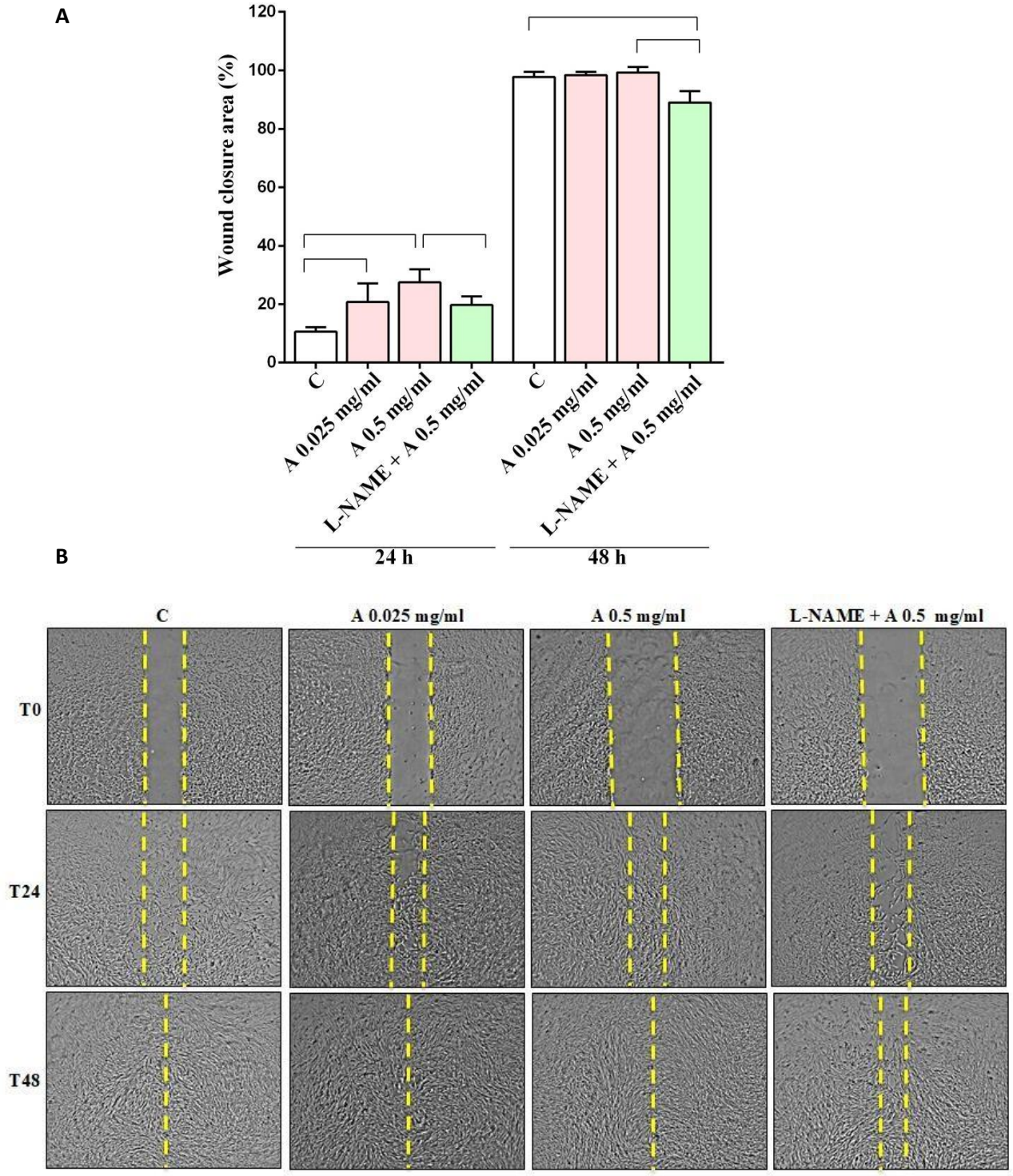

Figure 22: Effects of HUVEC/RPE cell co-culture on RPE cell migration after Aflibercept stimulation. Abbreviations are as in previous Figures. In A, quantified data for the wound-healing assay are shown. In B, an example of photograph of the wound of each time (time 0 and after 24 h and 48 h), are shown. The images were taken at 4X magnification. The wound area and the percentage of healing were calculated for each time point. Reported data are means ± SD of five independent experiments for each experimental protocol. Short square brackets indicate significance between groups ($P<0.05$).

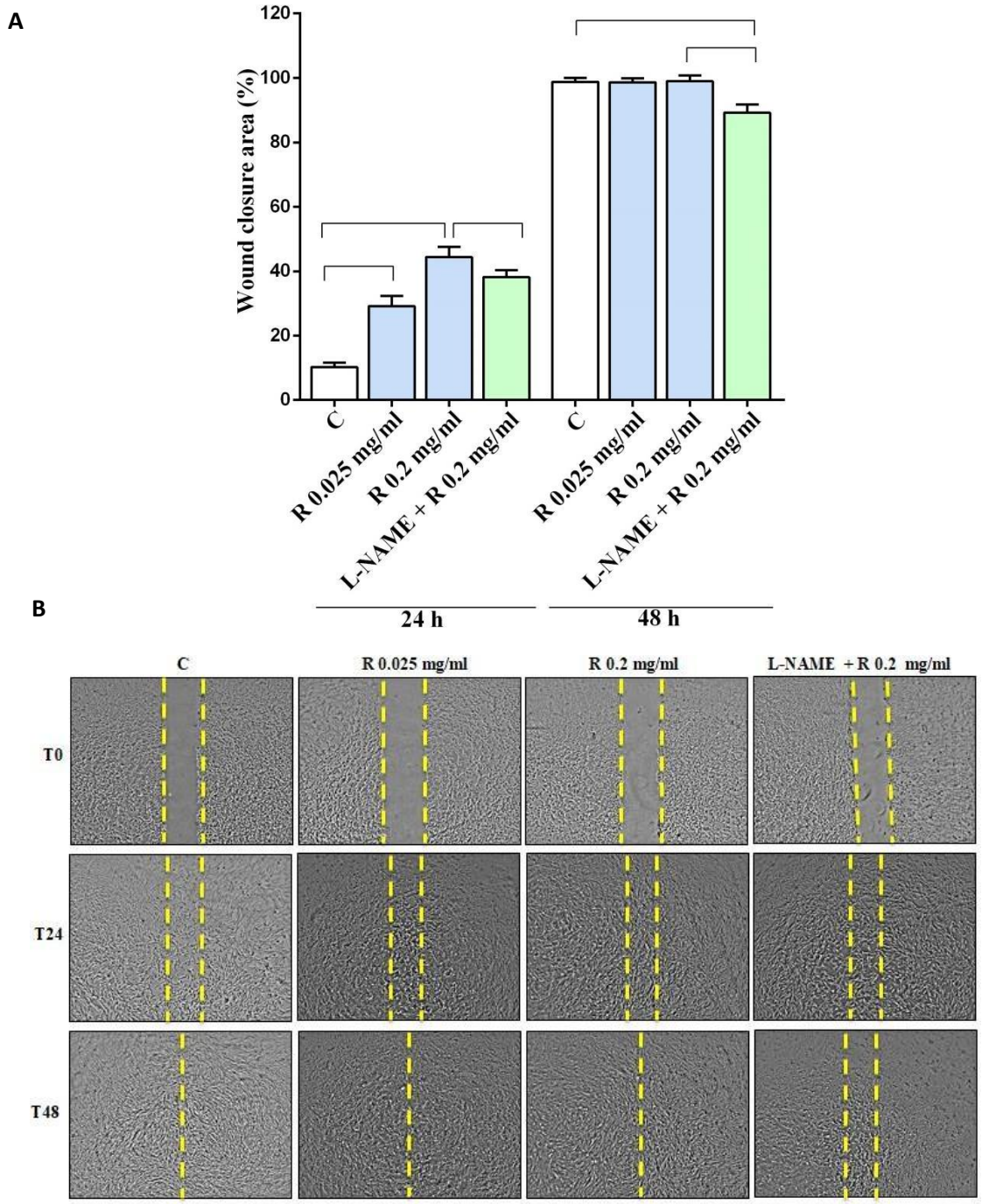

Figure 23: Effects of HUVEC/RPE cell co-culture on RPE cell migration after Ranibizumab stimulation. Abbreviations are as in previous Figures. In A, quantified data for the wound-healing assay are shown. In B, an example of photograph of the wound of each time (time 0 and after 24 h and 48 h), are shown. The images were taken at 4X magnification. The wound area and the percentage of healing were calculated for each time point. Reported data are means ± SD of five independent experiments for each experimental protocol. Short square brackets indicate significance between groups ($P<0.05$).

Aflibercept (Figure 22) and Ranibizumab (Figure 23), were able to increase RPE cell migration with a maximum effect at the major dose until 24 h from the wound. These effects were reduced when HUVEC were pretreated with the NOS inhibitor, L-NAME.

5.4 Effects of HUVEC/RPE cell co-culture on reactive oxygen species (ROS) production by RPE cells by using the DCFDA-Cellular ROS Detection Assay kit

The experiments were conducted by stimulating HUVEC with Aflibercept (0.025 mg/ml and 0.5 mg/ml) or Ranibizumab (0.025 mg/ml and 0.2 mg/ml) for 30 min, and the effects were analyzed on RPE cells in peroxidative conditions (200 µM H_2O_2 for 30 min). The acute effects on ROS release are visible in Figure 24.

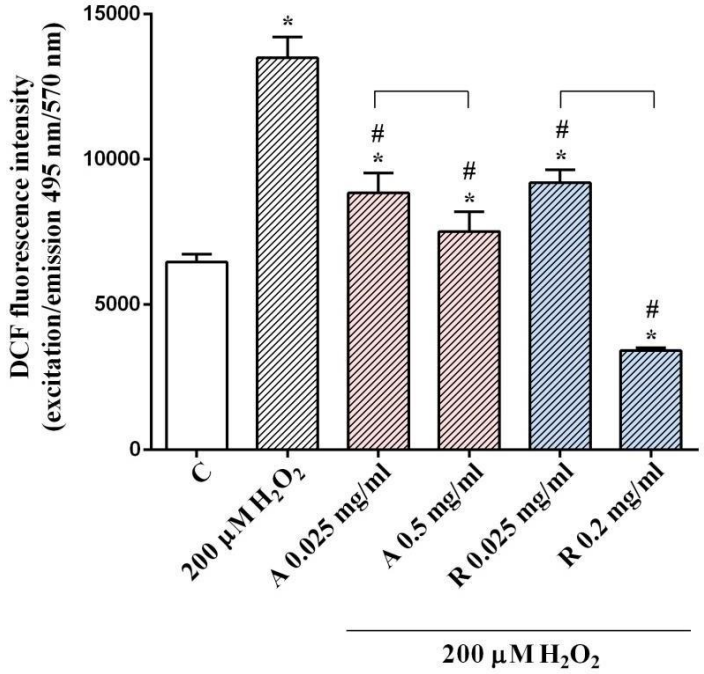

Figure 24: Effects of HUVEC/RPE cell co-culture on ROS production in RPE cells. Abbreviations are as in previous Figures. Results are expressed as DCF fluorescence intensity, which is proportional to the amount of intracellular ROS. Reported data are means ± SD of five independent experiments for each experimental protocol. Significance between groups: *P<0.05 vs C; #P<0.05 vs 200 µM H_2O_2. Short square brackets indicate significance between groups (P<0.05).

As shown in Figure 24, the stimulation of HUVEC cells with the two anti-VEGF drugs, was able to reduce ROS production by RPE cells in a dose-dependent manner with a maximum effect at 0.5 mg/ml for Aflibercept and 0.2 mg/ml for Ranibizumab.

5.5 Effects of HUVEC/RPE cell co-culture on RPE cell apoptosis by using Western blot analysis

In order to study if HUVEC cells stimulated with Aflibercept or Ranibizumab were able to modulate the apoptotic process in RPE cells, the expression of Cleaved Caspase 9 and Cytochrome C (Figure 25) was examined by Western blot and densitometric analysis. Furthermore, the effects

on the activation of Akt and ERK1/2 (Figure 26) were further investigated. The experiments were conducted by stimulating HUVEC cells with 0.5 mg/ml Aflibercept or 0.2 mg/ml Ranibizumab for 30 min, and the effects were analyzed on RPE cells in both physiological and peroxidative conditions (200 µM H_2O_2 for 6 h).

5.5.1 Effects on Cleaved Caspase 9 and Cytochrome C expression in RPE cells

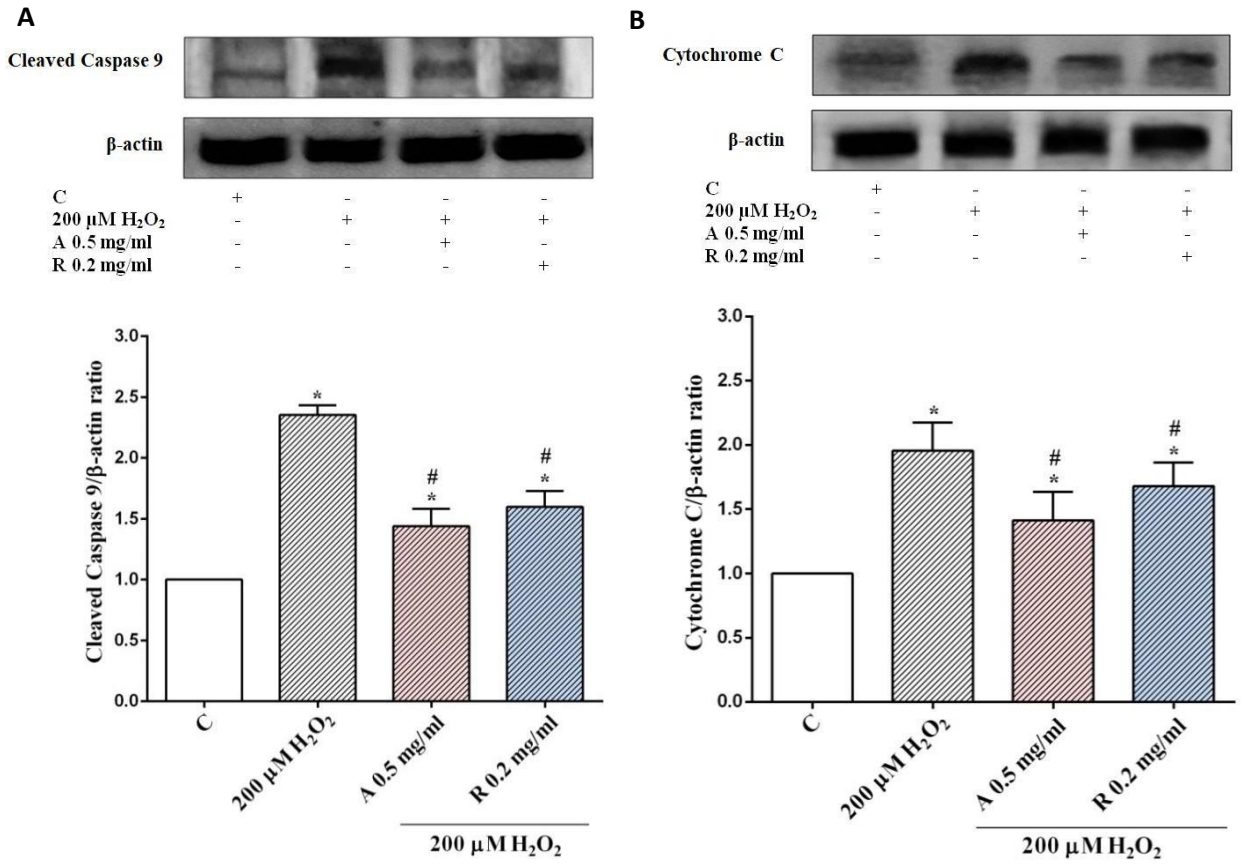

Figure 25: Variation in Cleaved Caspase 9 and Cytochrome C expression in RPE cells measured by Western blot and densitometric analysis. In A and B densitometric analysis and an example of Western blot taken from 5 different experiments of Cleaved Caspase 9 and Cytochrome C, respectively, are shown. Abbreviations are as in previous Figures. The data were normalized versus control value. Reported data are means ± SD of five independent experiments for each experimental protocol. Significance between groups: *P<0.05 vs C; #P<0.05 vs 200 µM H_2O_2.

As shown in Figure 25, the co-culture with HUVEC cells pretreated with Aflibercept and Ranibizumab, was able to counteract the effects of H_2O_2 on apoptosis in RPE cells, as evidenced by the inhibition of the expression of the Cleaved Caspase 9 and Cytochrome C.

5.5.2 Effects on Akt and ERK1/2 activation in RPE cells

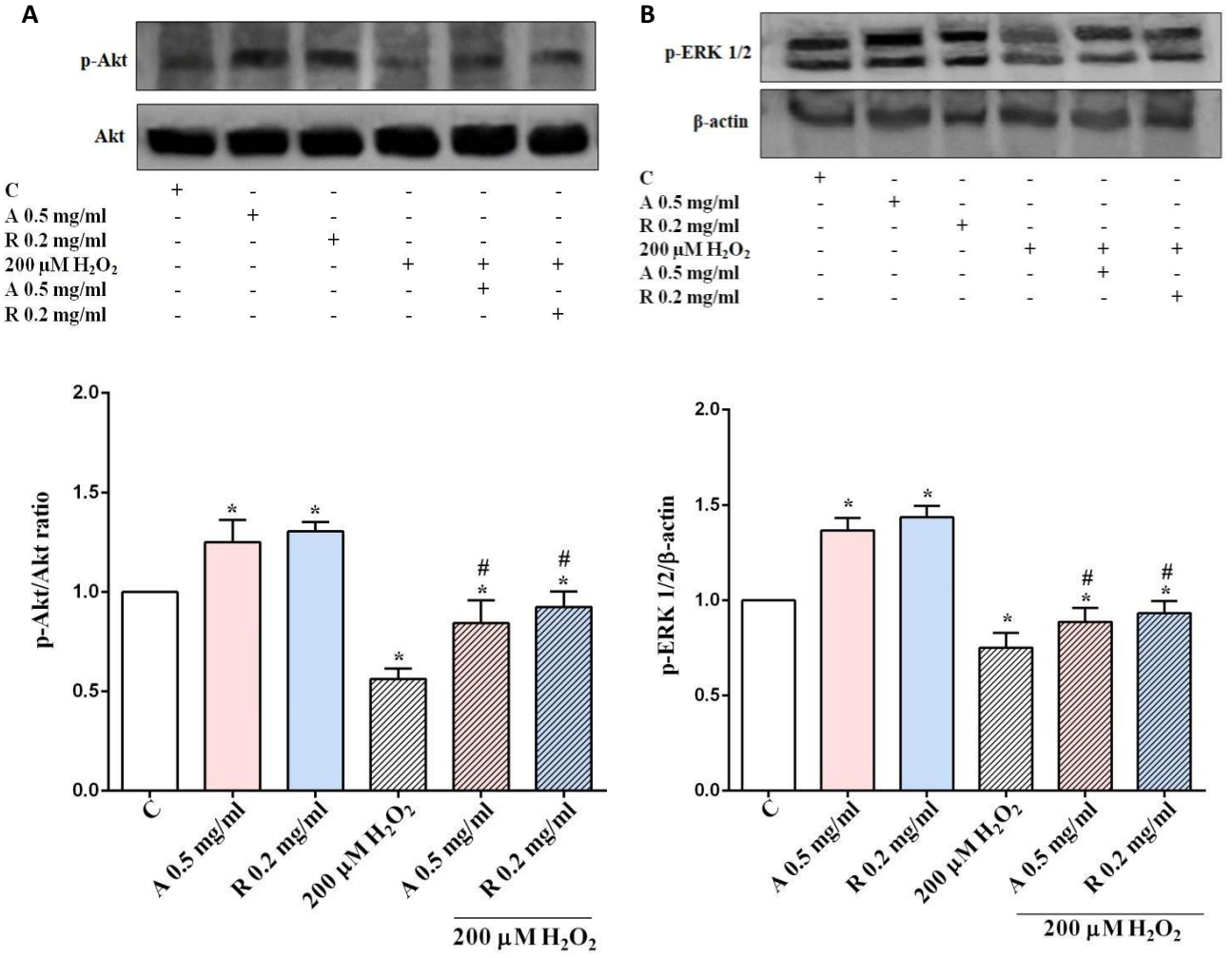

Figure 26: Variation in Akt and ERK 1/2 phosphorylation in RPE cells, measured by Western blot and densitometric analysis. In A and B densitometric analysis and an example of Western blot taken from 5 different experiments of p-Akt and p-ERK1/2 respectively, are shown. Abbreviations are as in previous Figures. The data were normalized versus control value. Reported data are means ± SD of five independent experiments for each experimental protocol. Significance between groups: *P<0.05 vs C; #P<0.05 vs 200 µM H_2O_2.

As shown in Figure 26, the co-culture with HUVEC cells, stimulated with Aflibercept or Ranibizumab, increased p-Akt and p-ERK1/2 in RPE cells cultured in physiologic conditions and prevented the inhibition of these survival kinases caused by H_2O_2.

Discussion

AMD is the leading cause of visual impairment and blindness in patients over 60 years old (Bian Z.M. *et al*., 2018). Given the enormous impact of AMD on an aging population, much public interest and research has been focused on it in the past decade. AMD initially occurs in a "dry" form with pathological changes in the RPE and drusen formation, and can progress to geographic atrophy and/or "wet" form of AMD with CNV (Zhuang P. *et al*., 2010). The RPE, a monolayer located between the photoreceptors and the vascular choroid, is constantly damaged by oxidative stress, particularly because of ROS.

RPE cells play vital roles in providing nutritional and structural support for the retina, and any sustained damage may consequently lead to loss of vision (Atienzar-Aroca S. *et al*., 2016; Luo X. *et al*., 2018). By protecting the retina from excess light and maintaining photoreceptor survival, RPE cells are capable of modulating sub-retinal ion balance and promoting the clearance of photoreceptor outer segments. Unfortunately, they do not renew after differentiation, inevitably resulting RPE cell apoptosis caused by long-term oxidative damage. In severe AMD cases, these apoptotic RPE cells release VEGF, the most significant pro-angiogenic factor. High levels of intraocular VEGF-A are found in CNV tissue from patients with AMD (Zampros I. *et al*., 2012). The malfunction of choroid circulation during the early stage of AMD, which leads to break down of Bruch's membrane, serves as an entrance for new and immature choroidal vessels to grow into the subretinal space that leads to the formation of CNV. In the severe late stage of the disease, CNV can leak fluid as well as hemorrhage in the subretinal space resulting in blurry vision, visual distortion and sudden loss of vision. If left untreated, these lesions progress to form an organized fibrous scar, termed "disciform scar", which typically results in irreversible central vision loss (Zhuang P. *et al*., 2010). Improvement and facilitation of ocular blood flow are, thus, mandatory to prevent CNV from occurring.

Intravitreal anti-VEGF therapy with drugs like Aflibercept and Ranibizumab has hugely improved the vision prognosis of neo-vascular AMD. However, the cellular mechanisms and signaling pathways conferring their protective effect are only partially understood.

This study has shown for the first time that anti-VEGF agents, Aflibercept and Ranibizumab, play an important role in the modulation of cell viability and mitochondrial membrane potential in RPE cells and HUVEC, cultured in either physiological or pathological conditions, by mechanisms related to NO release and cell survival. In the first part of the study, the direct effects of the two anti-VEGF drugs on RPE cells, were investigated. RPE cells are widely considered as the fulcrum of AMD pathogenesis and extensively used for *in vitro* studies in ophthalmology (Ambati J. *et al*., 2012; Corydon T.J. *et al*., 2016). Moreover, because the normal interaction between RPE and

choroidal endothelial cells appears critical for the maintenance of the outer-retina structure and function, pathological alterations of this relationship could be the primary event leading to vision-threatening pathologies such as macular degeneration. A better characterization of the homeostatic RPE cells-choroidal endothelial cells relationships is therefore particularly significant (Spencer C. *et al*., 2017). Thus, in the second part of the study, some experiments were also conducted by performing co-culture experiments between RPE cells and HUVEC, in order to analyze the cross-talk between vascular endothelial cells, which were directly treated with the two anti-VEGF drugs, and RPE cells. Hydrogen peroxide treatment of cultured cells is a commonly-used model to test oxidative stress susceptibility or antioxidant efficiency in various cell types that are at high risk for oxidative damage *in vivo*, such as RPE cells. Hence, RPE is located adjacent to the outer retina where it performs functions essential for photoreceptor survival. Oxidative stress to the largely non-mitotic RPE cell layer over time is theorized to produce tissue dysfunction that contributes to the development of AMD. The protection of RPE against oxidative damage would thus represent a potential therapeutic strategy for AMD (Stuart G.J. and Boulton M.E., 2012). In our study, we used H_2O_2 at a concentration which is widely adopted for inducing peroxidation (Kim M.H. *et al*., 2003; Kaczara P. *et al*., 2010; Li L. *et al*., 2015; Fong-Qi L. *et al*., 2003).

The results we have obtained have shown that Aflibercept and Ranibizumab, administrated at doses similar to the ones achievable in humans after intravitreal injections, and previously used in RPE cells (Malik D. *et al*., 2014), were able to increase the NO release by RPE cultured in physiological conditions. Opposite results were obtained in peroxidation, when both Aflibercept and Ranibizumab were able to reduce NO release caused by hydrogen peroxide. It is to note that similar findings were observed in HUVEC, which would highlight the involvement of NO in the mechanisms of action of the anti-VEGF agents on vasculature, too. Nitric oxide is generated from guanidine oxidation of L-arginine with the stoichiometric formation of L-citrulline by NOS in the presence of oxygen and NADPH (Sripathi S.R. *et al*., 2012). There are three different isoforms of NOS (Alderton W.K. *et al*., 2001), which are the inducible and calcium-independent NOS (iNOS), the constitutive and calcium-dependent neuronal NOS (nNOS) and endothelial NOS (eNOS) (Bhutto I.A. *et al*., 2010). While the constitutive NOSs, may act as a regulator of physiological phenomena, the inducible NOS, could be involved in longer-lasting cytotoxic and inflammatory functions (Goldstein I.M. *et al*., 1996). The fact that NO could exert protection or damage would depend on its concentration and to the relative activity of the constitutive or inducible NOS (Goldstein I.M. *et al*., 1996). In fact, while NO produced in low concentrations, as in the case of the eNOS activation, would act as a messenger and cytoprotective factor (Liaudet L. *et al*., 2000) the stimulation of iNOS and NO

overproduction, could increase RNS formation and cause cellular death. In the retina, NOS is found in retinal neurons, RPE cells, amacrine and ganglion cells, nerve fibers in the outer and inner plexiform layers, and in photoreceptors. Evidence emerged about the role of NO as a mediator of physiological, and possibly pathological, processes in all above retina structures (Sripathi S.R. *et al*., 2012; Goldstein I.M. *et al*., 1996; Ostwald P. and Roth S., 2012). In this context, small amount of eNOS-derived NO could act as a potent vasodilator and play a key role in the physiological regulation of ocular blood flow (Bhutto I.A. *et al*., 2010; Friedman E. *et al*., 1997; Grunwald J. *et al*., 1998). Furthermore, in RPE cells, NO contributes to the function of phagocytosis of rod outer segments and regulation of vascular endothelial growth factor gene expression. However, under oxidative stress, a high concentration of NO would react with superoxide anion (O_2^-) to produce peroxynitrite ($ONOO^-$), a potential cytotoxic and tyrosine nitrating molecule, which could lead to the accumulation of protein aggregates between photoreceptors and RPE cells, which would result in photoreceptor degeneration. Changes of NOS in AMD suggest that retinal degeneration is directly or indirectly related to local NO concentration in the RPE. Thus, NO does appear to play a role in the visual transduction system (Sripathi S.R. *et al*., 2012; Goldstein I.M. *et al*., 1996). Furthermore, eNOS itself has been reported to be a redox "hub", being regulated by GSH-dependent pathways. Hence, changes of GSH have been reported to cause eNOS "uncoupling", which would trigger ROS production from the oxygenase domain (Crabtree M.J. *et al*., 2013). The results we obtained about NO release and eNOS/iNOS activation/expression are in agreement with previous findings. Hence, while eNOS was found to be mainly involved in NO release in physiological conditions, iNOS expression, as well as, eNOS activation were found to be increased during peroxidation.

In previous studies, long-term exposure of RPE to anti-VEGF agents had no effect on cell viability. It was even shown by Oh et al., that anti-VEGF agents interfered with the physiological functions of RPE cells under high-glucose conditions, by decreasing cell viability and proliferation (Oh J.R. *et al*., 2017). Regarding mitochondria function, so far data are quite scarce and controversial. Mitochondrial membrane potential has been considered as a good indicator of the energy status of the mitochondria and, above all, of cellular homeostasis. Interestingly, changes in mitochondrial membrane potential have been reported to be correlated with cell survival or death through apoptosis (Javadov S. *et al*., 2007). Apoptotic signaling is mediated by the collapse of the mitochondrial membrane potential induced by mitochondrial transition pores opening. Loss of mitochondrial membrane potential would lead to depolarization of the inner mitochondrial membrane and by the subsequent release of mitochondrial Cytochrome C and downstream

activation of effector caspases (Ormel J. *et al*., 2011; Green D.R. and Reed J.C., 1998; Russell J.W. *et al*., 2002).

In a previous study by Malik et al. (Malik D. *et al*., 2014), neither Ranibizumab or Aflibercept produced any evidence of mitochondrial beneficial effect at clinical doses, whereas mitochondrial toxicity was observed at clinically relevant doses. In contrast, Sheu et al. (Sheu S.J. *et al*., 2015), hypothesized that the early protective action on mitochondrial bioenergetic capacity could predict possible long term antioxidative effects of Aflibercept and Ranibizumab in the eye. Overall, this is the first study showing protective effects of anti-VEGF agents on cell viability and mitochondrial membrane potential.

The latter finding could be of significant clinical relevance. Hence, previous data have shown a clear association between RPE health and compromised mitochondrial function. High numbers of mitochondria are present in metabolically active cells like RPE cells while their number decreases with age, particularly in AMD (Juel H.B. *et al*., 2013; Liang F.Q. *et al*., 2003; Malek G, *et al*., 2012). Experimental findings have also shown a link between mitochondrial impairment and RPE degeneration, which would arise as a consequence of an in balance of the cellular redox system.

In particular, mitochondrial depolarization has been reported to precede RPE cell death caused by peroxidation through the reduction of energy production, as well as, the increase in Cytochrome C release and ROS generation (Barot M. *et al*., 2011; Armstrong J.S., 2006; Green D.R. and Kroemer G., 2004).

It is noteworthy that in our study both anti-VEGF agents, in addition to preventing the fall of cell viability and mitochondrial membrane potential, were also able to increase cell proliferation and migration, and counteract the effects of H_2O_2.

Also this aspect could be of particular relevance in clinics. Hence, there are emerging signals that anti-VEGF treatment can potentially increase development of RPE cell atrophy and even macular atrophy, leading to geographic atrophy (GA) (Gemenetzi M. *et al*., 2017 Lois N. *et al*., 2013). In eyes with neovascular AMD undergoing multiple anti-VEGF injections, Lois et al., (Lois N. *et al*., 2013) reported progression of RPE atrophy in approximately 60% of eyes. Moreover, the number of anti-VEGF injections was significantly associated with the progression of atrophy with each additional anti-VEGF injection increasing the odds of developing atrophy by a factor of 1.35. Data from randomized clinical trials using Ranibizumab are controversial. On the one hand, the "Comparison of AMD Treatments Trials (CATT)" reported that after a 5-year treatment, higher rate of GA was associated with the specific clinical characteristics of choroidal neovascularization lesion, whereas no significant difference was found between the two drugs or the dosing regimen

(Grunwald J.E. *et al*., 2017). On the other hand, data from the "Inhibition of VEGF in Age-related choroidal Neovascularization (IVAN)" trial reported that after a 2-year treatment, GA was not different between two drug groups but it was significantly lower when discontinuous treatment was applied (Chakravarthy U. *et al*., 2013). Long-term data on the use of Ranibizumab in neovascular AMD documented that macular atrophy progression was major determinant of final visual acuity (Bhisitkul R.B. *et al*., 2015). Our data showing protective effects elicited by anti-VEGF agents in RPE cell proliferation and migration are in contrast with findings reported from *in vivo* studies, evidencing tears in the RPE after Aflibercept and Ranibizumab treatment (Wons J. *et al*., 2017). Changes in ocular microenvironment or effects of those anti-VEGF agents on retinal cells other than RPE cells, as well as, in their cross-talk, could be at basis of these discrepancies. Although the exact mechanisms of anti-VEGF effect on macular atrophy has not been fully elucidated, data from the present study indicate that the keeping of mitochondria function could be hypothesized to play a key role.

The protective effect Aflibercept and Ranibizumab on RPE cells response to oxidative stress, has been confirmed by the analysis of ROS release.

Oxidative stress, which is caused by the accumulation of intracellular ROS or RNS, is one of the leading factors triggering RPE cell apoptosis. Furthermore, the accumulation of ROS in mitochondria can lead to apoptotic cell death and ROS may also have direct effects on cellular structure and function. In our study Aflibercept and Ranibizumab, were able to reduce ROS production induced by H_2O_2, and to decrease apoptosis as shown by Annexin V/PI staining and Western blot. Western blot analysis performed on RPE cells, confirmed data on peroxidation about protective effects elicited by anti VEGF agents. In fact, both Aflibercept and Ranibizumab were able to counteract the activation of apoptotic markers such as Cytochrome C and Caspase 9. On the other hand, in our study, short-term exposure of RPE cells to H_2O_2 was able to reduce Akt activation, as previously shown in the same cellular model (Baek S.M. *et al*., 2016), an effect that was hindered by pretreatment of RPE cells with either Aflibercept or Ranibizumab. Thus, although it was not clearly examined, the activation of intracellular signaling downstream Akt and ERK1/2 could be hypothesized to be involved in the protective effects elicited by the anti-VEGF agents against AMD. The signaling pathways downstream Akt and ERK1/2 activation are known to be involved in the regulation of cellular proliferation, differentiation, and survival processes in many cell lines, amongst which are RPE cells. In particular, the stimulators of PI3K/Akt could represent a promising therapeutic tool for the prevention of the RPE degeneration, and theoretically, for the treatment of eye disorders, such as AMD (Zheng W. *et al*., 2018; Zha X. *et al*., 2015). In Figure 1, a

schematic representation of the intracellular signalling modulated by the anti-VEGF drugs in aged RPE cells is shown.

Interesting data were obtained by experiments of HUVEC/RPE cell co-culture. HUVEC cells stimulated in physiologic conditions with Aflibercept or Ranibizumab, were able to increase the NO release by RPE cells. Interestingly, the effects of the two anti-VEGF agents on NO release were reduced in the presence of L-NAME, as well as, in the presence of PI3K, Akt, ERK1/2, or p38MAPK inhibitors. Thus, at the basis of the effects of NO release by RPE cells caused by HUVEC stimulation with Aflibercept or Ranibizumab in physiologic conditions, there would be the activation of an intracellular signalling in HUVEC leading to PI3K, Akt, ERK1/2, p38MAPK activation and eNOS phosphorylation (Ciccarelli M. *et al*., 2007; Grossini E. P. *et al*., 2012). Hence, PI3K/Akt and MAPK pathways, are widely known to be involved in eNOS activation by phosphorylation on Ser^{1177}, or through the activation of calcium/calmodulin kinase II (CAMKII).
In contrast, in peroxidative conditions, the two agents were able to reduce the excessive release of NO caused by H_2O_2, an effect which was counteracted by the same inhibitors.
The protective effects of anti VEGF on mitochondrial function and against ROS release could be speculated to play a role in the above effect. Hence, changes in oxidant/antioxidant balance could activate eNOS "uncoupling", which would trigger ROS/RNS production from the oxygenase domain, and increase iNOS expression. Further studies will be, however, mandatory to better clarify those issues.

Moreover, as observed in RPE cells directly treated with Aflibercept or Ranibizumab, also in co-culture experiments, an increase of cell viability, and a prevention of mitochondrial membrane potential collapse in RPE cells, were evident, in both physiological and peroxidative conditions. These effects were reduced or inhibited by the HUVEC pre-treatment with the same inhibitors used for NO studies. Furthermore, the effects of H_2O_2 on ROS release were reduced. Western blot analysis also confirmed those findings, by showing a reduction of apoptotic markers such as Cytochrome C and Caspase 9, and an increased activation of Akt and ERK1/2 kinases. It is important to note that, in co-culture conditions, the effect of Aflibercept and Ranibizumab against peroxidation, were much more evident than those observed with the direct stimulation of RPE cells. Thus, the co-culture experiments would confirm the importance of the cross talk between HUVEC and RPE cells in the prevention of oxidative stress damage and RPE cell apoptosis, and in eliciting the protective effects of Aflibercept and Ranibizumab. Differences obtained with treatment of RPE cells alone or in co-culture with HUVEC could be related to the role of paracrine stimuli derived

from vascular endothelial cells, that could modulate RPE cell viability/mitochondrial membrane potential. The paracrine effects of HUVEC may include the role of exosomes, which are small vesicles, between 50 and 150 nm in diameter, released by a number of different cell types, including endothelial cells. Exosomes contain proteins, DNA, mRNA, cytokines, and growth factors, which could make these vesicles essential in cell communication. It is to note that exosomes could be found in many corporal fluids, including blood, saliva, breast milk and even aqueous humour and would play an important role in the cellular microenvironment (Atienzar-Aroca S. *et al*., 2016). Although not clearly examined, the results obtained in the presence of inhibitors would also highlight the involvement of both MAPK and Akt in the intracellular signalling activated in HUVEC by anti-VEGF drugs and involved in their effects on RPE cells.

Interesting results were also observed on RPE cell proliferation and migration, which was, however, less marked than those found with the direct treatment of RPE cells. In addition, these findings were confirmed by the increased expression of p21, which is well known to promote cell survival in response to oxidative stress (Gehen S.C. *et al*., 2008). Furthermore, it is to note that the activated cell migration of RPE cells was reduced in the presence of L-NAME, which indicates that NO may function as a regulator of cell motility during wound healing (Figure 2).

6.1 Conclusions

This study has shown for the first time new mechanisms involving NO, and mitochondria, in the actions of Aflibercept and Ranibizumab in RPE cells. Our results, showing the effects of anti-VEGF agents in both physiologic and pathologic contexts, could not only increase knowledge about the physiology of RPE cells, but also could have important implication in clinical conditions. Our data may indicate that the progression of atrophy in patients with neovascular AMD treated with Ranibizumab or Aflibercept are not due to the treatment itself, but that additional local factors may play an important role. Specific subtypes of neovascular AMD have shown different natural evolution, thus with major probability to progress to the atrophy stage. Therefore, further clinical and experimental studies are needed to better understand the interaction between anti-VEGF treatment and the progression of atrophy in patients with AMD.

6.2 Future perspectives

As concerning the first part of the study, in the next future, we want to study in deep the mechanisms involved in the NO production, analyzing the effects of the two anti-VEGF drugs in the regulation of antioxidant systems. Furthermore, the use of selective inhibitors for both NOS isoforms, could help to better understand their mechanism of action. As regarding the second part of

the study, we would like to analyze the supernatant released by HUVEC and RPE cells, by using proteomic analysis. Thanks to mass spectrometry, it would be possible to investigate the highest number of proteins present in the supernatant, to quantify their level of expression, and post-translational modifications, to examine any protein interactions, as well as their sub-cellular distribution. Moreover, we would like to verify the hypothesis about the possible role of the exosomes in the cross-talk between HUVEC and RPE cells. For this purpose, the supernatant would be subjected to ultracentrifuge, in order to isolate any exosomes. Next, in order to characterize isolated nanoparticles, and to determine the size and concentration, the NanoSight instrument would be used.

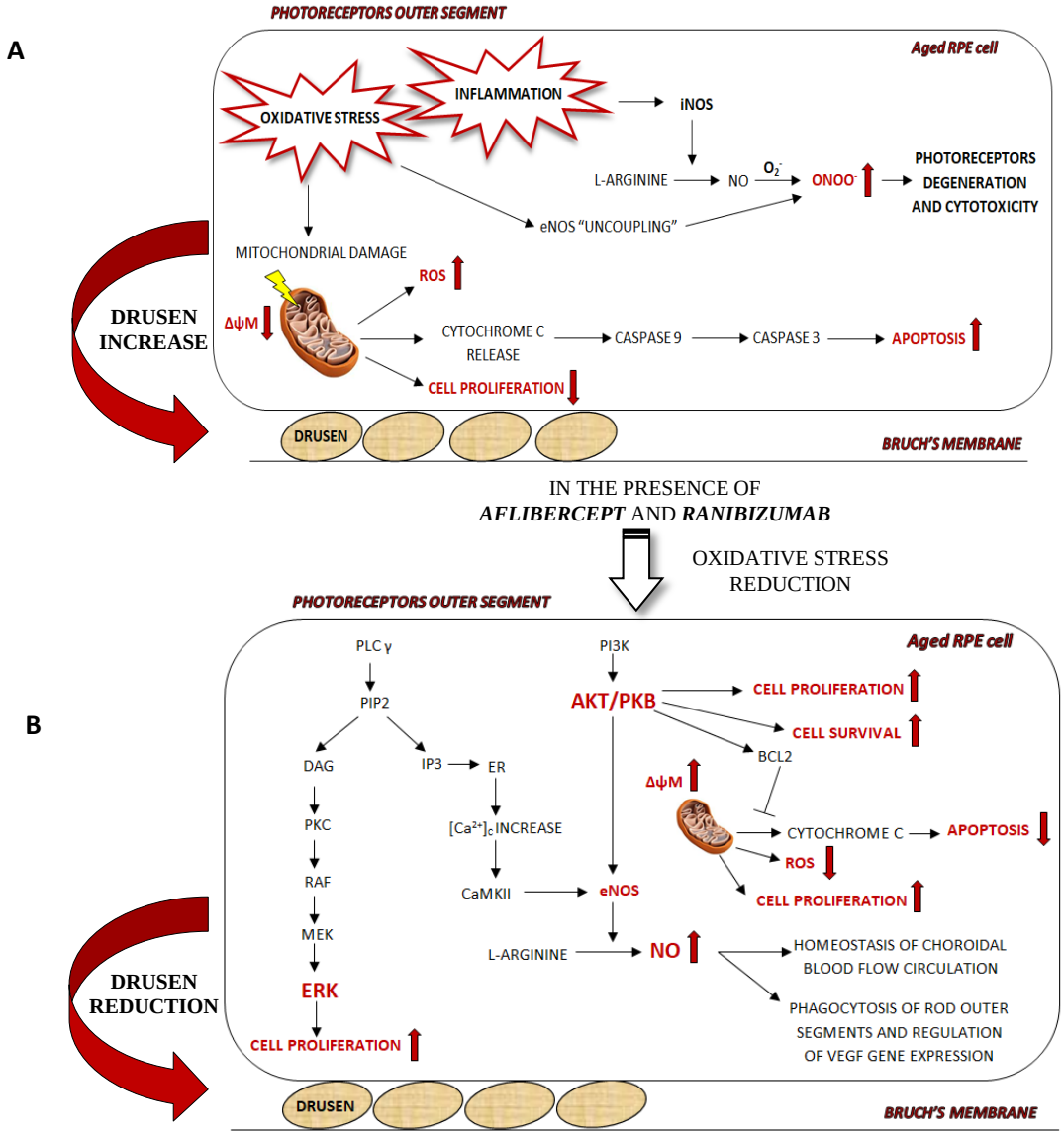

Figure 1: Graphical rapresentation about the effects of Aflibercept and Ranibizumab. The pathways are simplified, and only selected components are shown. In A, the role of aged RPE in AMD pathogenesis is shown. Oxidative stress and inflammation have a major role in the development and progression of AMD. An increase of peroxidation induces a reduction of mitochondrial membrane potential, resulting in cytochrome C release from mitochondrial membrane and activation of the apoptotic cascade. Mitochondrial damage is followed by a higher generation of ROS and a decrease in cell proliferation. The increase in inflammation causes the increase in iNOS expression with consequent excessive production of NO. Under oxidative stress, a high concentration of NO would react with O_2^- to produce $ONOO^-$, a potential cytotoxic and tyrosine nitrating molecule, which could lead to the accumulation of protein aggregates between photoreceptors and RPE, which would result in photoreceptor degeneration. Oxidative stress also causes eNOS "uncoupling", which would trigger ROS production from the oxygenase domain. The progressive dysfunction of the RPE, photoreceptor loss, and retinal degeneration, are followed by the drusen accumulation. In B, the effects of Aflibercept and Ranibizumab on aged RPE, are shown. In the presence of the two anti-VEGF drugs, there is a reduction of oxidative stress and an activation of MAPK and PI3K/Akt pathways, which causes an increase of cell viability, cell proliferation and mitochondrial membrane potential. The activation of anti-apoptotic BCL2 inhibits the release of cytochrome C from mitochondrial membrane. The increase of intracellular Ca^{2+} induced calcium/calmodulin kinase II (CAMKII) would be followed by eNOS activation. eNOS is also activated by phosphorylation on Ser^{1177}.

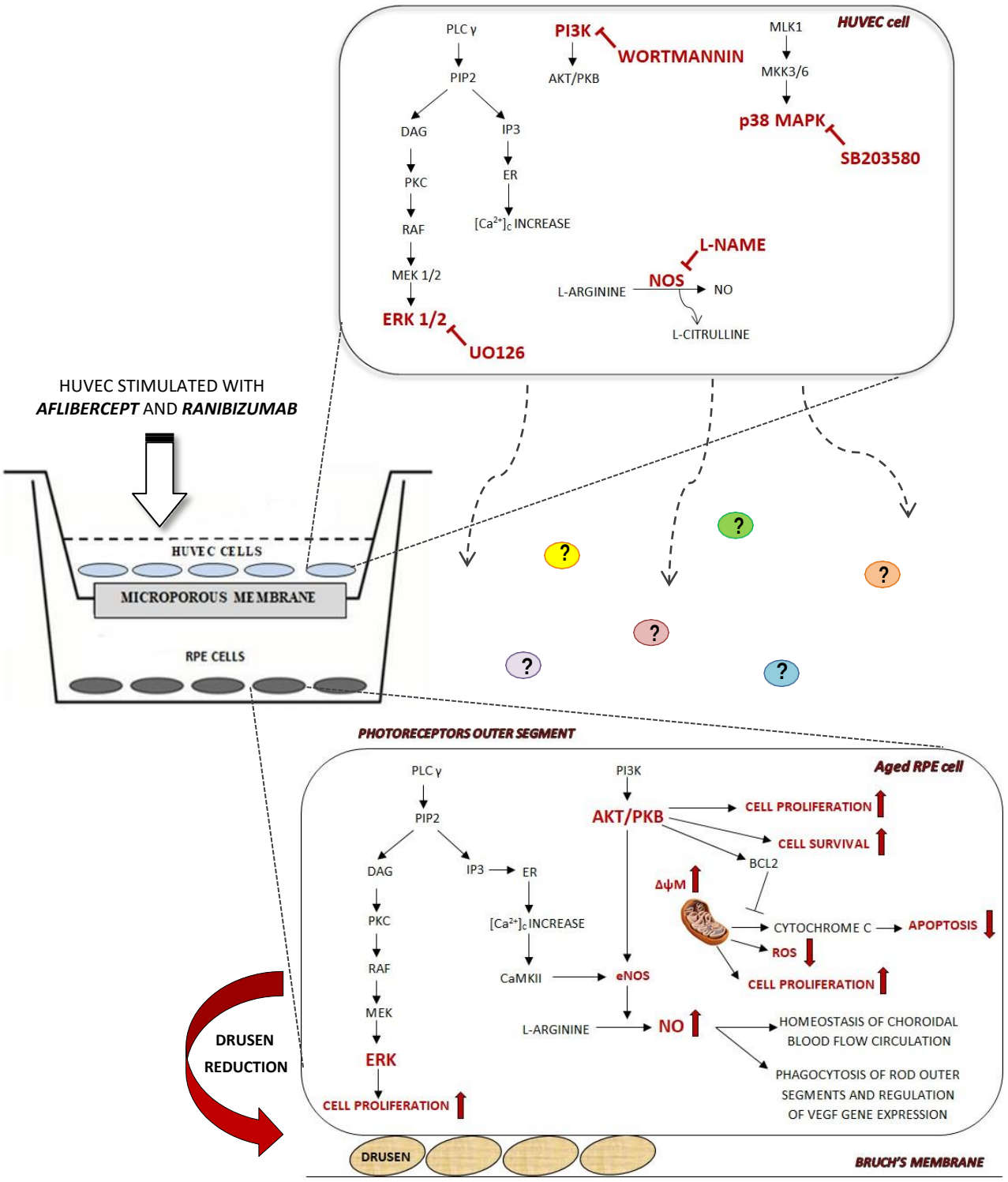

Figure 2: Graphical rapresentation about the HUVEC/RPE cross-talk. The pathways are simplified, and only selected components are shown. The HUVEC with Aflibercept and Ranibizumab, are able to increase proliferation, survival, NO release, and to improve mitochondrial membrane potential (ΔΨM) of aged RPE. On the contrary, ROS and RPE apoptosis are reduced. The above effects are related to the activation of signalling involving ERK1/2 and Akt that would lead to the keeping cell viability and mitochondrial function and to a "physiologic" NO release by eNOS. All the above events, accompanied by the modulation of choroidal perfusion and of the phagocytosis of rod outer segments and VEGF expression, would counteract drusen formation in the Bruch's membrane. Although not clearly examined, some paracrine stimuli could be involved in the cross-talk between HUVEC and RPE.

Bibliography

1. Ablonczy, Z., Dahrouj, M., Tang, P.H., Liu, Y., Sambamurti, K., Marmorstein, A.D., Crosson, C.E. (2011). Human retinal pigment epithelium cells as functional models for the RPE in vivo. Invest. Ophthalmol. Vis. Sci. *52*, 8614-20
2. Agrawal, S., Joshi, M., Christoforidis, J.B. (2013). Vitreous inflammation associated with intravitreal anti-VEGF pharmacotherapy. Mediators Inflamm. *2013*, 943409
3. Alderton, W.K., Cooper, C.E., Knowles, R.G. (2001). Nitric oxide synthases: structure, function and inhibition. Biochem. J. *357*, 593-615
4. Ambati, J., Fowler, B.J. (2012). Mechanisms of age-related macular degeneration. Neuron. *75*, 26-39
5. Armstrong, J.S. (2006). Mitochondrial membrane permeabilization: the sine qua non for cell death. Bioessays *28*, 253-260
6. Arya, M., Sabrosa, A.S., Duker, J.S., Waheed, N.K. (2018). Choriocapillaris changes in dry age-related macular degeneration and geographic atrophy: a review. Eye Vis (Lond). 5:22
7. Atienzar-Aroca, S., Flores-Bellver, M., Serrano-Heras, G., Martinez-Gil, N., Barcia, J.M., Aparicio, S., Perez-Cremades, D., Garcia-Verdugo, J.M., Diaz-Llopis, M., Romero, F.J., Sancho-Pelluz, J. (2016). Oxidative stress in retinal pigment epithelium cells increases exosome secretion and promotes angiogenesis in endothelial cells. J. Cell. Mol. Med. *20*, 1457-66
8. Atienzar-Aroca, S., Flores-Bellver, M., Serrano-Heras, G., Martinez-Gil, N., Barcia, J.M., Aparicio, S., Perez-Cremades, D., Garcia-Verdugo, J.M., Diaz-Llopis, M., Romero, F.J., Sancho-Pelluz. (2016). Oxidative stress in retinal pigment epithelium cells increases exosome secretion and promotes angiogenesis in endothelial cells. J. Cell. Mol. Med. *20*, 1457-1466
9. Baek, S.M., Yu, S.Y., Son, Y., Hong, H.S. (2016). Substance P promotes the recovery of oxidative stress-damaged retinal pigmented epithelial cells by modulating Akt/GSK-3β signaling. Mol. Vis. *22*, 1015-1023
10. Bandello, F., Sacconi, R., Querques, L., Corbelli, E., Cicinelli, M.V., Querques, G. (2017). Recent advances in the management of dry age-related macular degeneration: A review. F1000Res. *6*, 245
11. Barot, M., Gokulgandhi, M.R., Mitra, A.K. (2011). Mitochondrial Dysfunction in Retinal Diseases. Curr. Eye Res. *36*, 1069-107
12. Bergen, A.A., Arya, S., Koster, C., Pilgrim, M.G., Wiatrek-Moumoulidis, D., Van Der Spek, P.J., Hauck, S.M., Boon, C.J.F., Emri, E., Stewart, A.J., Lengyel, I. (2018). On the origin of proteins in human drusen: The meet, greet and stick hypothesis. Prog. Retin. Eye Res. *S1350-9462*, 30041-7
13. Bhisitkul, R.B., Mendes, T.S., Rofagha, S., Enanoria, W., Boyer, D.S., Sadda, S.R., Zhang, K. (2015). Macular atrophy progression and 7-year vision outcomes in subjects from the ANCHOR, MARINA, and HORIZON studies: the SEVEN-UP study. Am. J. Ophthalmol. *159*, 915-924
14. Bhutto, I.A., Baba, T., Merges, C., McLeod, D.S., Lutty, G.A. (2010). Low nitric oxide synthases (NOSs) in eyes with age-related macular degeneration (AMD). Exp Eye Res. *90*, 155-67
15. Bian, Z.M., Field, M.G., Elner, S.G., Kahlenberg, J.M., Elner, V.M. (2018). Distinct CD40L receptors mediate inflammasome activation and secretion of IL-1β and MCP-1 in cultured human retinal pigment epithelial cells. Exp. Eye Res. *170*, 29-39
16. Blasiak, J., Glowacki, S., Kauppinen, A., Kaarniranta, K. (2013). Mitochondrial and nuclear DNA damage and repair in age-related macular degeneration. Int. J. Mol. Sci. *14*, 2996-3010
17. Blasiak, J., Petrovski, G., Veréb, Z., Facskó, A., Kaarniranta, K. (2014). Oxidative stress, hypoxia, and autophagy in the neovascular processes of age-related macular degeneration. Biomed. Res. Int. *2014*, 768026
18. Boltz, A., Luksch, A., Wimpissinger, B., Maar, N., Weigert, G., Frantal, S., Brannath, W., Garhöfer, G., Ergun, E., Stur, M., Schmetterer, L. (2010). Choroidal blood flow and progression of age-related macular degeneration in the fellow eye in patients with unilateral choroidal neovascularization. Invest. Ophthalmol. Vis. Sci.*51*, 4220-5

19. Booij, J.C., Baas, D.C., Beisekeeva, J., Gorgels, T.G., Bergen, A.A. (2010). The dynamic nature of Bruch's membrane. Prog. Retin Eye Res. *29*, 1-18
20. Carr, A.J., Smart, M.J., Ramsden, C.M., Powner, M.B., Da Cruz, L., Coffey, P.J. (2013). Development of human embryonic stem cell therapies for age-related macular degeneration. Trends Neurosci. 36, 385-95
21. Chakravarthy, U., Harding, S.P., Rogers, C.A., Downes, S.M., Lotery, A.J., Culliford, L.A., Reeves, B.C. (2013). IVAN study investigators: Alternative treatments to inhibit VEGF in age-related choroidal neovascularisation: 2-year findings of the IVAN randomised controlled trial. Lancet *382*, 1258-1267
22. Chen, W.J., Wu, C., Xu, Z., Kuse, Y., Hara, H., Duh, E.J. (2016). Nrf2 protects photoreceptor cells from photo-oxidative stress induced by blue light. Exp Eye Res. *154*, 151-158
23. Chiou, G.C. (2001). Review: effects of nitric oxide on eye diseases and their treatment. J. Ocul. Pharmacol. Ther. *17*, 189-98
24. Ciccarelli, M., Cipolletta, E., Santulli, G., Campanile, A., Pumiglia, K., Cervero, P., Pastore, L., Astone, D., Trimarco, B., Iaccarino, G. (2007). Endothelial beta2 adrenergic signaling to AKT: role of Gi and SRC. Cell Signal. *19*, 1949-55
25. Corydon, T.J., Mann, V., Slumstrup, L., Kopp, S., Sahana, J., Askou, A.L., Magnusson, N.E., Echegoyen, D., Bek, T., Sundaresan, A., Riwaldt, S., Bauer, J., Infanger, M., Grimm, D. (2016). Reduced expression of cytoskeletal and extracellular matrix genes in human adult retinal pigment epithelium cells exposed to simulated microgravity. Cell. Physiol. Biochem. *40*, 1-17
26. Crabtree, M.J., Brixey, R., Batchelor, H., Hale, A.B., Channon, K.M. (2013). Integrated redox sensor and effector functions for tetrahydrobiopterin- and glutathionylation-dependent endothelial nitric-oxide synthase uncoupling. J. Biol. Chem. *288*, 561-569
27. Datta, S., Cano, M., Ebrahimi, K., Wang, L., Handa, J.T. (2017). The impact of oxidative stress and inflammation on RPE degeneration in non-neovascular AMD. Prog. Retin. Eye Res. *60*, 201-218
28. De Cillà, S., Farruggio, S., Vujosevic, S., Raina, G., Filippini, D., Gatti, V., Clemente, N., Mary, D., Vezzola, D., Casini, G., Rossetti, L., Grossini, E. (2017). Anti-Vascular Endothelial Growth Factors Protect Retinal Pigment Epithelium Cells Against Oxidation by Modulating Nitric Oxide Release and Autophagy. Cell. Physiol. Biochem. *42*, 1725-1738
29. Ehlken, C., Jungmann, S., Böhringer, D., Agostini, H.T., Junker, B., Pielen, A. (2014). Switch of anti-VEGF agents is an option for nonresponders in the treatment of AMD. Eye (Lond). *28*, 538-45
30. Enseleit, F., Michels, S., Ruschitzka, F. (2010). Anti-VEGF therapies and blood pressure: more than meets the eye. Curr. Hypertens. Rep. *12*, 33-8
31. Evereklioglu, C., Er, H., Doganay, S., Cekmen, M., Turkoz, Y., Otlu, B., Ozerol, E. (2003). Nitric oxide and lipid peroxidation are increased and associated with decreased antioxidant enzyme activities in patients with age-related macular degeneration. Doc. Ophthalmol. *106*, 129-36
32. Falavarjani, K.G., Nguyen, Q.D. (2013). Adverse events and complications associated with intravitreal injection of anti-VEGF agents: a review of literature. Eye (Lond) *27*, 787-94
33. Fehér, J., Kovács, B., Kovács, I., Schvöller, M., Corrado, B.G. (2007). Metabolic therapy for early treatment of age-related macular degeneration. Orv. Hetil *148*, 2259-68
34. Fiebai, B., Odogu, V. (2017). Intravitreal Anti Vascular Endothelial Growth Factor Agents in The Management of Retinal Diseases: An Audit. Open Ophthalmol. J. *11*, 315-321
35. Fong-Qi, L., Bernard, F.G. (2003). Oxidative stress-induced mitochondrial DNA damage in human retinal pigment epithelial cells: a possible mechanism for RPE aging and age-related macular degeneration. Experimental Eye Research *76*, 397-403
36. Friedman, E. (1997). A hemodynamic model of the pathogenesis of age-related macular degeneration. Am. J. Ophthalmol. *124*, 677-82

37. Gehen, S.C., Staversky, R.J., Bambara, R.A., Keng, P.C., O'Reilly, M.A. (2008). hSMG-1 and ATM sequentially and independently regulate the G1 checkpoint during oxidative stress. Oncogene *27*, 4065-74.
38. Gemenetzi, M., Lotery, A.J., Patel, P.J. (2017). Risk of geographic atrophy in age-related macular degeneration patients treated with intravitreal anti-VEGF agents. Eye (Lond) *31*, 1-9
39. Goldstein, I.M., Ostwald, P., Roth, S. (1996). Nitric oxide: a review of its role in retinal function and disease. Vision Res. *36*, 2979-2994
40. Green, D.R., Kroemer, G. (2004). The pathophysiology of mitochondrial cell death. Science *305*, 626-9
41. Green, D.R., Reed, J.C. (1998). Mitochondria and apoptosis. Science *281*, 1309-12
42. Green, W.R., Key, S.N. (2005). Senile macular degeneration: a histopathologic study. 1977. Retina *25*, 180-250
43. Grossini, E., Caimmi, P., Molinari, C., Uberti, F., Mary, D., Vacca, G. (2012). CCK receptors-related signaling involved in nitric oxide production caused by gastrin 17 in porcine coronary endothelial cells. Mol. Cell. Endocrinol. *350*, 20-30
44. Grossini, E., Farruggio, S., Raina, G., Mary, D., Deiro, G., Gentilli, S. (2018). Effects of Genistein on Differentiation and Viability of Human Visceral Adipocytes. Nutrients *10*, pii: E978
45. Grossini, E., Gramaglia, C., Farruggio, S., Bellofatto, K., Anchisi, C., Mary, D., Vacca, G., Zeppegno, P. (2014). Asenapine increases nitric oxide release and protects porcine coronary artery endothelial cells against peroxidation. Vascul. Pharmacol. *60*, 127-141
46. Grossini, E., Marotta, P., Farruggio, S., Sigaudo, L., Qoqaiche, F., Raina, G., De Giuli, V., Mary, D., Vacca, G., Pollastro, F. (2015). Effects of Artemetin on Nitric Oxide Release and Protection against Peroxidative Injuries in Porcine Coronary Artery Endothelial Cells. Phytother. Res. *29*, 1339-1348
47. Grossini, E., Raina, G., Farruggio, S., Camillo, L., Molinari, C., Mary, D., Walker, G.E., Bona, G., Vacca, G., Moia, S., Prodam, F., Surico, D. (2016). Intracoronary Des-Acyl Ghrelin Acutely Increases Cardiac Perfusion Through a Nitric Oxide-Related Mechanism in Female Anesthetized Pigs. Endocrinology *157*, 2403-15
48. Grunwald, J., Hariprasad, S., DuPont, J., Maguire, M.G., Fine, S.L., Brucker, A.J., Maguire, A.M., Ho, A.C. (1998). Foveolar choroidal blood flow in age-related macular degeneration. Invest. Ophthalmol. Vis. Sci. *39*, 385-390
49. Grunwald, J.E., Pistilli, M., Daniel, E., Ying, G.S., Pan, W., Jaffe, G.J., Toth, C.A., Hagstrom, S.A., Maguire, M.G., Martin, D.F. (2017). Comparison of Age-Related Macular Degeneration Treatments Trials Research Group: Incidence and Growth of Geographic Atrophy during 5 Years of Comparison of Age-Related Macular Degeneration Treatments Trials. Ophthalmology *124*, 97-104
50. Gupta, N., Mansoor, S., Sharma, A., Sapkal, A., Sheth, J., Falatoonzadeh, P., Kuppermann, B.D., Kenney, M.C. (2013). Diabetic Retinopathy and VEGF. Open Ophthalmol. J. *7*, 4-10
51. Halliwell, B. (2007). Oxidative stress and cancer: have we moved forward? Biochem. J. *401*, 1-11
52. Handa, J.T. (2012). How does the macula protect itself from oxidative stress? Mol. Aspects Med. *33*, 418-35
53. Handa, J.T., Cano, M., Wang, L., Datta, S., Liu, T. (2017). Lipids, oxidized lipids, oxidation-specific epitopes, and Age-related Macular Degeneration. Biochim. Biophys. Acta. *1862*, 430-440
54. Hernández-Zimbrón, L.F., Zamora-Alvarado, R., Ochoa-De la Paz, L., Velez-Montoya, R., Zenteno, E., Gulias-Cañizo, R., Quiroz-Mercado, H., Gonzalez-Salinas, R. (2018). Age-Related Macular Degeneration: New Paradigms for Treatment and Management of AMD. Oxid. Med. Cell. Longev. *2018*, 8374647

55. Hernández-Zimbrón, L.F., Zamora-Alvarado, R., Ochoa-De la Paz, L., Velez-Montoya, R., Zenteno, E., Gulias-Cañizo, R., Quiroz-Mercado, H., Gonzalez-Salinas, R. (2018). Age-Related Macular Degeneration: New Paradigms for Treatment and Management of AMD. Oxid Med Cell Longev. 8374647
56. Honda, K., Casadesus, G., Petersen, R.B., Perry, G., Smith, M.A. (2004). Oxidative stress and redox-active iron in Alzheimer's disease. Ann. N.Y. Acad. Sci. *1012*, 179-82
57. http://bdbiosciences.com/kr/instruments/accuri/a rticles/archive/2015_02/index.jsp
58. https://c60canada.com/2018/04/23/age-related-macular-degeneration-treatment-possibly
59. https://discoveryeye.org/layers-of-the-retina
60. https://terraceeyecentre.com.au/conditions-treated/age-related-macular-degeneration
61. https://terraceeyecentre.com.au/conditions-treated/age-related-macular-degeneration
62. https://www.abcam.com/dcfda--h2dcfda-cellular-ros-assay-kit-ab113851.html
63. https://www.closerlookatstemcells.org/stem-cells-medicine/macular-degeneration
64. https://www.naturaleyecare.com/glossary/macula-definition
65. https://www.nbsbio.co.uk
66. https://www.researchgate.net/figure/Conversion-of-MTT-to-formazan-by-NADH-dependent-reductases_fig36_265025671
67. https://www.scienceofamd.org
68. https://www.semanticscholar.org/paper/Nitric-oxide-release%3A-part-III.-Measurement-and-Coneski
69. Huo, X., Li, Y., Jiang, Y., Sun, X., Gu, L., Guo, W., Sun, D. (2015). Inhibition of ocular neovascularization by co-inhibition of VEGF-A and PLGF. Cell. Physiol. Biochem. *35*, 1787-96
70. Jarrett, S.G., Boulton, M.E. (2012). Consequences of oxidative stress in age-related macular degeneration. Mol. Aspects Med. *33*, 399-417
71. Javadov, S., Karmazyn, M. (2007). Mitochondrial permeability transition pore opening as an endpoint to initiate cell death and as a putative target for cardioprotection. Cell. Physiol. Biochem. *20*, 1-22
72. Juel, H.B., Faber, C., Svendsen, S.G., Vallejo, A.N., Nissen, M.H. (2013). Inflammatory cytokines protect retinal pigment epithelial cells from oxidative stress-induced death. PLoS One *8*, e64619
73. Justilien, V., Pang, J.J., Renganathan, K., Zhan, X., Crabb, J.W., Kim, S.R., Sparrow, J.R., Hauswirth, W.W., Lewin, A.S. (2007). SOD2 knockdown mouse model of early AMD. Invest. Ophthalmol. Vis. Sci. *48*, 4407-20.
74. Kaarniranta, K., Salminen, A., Haapasalo, A., Soininen, H., Hiltunen, M. (2011). Age-related macular degeneration (AMD): Alzheimer's disease in the eye? J Alzheimers Dis. *24*, 615-31
75. Kaarniranta, K., Sinha, D., Blasiak, J., Kauppinen, A., Veréb, Z., Salminen, A., Boulton, M.E., Petrovski, G. (2013). Autophagy and heterophagy dysregulation leads to retinal pigment epithelium dysfunction and development of age-related macular degeneration. Autophagy *9*, 973-84
76. Kaczara, P., Sarna, T., Burke, J.M. (2010). Dynamics of H_2O_2 Availability to ARPE-19 Cultures in Models of Oxidative Stress. Free Radic. Biol. Med. *48*, 1064-1070
77. Kang, S., Choi, H., Rho, C.R. (2016). Differential Effects of Bevacizumab, Ranibizumab, and Aflibercept on the Viability and Wound Healing of Corneal Epithelial Cells. J. Ocul. Pharmacol. Ther. *32*, 671-676
78. Kannan, R., Zhang, N., Sreekumar, P.G., Spee, C.K., Rodriguez, A., Barron, E., Hinton, D.R. (2006). Stimulation of apical and basolateral VEGF-A and VEGF-C secretion by oxidative stress in polarized retinal pigment epithelial cells. Mol. Vis. *12*, 1649-59
79. Kanwar, M., Chan, P.S., Kern, T.S., Kowluru, R.A. (2007). Oxidative damage in the retinal mitochondria of diabetic mice: possible protection by superoxide dismutase. Invest. Ophthalmol. Vis. Sci. *48*, 3805-11

80. Karunadharma, P.P., Nordgaard, C.L., Olsen, T.W., Ferrington, D.A. (2010). Mitochondrial DNA damage as a potential mechanism for age-related macular degeneration. Investigat. Ophthalmol. Visual Sci. *51*, 5470-9
81. Kasahara, E., Lin, L.R., Ho, Y.S., Reddy, V.N. (2005). SOD2 protects against oxidation-induced apoptosis in mouse retinal pigment epithelium: implications for age-related macular degeneration. Invest. Ophthalmol. Vis. Sci. *46*, 3426-34
82. Kauppinen, A., Paterno, J.J., Blasiak, J., Salminen, A., Kaarniranta, K. (2016). Inflammation and its role in age-related macular degeneration. Cell. Mol. Life Sci. *73*, 1765-86
83. Keles, S., Ates, O., Kartal, B., Alp, H.H., Ekinci, M., Ceylan, E., Ondas, O., Arpali, E., Dogan, S., Yildirim, K., Keles, M.S. (2014). Evaluation of cardiovascular biomarkers in patients with age-related wet macular degeneration. Clin. Ophthalmol. *8*, 1573-8
84. Kim, M.H., Chung, J., Yang, J.W., Chung, S.M., Kwag, N.H., Yoo, J.S. (2003). Hydrogen peroxide-induced cell death in a human retinal pigment epithelial cell line, ARPE-19. Korean J. Ophthalmol. *17*, 19-28
85. Kimoto, K., Kubota, T. (2012). Anti-VEGF Agents for Ocular Angiogenesis and Vascular Permeability. J. Ophthalmol. *2012*, 852-83
86. Klettner, A., Tahmaz, N., Dithmer, M., Richert, E., Roider, J. (2014). Effects of aflibercept on primary RPE cells: toxicity, wound healing, uptake and phagocytosis. Br. J. Ophthalmol. *98*, 1448-52
87. Li, L., Wei, W., Zhang, Y., Tu, G., Zhang, Y., Yang, J., Xing, Y. (2015). SirT1 and STAT3 protect retinal pigmented epithelium cells against oxidative stress. Mol. Med. Rep. *12*, 2231-8
88. Liang, F.Q., Godley, B.F. (2003). Oxidative stress-induced mitochondrial DNA damage in human retinal pigment epithelial cells: a possible mechanism for RPE aging and age-related macular degeneration. Exp. Eye Res. *76*, 397-403
89. Liaudet, L., Soriano, F.G., Szabó, C. (2000). Biology of nitric oxide signaling. Crit. Care Med. N37-52
90. Lois, N., McBain, V., Abdelkader, E., Scott, N.W., Kumari, R. (2013). Retinal pigment epithelial atrophy in patients with exudative age-related macular degeneration undergoing anti-vascular endothelial growth factor therapy. Retina *33*, 13-22
91. Luo, X., Gu, S., Zhang, Y., Zhang, J. (2018). Kinsenoside Ameliorates Oxidative Stress-Induced RPE Cell Apoptosis and Inhibits Angiogenesis via Erk/p38/NF-κB/VEGF Signaling. Front. Pharmacol. *9*, 240
92. Malek, G., Dwyer, M., McDonnell, D. (2012). Exploring the potential role of the oxidant-activated transcription factor aryl hydrocarbon receptor in the pathogenesis of AMD. Adv. Exp. Med. Biol. *723*, 51-59
93. Malik, D., Tarek, M., Caceres del Carpio, J., Ramirez, C., Boyer, D., Kenney, M.C., Kuppermann, B.D. (2014). Safety profiles of anti-VEGF drugs: bevacizumab, ranibizumab, aflibercept and ziv-aflibercept on human retinal pigment epithelium cells in culture. Br. J. Ophthalmol. *98*, Suppl 1:i11-16
94. Mitter, S.K., Song, C., Qi, X., Mao, H., Rao, H., Akin, D., Lewin, A., Grant, M., Dunn, W., Ding, J., Bowes, R.C., Boulton, M. (2014). Dysregulated autophagy in the RPE is associated with increased susceptibility to oxidative stress and AMD. Autophagy *10*, 1989-2005
95. Modi, Y.S., Tanchon, C., Ehlers, J.P. (2015). Comparative safety and tolerability of anti-VEGF therapy in age-related macular degeneration. Drug Saf. *38*, 279-93
96. Oh, J.R., Han, J.W., Kim, Y.K., Ohn, Y.H., Park, T.K. (2017). The effects of anti-vascular endothelial growth factor agents on human retinal pigment epithelial cells under high glucose conditions. Int. J. Ophthalmol. *10*, 203-210
97. Ormel, J., De Jonge, P. (2011). Unipolar depression and the progression of coronary artery disease: toward an integrative model. Psychother. Psychosom. *80*, 264-274.

98. Ostwald, P., Roth, S. (2012). Nitric oxide leads to cytoskeletal reorganization in the retinal pigment epithelium under oxidative stress. Adv. Biosci. Biotechnol. *3*, 1167-1178
99. Peddada, K.V., Brown, A., Verma, V., Nebbioso, M. (2018). Therapeutic potential of curcumin in major retinal pathologies. Int. Ophthalmol.
100. Penn, J.S., Madan, A., Caldwell, R.B., Bartoli, M., Caldwell, R.W., Hartnett, M.E. (2008). Vascular endothelial growth factor in eye disease. Prog. Retin. Eye Res. *27*, 331-71
101. Pinazo, D., Gallego-Pinazo, R., García-Medina, J.J., Zanón-Moreno, V., Nucci, C., Dolz-Marco, R., Martínez-Castillo, S., Galbis-Estrada, C., Marco-Ramírez, C., López-Gálvez, M.I., Galarreta, D.J., Díaz-Llópis, M. (2014). Oxidative stress and its downstream signaling in aging eyes. Clin. Interv. Aging *9*, 637-52
102. Plyukhova, A.A., Budzinskaya, M.V. (2018). The role of anti-VEGF therapy in geographic atrophy progression. Vestn. Oftalmol. *134*, 289-293
103. Prasad, S., Galetta, S.L. (2011). Anatomy and physiology of the afferent visual system. Handb. Clin. Neurol. *102*, 3-19
104. Ranjbar, M., Brinkmann, M.P., Tura, A., Rudolf, M., Miura, Y., Grisanti, S. (2016). Ranibizumab interacts with the VEGF-A/VEGFR-2 signaling pathway in human RPE cells at different levels. Cytokine *83*, 210-216
105. Ranjbar, M., Brinkmann, M.P., Zapf, D., Miura, Y., Rudolf, M., Grisanti, S. (2016). Fc Receptor Inhibition Reduces Susceptibility to Oxidative Stress in Human RPE Cells Treated with Bevacizumab, but not Aflibercept. Cell. Physiol. Biochem. *38*, 737-47
106. Russell, J.W., Golovoy, D., Vincent, A.M., Mahendru, P., Olzmann, J.A., Mentzer, A., Feldman, E.L. (2002). High glucose-induced oxidative stress and mitochondrial dysfunction in neurons. FASEB J. *16*, 1738-48
107. Saenz-de-Viteri, M., Fernández-Robredo, P., Hernández, M., Bezunartea, J., Reiter, N., Recalde, S., García-Layana, A. (2016). Single- and repeated-dose toxicity study of bevacizumab, ranibizumab, and aflibercept in ARPE-19 cells under normal and oxidative stress conditions. Biochem. Pharmacol. *103*, 129-39
108. Salvi, S.M., Akhtar, S., Currie, Z. (2006). Ageing changes in the eye. Postgrad. Med. J 82, 581–587
109. Santos, A.L., Lindner, A.B. (2017). Protein Posttranslational Modifications: Roles in Aging and Age-Related Disease. Oxid Med Cell Longev. 2017: 5716409
110. Schicht, M., Hesse, K., Schröder, H., Naschberger, E., Lamprecht, W., Garreis, F., Paulsen, F.P., Bräuer, L. (2017). Efficacy of aflibercept (EYLEA®) on inhibition of human VEGF in vitro. Ann. Anat. *211*, 135-139
111. Schottler, J., Randoll, N., Lucius, R., Caliebe, A., Roider, J., Klettner, A. (2018). Long-term treatment with anti-VEGF does not induce cell aging in primary retinal pigment epithelium. Exp. Eye Res. *171*, 1-11
112. Scott, A.W., Bressler, S.B. (2013). Long-term follow-up of vascular endothelial growth factor inhibitor therapy for neovascular age-related macular degeneration. Curr. Opin. Ophthalmol. *24*, 190-6
113. Shen, W., Yau, B., Lee, S.R., Zhu, L., Yam, M., Gillies, M.C. (2017). Effects of Ranibizumab and Aflibercept on Human Müller Cells and Photoreceptors under Stress Conditions. Int. J. Mol. Sci. *18*, pii: E533
114. Sheu, S.J., Chao, Y.M., Liu, N.C., Chan, J.Y. (2015). Differential effects of bevacizumab, ranibizumab and aflibercept on cell viability, phagocytosis and mitochondrial bioenergetics of retinal pigment epithelial cell. Acta Ophthalmol. *93*, e631-43
115. Spencer, C., Abend, S., McHugh, K.J., Saint-Geniez, M. (2017). Identification of a synergistic interaction between endothelial cells and retinal pigment epithelium. J. Cell. Mol. Med. *21*, 2542-2552

116. Spraul, C.W., Lang, G.E., Grossniklaus, H.E., Lang, G.K. (1999). Histologic and morphometric analysis of the choroid, Bruch's membrane, and retinal pigment epithelium in postmortem eyes with age-related macular degeneration and histologic examination of surgically excised choroidal neovascular membranes. Surv. Ophthalmol. *44*, S10-32
117. Sreekumar, P.G., Kannan, R., de Silva, A.T., Burton, R., Ryan, S.J., Hinton, D.R. (2006). Thiol regulation of vascular endothelial growth factor-A and its receptors in human retinal pigment epithelial cells. Biochem. Biophys. Res. Commun. *346*, 1200-6
118. Sripathi, S.R., He, W., Um, J.Y., Moser, T., Dehnbostel, S., Kindt, K., Goldman, J., Frost, M.C., Jahng, W.J. (2012). Nitric oxide leads to cytoskeletal reorganization in the retinal pigment epithelium under oxidative stress. Adv. Biosci. Biotechnol. *3*, 1167-1178
119. Stocker, R., Keaney, J.F. (2004). Role of oxidative modifications in atherosclerosis. Physiol. Rev 84, 1381-478
120. Stuart, G.J., Boulton, M.E. (2012). Consequences of oxidative stress in age-related macular degeneration. Mol. Aspects Med. *33*, 399-417
121. Surico, D., Ercoli, A., Farruggio, S., Raina, G., Filippini, D., Mary, D., Minisini, R., Surico, N., Pirisi, M., Grossini, E. (2017). Modulation of Oxidative Stress by 17 β-Estradiol and Genistein in Human Hepatic Cell Lines In Vitro. Cell. Physiol. Biochem. *42*, 1051-1062
122. Surico, D., Farruggio, S., Marotta, P., Raina, G., Mary, D., Surico, N., Vacca, G., Grossini, E. (2015). Human chorionic gonadotropin protects vascular endothelial cells from oxidative stress by apoptosis inhibition, cell survival signalling activation and mitochondrial function protection. Cell. Physiol. Biochem. *36*, 2108-2120
123. Totan, Y., Cekiç, O., Borazan, M., Uz, E., Sögüt, S., Akyol, O. (2001). Plasma malondialdehyde and nitric oxide levels in age related macular degeneration. Br. J. Ophthalmol. *85*, 1426-8
124. Totan, Y., Koca, C., Erdurmuş, M., Keskin, U., Yiğitoğlu, R. (2015). Endothelin-1 and Nitric Oxide Levels in Exudative Age-Related Macular Degeneration. J. Ophthalmic. Vis. Res. *10*, 151-4
125. Wang, L., Clark, M.E., Crossman, D.K.., 2 Kojima, K., Messinger, J.D., Mobley, J.A.., Curcio, C.A. (2010). Abundant Lipid and Protein Components of Drusen. PLoS One. *5*, e10329
126. Wang, Y., Fei, D., Vanderlaan, M., Song, A. (2004). Biological activity of bevacizumab, a humanized anti-VEGF antibody in vitro. Angiogenesis. *7*, 335-45
127. Weiyong, S., Belinda, Y., So-Ra, L., Ling, Z., Yam, M., Gillies, M.C. (2017). Effects of Ranibizumab and Aflibercept on Human Müller Cells and Photoreceptors under Stress Conditions. Int. J. Mol. Sci. *18*, pii: E533
128. Wetzig, P.C. (1988). Treatment of drusen-related aging macular degeneration by photocoagulation. Trans Am Ophthalmol. Soc. *86*, 276-90
129. Willoughby, C.E., Ponzin, D., Ferrari S., Lobo A., Landau, K., Omidi, Y. (2010). Anatomy and physiology of the human eye: effects of mucopolysaccharidoses disease on structure and function–a review. Clinical and Experimental Ophthalmology *38*, 2-11
130. Wons, J., Wirth, M.A., Graf, N., Becker, M.D., Michels, S. (2017). Comparison of progression rate of retinal pigment epithelium loss in patients with neovascular age-related macular degeneration treated with Ranibizumab and Aflibercept. J. Ophthalmol. *2017*, 7432739
131. Yorston, D. (2014). Anti-VEGF drugs in the prevention of blindness. Community Eye Health *27*, 44-6
132. Young, R.W. (1988). Solar radiation and age-related macular degeneration. Surv. Ophthalmol. *32*, 252-69
133. Zając-Pytrus, H.M., Pilecka, A., Turno-Kręcicka, A., Adamiec-Mroczek, J., Misiuk-Hojło, M. (2015). The Dry Form of Age-Related Macular Degeneration (AMD): The Current Concepts of Pathogenesis and Prospects for Treatment. Adv. Clin. Exp. Med. *24*, 1099-104

134. Zampros, I., Praidou, A., Brazitikos, P., Ekonomidis, P., Androudi, S. (2012). Antivascular Endothelial Growth Factor Agents for Neovascular Age-Related Macular Degeneration. Journal of Ophthalmology *2012*, 319-728
135. Zha, X., Wu, G., Zhao, X., Zhou, L., Zhang, H., Li, J., Ma, L., Zhang, Y. (2015). PRDX6 Protects ARPE-19 Cells from Oxidative Damage via PI3K/AKT Signaling. Cell. Physiol. Biochem. *36*, 2217-28
136. Zhao, Z., Sun, T., Jiang, Y., Wu, L., Cai, X., Sun, X., Sun, X. (2014). Photooxidative damage in retinal pigment epithelial cells via GRP78 and the protective role of grape skin polyphenols. Food Chem. Toxicol. *74*, 216-24.
137. Zheng, W., Meng, Q., Wang, H., Yan, F., Little, P.J., Deng, X., Lin, S. (2018). IGF-1-Mediated Survival from Induced Death of Human Primary Cultured Retinal Pigment Epithelial Cells Is Mediated by an Akt-Dependent Signaling Pathway. Mol. Neurobiol. *55*, 1915-1927
138. Zhuang, P., Shen, Y., Chiou George, C.Y. (2010). Effect of flavone on the ocular blood flow and formation of choroidal novascularization. Int. J. Ophthalmol. *3*, 95-98